

Higher Dimensional Gravity, Black Holes and Brane Worlds

A thesis
submitted in partial fulfilment
of the requirements for the Degree
of
Doctor of Philosophy in Physics
in the
University of Canterbury

by

Benedict Carter



University of Canterbury
2006

Disclaimer

The work described in this thesis was carried out under the supervision of Dr D.L. Wiltshire in the Department of Astronomy and Physics, University of Canterbury. Chapters two–four are comprised of original work except where explicit reference is made to the work of others. Chapter two is based on work done in collaboration with Ishwaree Neupane, published in *Phys. Rev. D* **72** (2005) 043534. Chapter three is based on work published in *Class. Quant. Grav.* **22** (2005) 4551. Chapter four is based on work done in collaboration with Alex Nielsen and David Wiltshire, in *hep-th/0602086*, submitted to *J. High Energy Physics*. No part of this thesis has been submitted for any degree, diploma or other qualification at any other University.

Acknowledgements

I'd like to thank my supervisor, David Wiltshire for his support and guidance. I am grateful to Ishwaree Neupane for his collaboration. Many thanks to Matt Visser for his encouragement and fruitful discussions. I would like to thank Isis and Brad Cartridge, Alex Nielsen, Ben Leith, Duncan Wright, Kahae Han, Ewan Orr, Marni Sheppeard and everyone else who has already left (you know who you are) for providing support, comradeship, entertainment, intelligent discussion and much needed distractions. Finally, I would like to thank Wibke Ehlers for her companionship, support and humour.

Dedication

I dedicate this thesis to my parents, Miles and Rosemary Carter, for their unending encouragement, emotional support, guidance and belief in me throughout the entirety of my education.

Contents

1	Introduction	1
1.1	Pushing the Limits of General Relativity	1
1.2	Black Holes in Four Dimensions	2
1.2.1	The Schwarzschild Solution	2
1.2.2	The Kerr Solution	3
1.2.3	Black Hole Thermodynamics	5
1.2.4	Alternatives to Black Holes	8
1.3	Higher Dimensional Black Holes	10
1.3.1	Uncompactified Extra Dimensions	11
1.3.2	Compactified Extra Dimensions	14
1.3.3	Analysis of Higher Dimensional Black Holes	18
1.4	Brane Worlds	18
1.4.1	Large Extra (Compact) Dimensions	19
1.4.2	Warped extra dimensions	21
1.4.3	Hybrid Brane world Models	23
1.5	Overview of Thesis	23
2	Stability of Higher Dimensional Rotating (Kerr) AdS Black Holes	25
2.1	Higher Dimensional Black Holes and String-Theory	25
2.2	AdS and Kerr-AdS metrics	27
2.3	Thermodynamics of Kerr AdS Solutions	29

2.3.1	Thermal Phase Transition	30
2.3.2	The first law of AdS bulk thermodynamics	40
2.3.3	The specific heat and thermodynamic stability	41
2.3.4	The temperature bound for rotating black holes	47
2.3.5	Rotation and the AdS-CFT correspondence	50
2.4	The stability of the background of Kerr-AdS spacetime under gravitational perturbations	51
2.4.1	The Lichnerowicz operator	52
2.4.2	Dependence on radial coordinate only	53
2.4.3	Anti de-Sitter spacetime in odd dimensions	56
2.4.4	AdS spacetime in even dimensions	58
2.5	Conclusion	60
3	Gravastars with generalised exteriors	62
3.1	Gravastars	62
3.2	Schwarzschild-(A)dS Gravastar	65
3.2.1	Definitions	65
3.2.2	Solutions	66
3.3	Reissner-Nordström gravastar	72
3.4	Conclusion	77
4	Hybrid Brane Worlds in the Salam-Sezgin Model	78
4.1	Hybrid Brane Worlds	78
4.2	Salam-Sezgin fluxbranes	81
4.3	Adding a thin brane	84
4.3.1	Consistency conditions when adding a thin-brane	86
4.4	Static potential of the massless scalar field	88
4.4.1	Scalar propagator	88
4.4.2	Boundary and matching conditions	91

4.4.3	Static potential on the brane	92
4.4.4	Nonlinear gravitational waves on the brane	98
4.5	The hierarchy problem	99
4.6	General fluxbrane and dual static black hole-like solutions	102
4.7	Conclusion	109
A	Physical Units	111
B	Series solutions for a static scalar potential in a Salam-Sezgin Super-gravitational hybrid braneworld	112
B.1	Abstract	112
B.2	Introduction	113
B.3	The Model	114
B.4	The Solution	115
B.5	Conclusion	117
B.6	Acknowledgements	117
References		118

Abstract

Current research is focussed on extending our knowledge of how gravity behaves on small scales and near black hole horizons, with various modifications which may probe the low energy limits of quantum gravity. This thesis is concerned with such modifications to gravity and their implications.

In chapter two thermodynamic and classical gravitational stability analyses are performed on higher dimensional Kerr anti-de Sitter black holes. We find conditions for the black holes to be able to be in thermal equilibrium with their surroundings and for the background to be stable against classical tensor perturbations.

In chapter three new spherically symmetric gravastar solutions, stable to radial perturbations, are found by utilising the construction of Visser and Wiltshire. The solutions possess an anti-de Sitter or de Sitter interior and a Schwarzschild-(anti)-de Sitter or Reissner–Nordström exterior. We find a wide range of parameters which allow stable gravastar solutions, and present the different qualitative behaviors of the equation of state for these parameters.

In chapter four a six-dimensional warped brane world compactification of the Salam-Sezgin supergravity model is constructed by generalizing an earlier hybrid Kaluza–Klein / Randall–Sundrum construction. We demonstrate that the model reproduces localized gravity on the brane in the expected form of a Newtonian potential with Yukawa–type corrections. We show that allowed parameter ranges include values which potentially solve the hierarchy problem. The class of solutions given applies to Ricci–flat geometries in four dimensions, and consequently includes brane world realisations of the Schwarzschild and Kerr black holes as particular examples. Arguments are given which suggest that the hybrid compactification of the Salam–Sezgin model can be extended to reductions to arbitrary Einstein space geometries in four dimensions.

This work furthers our understanding of higher dimensional general relativity, which is potentially interesting given the possibility that higher dimensions may become observable at the TeV scale, which will be probed in the Large Hadron Collider in the next few years.

Chapter 1

Introduction

1.1 Pushing the Limits of General Relativity

Black holes are perhaps the most interesting objects in general relativity. A black hole is a solution to Einstein’s equations which is generically characterized by having at least one gravitational trapping horizon – a boundary of a region where the gravitational field is so great that not even light can escape from it. Exact black hole solutions of Einstein’s field equation are generally found to also contain singularities within the horizon. In fact, Hawking and Penrose proved that as long as matter in a generic spacetime satisfies the strong energy condition and there exists a closed trapped surface then the spacetime will be not be geodesically complete, implying the existence of a singularity. At such singularities the curvature of the manifold typically (but not necessarily) becomes infinite. While the properties of horizons are taken to be physically acceptable by the majority of the scientific community, it is assumed that black hole singularities are unphysical. Hence it is expected that near the singularity general relativity breaks down and that a theory of quantum gravity will be required in order to accurately describe the physics [1, 2]. Unfortunately, gravity has proven to be difficult to directly quantise [3, 4] and as such current work is focussed on extending our knowledge of how gravity behaves on small scales and near black hole horizons, with various modifications designed to link up with the suspected low energy limits of quantum gravity. This thesis is concerned with such modifications to gravity and their implications.

1.2 Black Holes in Four Dimensions

1.2.1 The Schwarzschild Solution

The simplest example of a black hole is given by the Schwarzschild solution [5] to Einstein's vacuum equations. The Schwarzschild metric in Schwarzschild coordinates¹ is

$$ds^2 = -\Delta dt^2 + \Delta^{-1} dr^2 + r^2 d\theta^2 + r^2 \sin^2 \theta d\phi^2, \quad (1.1)$$

where

$$\Delta(r) = 1 - \frac{2GM}{r}, \quad (1.2)$$

M is the gravitational mass of the system measured at spatial infinity and G is Newton's constant. The horizon for the Schwarzschild geometry is located by the condition $\Delta = 0$ in these coordinates, i.e. at $r = 2GM$. The Schwarzschild geometry has four Killing vectors, $\frac{\partial}{\partial t}$ and the three rotational Killing vectors of $SO(3)$, corresponding to spherical symmetry. In fact, by Birkhoff's theorem the existence of the timelike Killing vector follows as a result of spherical symmetry in vacuum.

The Kretschmann scalar, $R^{abcd}R_{abcd}$, measures the curvature in a coordinate independent manner, and for Schwarzschild is given by

$$R^{abcd}R_{abcd} = \frac{48G^2M^2}{r^6}. \quad (1.3)$$

It diverges as $r \rightarrow 0$, which implies the existence of a curvature singularity at $r = 0$. Given that singularities are generally not thought to be physical, and cannot strictly speaking be described by a point in the manifold, it is clear that the classical theory of general relativity is incomplete and inaccurate in that regime. In some sense though, the existence of the singularity is moot, since it is trapped behind an event horizon, and hence any associated problems are unable to classically escape the black hole. The cosmic censorship hypothesis states that naked singularities cannot form in gravitational collapse from generic, initially non-singular states in an asymptotically flat space-time obeying the dominant energy condition. That is, “there are no naked singularities” [7].

¹These are not the coordinates Schwarzschild originally used [6].

Outside of the horizon where theoretical interest is centered, the fundamental importance of the Schwarzschild solution is that the behavior of the planets in our solar system can be excellently modelled as point particles in the Schwarzschild geometry, since they are at radial parameter distances $r > r_{\text{sun}} \gg 2M_{\text{sun}}$. For example, by using the Schwarzschild solution as the background metric and solving for the timelike geodesics of test particles, one can explain the perihelion precession of Mercury (and similarly for the other planets). The Schwarzschild solution was also used to calculate the bending of light due to the sun, correctly giving twice the Newtonian prediction. Irrespective of theoretical concerns about the nature of the Schwarzschild horizon and its interior interior, the exterior Schwarzschild solution presents an undeniably functional description of gravity in our solar system.

1.2.2 The Kerr Solution

The Kerr metric [8] is a simple, explicit, exact solution of the Einstein vacuum equations describing a rotating black hole in a four-dimensional spacetime, providing a non-trivial generalization of the Schwarzschild geometry. It has just two Killing vectors as opposed to the four of Schwarzschild geometry - it is stationary and axisymmetric. In Boyer-Lindquist coordinates, with $c = 1$, it is given by:

$$ds^2 = - \left(1 - \frac{2GMr}{\rho^2} \right) - \frac{2GMar \sin^2 \theta}{\rho^2} (dt d\phi + d\phi dt) + \frac{\rho^2}{\Delta} dr^2 + \rho^2 d\theta^2 + \frac{\sin^2 \theta}{\rho^2} [(r^2 + a^2)^2 - a^2 \Delta \sin^2 \theta] d\phi^2 \quad (1.4)$$

where

$$\Delta(r) = r^2 - 2GMr + a^2 \quad (1.5)$$

and

$$\rho^2(r, \theta) = r^2 + a^2 \cos^2 \theta. \quad (1.6)$$

The solution is parameterised by the two quantities, M and $a = J/M$. The mass M of the spacetime can be evaluated by Stokes' theorem for a conserved current, $K_\nu R^{\mu\nu}$, by

$$M = \frac{1}{4\pi G} \int_{\partial\Sigma} d^2x \sqrt{\gamma^{(2)}} n_\nu \sigma_\mu \nabla^\nu K^\mu, \quad (1.7)$$

where n_ν is the normal to the hypersurface Σ , σ_μ is the normal to the boundary of the hypersurface $\partial\Sigma$, $\sqrt{\gamma^{(2)}}$ is the determinant of the induced metric on the boundary of the hypersurface and K^μ is the time-translational Killing vector for the spacetime. The angular momentum can be similarly calculated,

$$J = \frac{1}{4\pi G} \int_{\partial\Sigma} d^2x \sqrt{\gamma^{(2)}} n_\nu \sigma_\mu \nabla^\nu R^\mu, \quad (1.8)$$

where R^μ is the axisymmetric rotational Killing vector. One can see that the in limit of $a \rightarrow 0$ in (1.4)-(1.6) leads to the Schwarzschild metric in Schwarzschild coordinates.

Interestingly, the Kerr solution can be written in terms of an exact “distortion” on a background spacetime giving the Kerr-Schild form of the Kerr solution [9],

$$ds^2 = g_{\mu\nu} dx^\mu dx^\nu = \eta_{\mu\nu} dx^\mu dx^\nu + \frac{2M}{U} (k_\mu dx^\mu)^2 \quad (1.9)$$

where k_μ is null and geodesic with respect to both the full metric $g_{\mu\nu}$ and the flat metric $\eta_{\mu\nu}$. Explicitly, in Cartesian coordinates x, y, z, t , one has [10]

$$\mathbf{k} = k_\mu dx^\mu = dt + \frac{r(xdx + ydy) + a(xdy - ydx)}{r^2 + a^2} + \frac{zdz}{r}, \quad (1.10)$$

and

$$U = r + \frac{a^2 z^2}{r^3}, \quad (1.11)$$

where r is defined² by

$$\frac{x^2 + y^2}{r^2 + a^2} + \frac{z^2}{r^2} = 1. \quad (1.12)$$

The Kerr-Schild form of the Kerr solution naturally generalises to higher dimensions and background spacetimes.

Generalisation of Schwarzschild and Kerr Solutions in Four Dimensions

The Schwarzschild solution has been generalised in a number of ways by relaxing various assumptions. For example, it is currently understood that 70% of the energy density of the universe is due to a repulsive dark energy, namely a fluid with pressure, P , and energy density, ρ , related by $p = \omega\rho$, $\omega < -1/3$, which violates the strong energy condition. The most well-known example of such a dark energy is a cosmological

²Note that r is *not* the usual radial coordinate in flat spacetime.

constant, Λ , for which $\omega = -1$, i.e. $P = -\rho = -\Lambda/8\pi G$. The cosmological constant was first introduced by Einstein with a finely tuned value in order to produce a static universe in which the repulsive vacuum energy exactly cancelled the gravitational attraction of additional pressureless matter. Willem de Sitter shortly thereafter derived cosmological solutions without any ordinary matter, in which the cosmological constant was not finely tuned and the Universe expanded forever [11].

Kottler generalised the Schwarzschild solution by including such a cosmological constant term to find black hole solutions with asymptotic constant curvature geometry [12]. The Schwarzschild (Anti) de Sitter metric is given by (1.1) where $\Delta(r) = 1 - 2GM/c^2r - \Lambda r^2/3$.

Similarly, Brandon Carter generalised the Kerr solution by adding a cosmological constant to the background spacetime in Kerr-Schild coordinates, and modifying the geodesics to find the Kerr-(A)dS solution [13, 14]. We will present this result more generally later in this chapter. Newman and coworkers [15] also generalised the Kerr geometry by adding electric and magnetic charge, which can be seen by making the replacement $2GMr \rightarrow 2GMr - G(Q^2 + P^2)$ in (1.4)–(1.6). The associated one-form electromagnetic potential for the Kerr-Newman solution is

$$\begin{aligned} A_t &= \frac{Qr - Pa \cos \theta}{\rho^2}, \\ A_\phi &= \frac{-Qar \sin^2 \theta + P(r^2 + a^2) \cos \theta}{\rho^2}. \end{aligned} \quad (1.13)$$

1.2.3 Black Hole Thermodynamics

In the early 1970s it was discovered that black holes obeyed certain laws of black hole mechanics:

- Zeroth law: A black hole in a stationary state has a constant surface gravity on the entire horizon \leftrightarrow A system in thermal equilibrium has constant temperature.
- First law:

$$\delta M = \frac{\kappa}{8\pi G} \delta A + \dots \leftrightarrow dE = TdA + \dots \quad (1.14)$$

- Second law:

$$\delta A \geq 0 \leftrightarrow dS \geq 0. \quad (1.15)$$

- Third law: That the area of a black hole cannot be reduced to zero in a finite number of steps. This remains as a conjecture which may not actually hold and in some versions is equivalent to the cosmic censorship hypothesis [16].

Bardeen, Carter and Hawking proved the zeroth and first laws for stationary axisymmetric (electro)vacuum asymptotically flat spacetimes [18]. The analogy to the thermodynamic laws, which is seen explicitly via the substitutions

$$E \leftrightarrow M, \quad S \propto A, \quad T \propto \kappa. \quad (1.16)$$

Early on Bekenstein suggested that some multiple of the area of the black hole horizon played the role of entropy due to the form of the second law [17]. However, it was initially emphasised by Hawking *et al.* that the laws were at best analogies, as classical black holes had zero temperature and, in general, non-zero surface gravity [18]. Three years later, by considering quantum field theory in the background of a Schwarzschild black hole, Hawking found a non-zero thermal radiation flux at infinity [19]. The radiation was due to the presence of the black hole horizon, which lead to the concrete realisation of the proportionality of the temperature and surface gravity,

$$T = \kappa/2\pi, \quad (1.17)$$

implying that the laws of black hole mechanics were also the laws of black hole thermodynamics.

Due to Hawking radiation, a black hole's horizon area is able to decrease, leading to a violation of the classical second law of black hole thermodynamics (the area theorem). However, the associated Hawking radiation has entropy, which led Bekenstein to propose the generalised second law of black hole thermodynamics [17],

$$\delta \left(S_{matter} + \frac{A}{4G} \right) \geq 0. \quad (1.18)$$

This has been checked in a variety of model dependant scenarios of widely varying nature, and has so far been validated [20]. This strongly suggests that the entropy of a black hole is of a far more generic nature than had been previously thought [21].

Whether black holes are thermodynamically stable is an important issue for quantum gravity. For example, the negative specific heat of Schwarzschild means that

the black hole cannot come into thermal equilibrium with the background spacetime and will lead to a runaway evaporation of the black hole into thermal radiation [19]. However, the semi-classical calculation used in a vacuum background, for example in a Schwarzschild background, must necessarily break down since once sufficient thermal radiation back reacts onto the geometry, the solution can no longer be considered vacuum. While the radiation is initially low temperature, because of the negative specific heat of the black hole the energy associated with the radiation will eventually become comparable to the energy of the radiating black hole. Additionally, it is not yet known how to deal with the end point of the evaporation process - it is once again expected that the physics after the breakdown of the semi-classical approximation will only be answered within the context of a quantum theory of gravity.

Both general relativity and quantum field theory conserve information. In general relativity with globally hyperbolic manifolds Cauchy data prescribed on an initial spacelike hypersurface uniquely determines the evolution of the full spacetime, while in quantum field theory one has a unitary evolution of quantum states. In both cases the information required to prescribe a state at early time is directly related to the information required to prescribe a state at later times [22]. The equations of motion governing the dynamics of the situation are time-reversible. However, according to the no hair “theorems” a black hole can be described by just a few parameters (e.g. M , J and Q for an Einstein electrovacuum black hole in four dimensions), meaning that any other information which passes over the event horizon becomes hidden. Semi-classically Hawking radiation given off by such a black hole is almost entirely thermal at infinity [19], meaning that information trapped behind the horizon does not escape via this process.

The problem can be illustrated by a thought experiment: Take two states of matter with the same M , J and Q , one a baryon gas and another a lepton gas and collapse them into identical black holes (of the same mass, charge and angular momentum). The thermal radiation collected at infinity will be identical in character for both black holes. The information of the initial states (baryon and lepton number) before they became black holes has therefore been ‘lost’ [22].

The problem might be attributed to the presence of a singularity, on which all geodesics entering the event horizon end, thereby destroying information that enters the horizon (as it cannot reach future infinity). Some suggested ‘resolutions’ to the information paradox include:

1. Unitarity is violated [23]–[25]. However, the chief proponent of this view, Hawking, has recently revised his opinion and now favours option two below, namely that quantum perturbations of the horizon allow information to escape [26]. Unfortunately the details of Hawking’s calculation have yet to appear.
2. The radiation emitted by the black hole is not thermal, but is correlated with the information that went into the formation of the black hole. This viewpoint has long been advocated by ’t Hooft, who has provided a number of toy models to describe this process [27]–[30].
3. The black hole does not radiate away entirely, leaving behind a remnant which still contains all the information that went into its formation.
4. Due to quantum gravitational effects, gravitational collapse halts before a horizon forms. The equation of state in the center of the black hole might be similar to (anti) de Sitter space. One would be left with a super dense object, presumably more dense than a neutron star.

We will discuss the last ‘resolution’ in more detail with the assumption that a horizon does not form, as it is similar in character to that of the neutron star model, which has enjoyed wide success with the discovery of pulsars. We note though that by removing the horizon, we remove the significance of the elegant black hole thermodynamic laws.

1.2.4 Alternatives to Black Holes

In chapter 3 we will examine a particular model which avoids the information paradox by removing the horizon. This can be achieved, for example, by halting gravitational collapse of the matter at some radius outside of the horizon radius. For this to happen,

one needs a new state of matter which resists further compression. The equation of state for the matter, in models considered to date, is that of (anti) de Sitter space, i.e., a non-zero pure vacuum energy.

A simple picture of the models under consideration is that of an (A)dS metric surrounded by a thin shell of matter. The matter making up the shell is some new state of matter that obeys the dominant energy condition. The metric exterior to the thin shell of matter is Kerr-Newman or some special simpler case. This picture, while speculative, is extremely similar to that of the neutron star and in fact carries on the long tradition of positing that super-dense stars are formed out of new states of matter [11],[31]–[37].

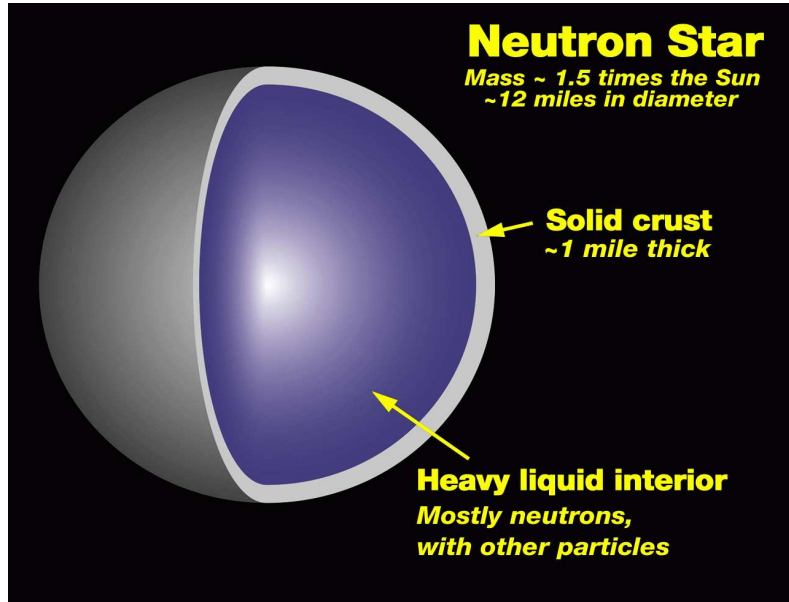


Figure 1.1: *A model of Neutron star internal structure. Source: NASA/Marshall Space Flight Center.*

In this scenario, one would need to check that the solution is consistent within the context of general relativity, resists further gravitational collapse, and is stable to radial perturbations. In chapter 3 we investigate a model which fits these requirements, the gravitational vacuum star (gravastar) of Mazur and Mottola [37]. In the simplified version as envisaged by Visser and Wiltshire [38], we extend the exterior geometry from Schwarzschild to both Schwarzschild (A)dS and Reissner–Nordström, and find conditions for stability against radial perturbations. This is of course a very simplified

model.

By analogy, if the one looks at actual models of neutron stars, one finds that the matter at the surface of a neutron star is composed of ordinary nuclei as well as electrons. The “atmosphere” of the star is roughly one meter thick, below which one encounters a solid “crust” whose thickness is approximately 5%–10% of the radius of the star [39, 40].

The outer layers of a neutron star are formed of a solid crust composed of a Coulomb lattice of very neutron rich nuclei immersed in a nearly uniform relativistic electron gas. In the deeper layers corresponding to densities beyond the drip threshold $\rho_{drip} \simeq 4 \times 10^{11} \text{ g cm}^{-3}$, nuclei are embedded in a sea of “free” neutrons which are expected to become superfluids in mature neutron stars whose temperature has dropped below the critical temperature for the onset of superfluidity [40]. The core is expected to contain superfluid neutrons coexisting with electrons and protons [41].

Realistic gravastars would be expected to display equally complex structures depending on the details of the physics governing the gravitational condensate matter state.

1.3 Higher Dimensional Black Holes

Given that Einstein’s general relativity is a classical theory, it is expected that it will break down as an accurate model of gravity on small distance scales/high curvature regions, and that to properly describe gravitational interactions on such small scales will require a theory of quantum gravity. We currently do not have such a theory, and so current work is focussed on modifying general relativity to find semi-classical models which will give rise to experimentally testable corrections to gravity on relevant scales.

One of the theories which is hoped to describe semi-classical gravity is M-theory³; see [43, 44] for reviews. M-theory is naturally framed in 10 + 1 dimensions, and as such faces difficulty in being reconciled with current observations which indicate a reality consisting of 3 + 1 dimensions.

³One other serious contender is loop quantum gravity; see [42] for a review.

One of the most important unanswered questions with regard to higher-dimensional unified models is why does spacetime appear to have *three* spatial dimensions? General relativity, and its precursors, special relativity and Galilean relativity do not prescribe the dimensionality of space. The fact that we observe three spatial and one time dimension is added into the description of reality within the framework of those mathematical structures by hand. General relativity is written in the framework of manifolds, spaces which may be curved and can possess a complicated topology, but in local regions “appear as” segments of \mathbb{R}^n . Given the generality available to the possible description of spacetime within this framework, one may ask the question “what is unique about the nature of three spatial dimensions that naturally selects it as physical reality”? Alternatively one may ask “assuming there are more than three spatial dimensions, why do we only observe three”? We will attempt to briefly address the attempts that have been made to answer both questions in this section.

1.3.1 Uncompactified Extra Dimensions

Why three?

Large extra dimensions were first considered by Ehrenfest [45]. Amongst other results, he found that for objects bound in a potential of the form

$$V \propto \frac{1}{r^{n-2}}, \quad (1.19)$$

where $r = \sqrt{x_1^2 + x_2^2 + \dots + x_n^2}$ is the metric in the space \mathbb{R}^n with coordinates x_i , $i = 1 \dots n$, that:

- All states were bound in \mathbb{R}^2 ,
- Bound states and unbound states were possible in \mathbb{R}^3 ,
- There were no bound states for $n > 3$ in \mathbb{R}^n – all states were ingoing or outgoing spirals.

Similarly one can attempt to generalise 4-dimensional GR models to higher dimensions, and investigate the physical consequences. For example, the Schwarzschild

solution may be generalised to arbitrary $D = n + 1$ dimensions in a straightforward manner. The solution, obtained by Tangherlini [46] is,

$$ds^2 = -\Delta dt^2 + \frac{dr^2}{\Delta} + r^2 d\Omega_{n-1}^2, \quad (1.20)$$

where n is the number of spatial dimensions, $d\Omega_{n-1}^2$ is the line element of a $(n - 1)$ –dimensional sphere, and Δ is given by

$$\Delta = 1 - \frac{2GM}{r^{n-2}}. \quad (1.21)$$

If a D –dimensional cosmological constant and electromagnetic field are included then one has

$$\Delta = 1 - \frac{2GM}{r^{n-2}} + \frac{GQ^2}{2\pi(n-1)(n-2)r^{2(n-2)}} - \frac{2\Lambda r^2}{(n)(n-1)}. \quad (1.22)$$

A study of the geodesic equations in the background (1.20,1.21) reveals that stable bound orbits do not exist if $n > 3$ [46]. Furthermore, if one requires that the effective potential governing the problem vanishes at infinity then values $n < 3$ are ruled out. Thus we are uniquely led to $n = 3$. An analysis of the Schrödinger equation for arbitrary D also leads to similar conclusions [46].

From an anthropic point of view then, four dimensional space-time seems to be favoured for allowing the most complex forms of life, given it allows for the most complex types of behavior for both classical and quantum orbits.

Higher Dimensional Generalisations of the Kerr–Newman solution

The Kerr–Newmann geometry was generalised to D dimensions by Myers and Perry [47]. By assuming Kerr–Schild form they found that, for even–dimensional spacetimes, $D = 2n \geq 4$, the appropriate null one–form which generalises (1.10) is

$$\mathbf{k} = k_\mu dx^\mu = dt + \sum_{i=1}^{n-1} \frac{r(x_i dx^i + y_i dy^i) + a_i(x_i dy^i - y_i dx^i)}{r^2 + a_i^2} + \frac{z dz}{r}, \quad (1.23)$$

with

$$U = \frac{1}{r} \left(1 - \sum_{i=1}^{n-1} \frac{a_i^2 (x_i^2 + y_i^2)}{(r^2 + a_i^2)^2} \right) \prod_{j=1}^{n-1} (r^2 + a_j^2), \quad (1.24)$$

and

$$\sum_{i=1}^{n-1} \frac{x_i^2 + y_i^2}{r^2 + a_i^2} + \frac{z^2}{r^2} = 1. \quad (1.25)$$

Substituting (1.23) and (1.24) into (1.9), one obtains the generalisation of the vacuum Kerr metric in $2n$ spacetime dimensions, with $(n - 1)$ independent rotation parameters a_i in $(n - 1)$ orthogonal spatial 2-planes.

If the number of spacetime dimensions is odd, $D = 2n + 1 \geq 5$, then there are $n \geq 2$ pairs of spatial coordinates and no z coordinate, and so the terms involving z are omitted, while U is then $1/r$ times the right-hand side of equation (1.24). Thus we find

$$\mathbf{k} = k_\mu dx^\mu = dt + \sum_{i=1}^{n-1} \frac{r(x_i dx_i + y_i dy_i) + a_i(x_i dy_i - y_i dx_i)}{r^2 + a_i^2}, \quad (1.26)$$

with

$$U = \frac{1}{r^2} \left(1 - \sum_{i=1}^{n-1} \frac{a_i^2(x_i^2 + y_i^2)}{(r^2 + a_i^2)^2} \right) \prod_{j=1}^{n-1} (r^2 + a_j^2), \quad (1.27)$$

and

$$\sum_{i=1}^{n-1} \frac{x_i^2 + y_i^2}{r^2 + a_i^2} = 1. \quad (1.28)$$

The higher dimensional black hole has a curvature singularity as expected, and $(D - 2)$ -dimensional spherical horizon topology. Remarkably, in higher dimensions there can still only be up to two horizons. Interestingly, it was found that for $D \geq 6$, Kerr black holes with fixed mass can have arbitrarily large angular momentum [47]. This occurs since the vanishing of one or two spin parameters is enough to guarantee the existence of a horizon. The other spin parameters can then take on arbitrary values. Recently, the Myers–Perry solution given above has been further generalised by Gibbons, Lu, Page and Pope to include a cosmological constant [10].

The black hole uniqueness theorem as stated by Israel, Penrose and Wheeler asserts that in vacuum a 4-dimensional stationary Einstein–Maxwell black hole is characterized solely by its mass, angular momentum and charge. This is consistent with the “no hair theorems” [48], which rule out regular black hole solutions with other independent charges, such as scalar charges, on a model by model basis. By now a number of “hairy black holes” in models with additional exotic forms of matter, such as the Skyrme black hole [49]–[51], are known.

The proof of the uniqueness theorem does not generalize to vacuum solutions in higher dimensions. In fact the recent black rings discovered by Emparan and Reall [52] provide alternatives to 5-dimensional Kerr–Newman black holes with the same mass,

charge and angular momentum, demonstrating that no electrovacuum uniqueness theorem holds in five, and presumably higher dimensions. The discovery of the black ring solutions in five dimensions shows that horizon topologies other than spherical are allowed in higher dimensions, but it is unclear precisely which topologies are allowed.

1.3.2 Compactified Extra Dimensions

Kaluza–Klein Compactification

While the work of Ehrenfest, Tangherlini and others argued for the naturalness of three large spatial dimensions, it had nothing to say about the possibility of $(4 + n)$ -dimensional theories which on large scales appear to be four dimensional. One way of realizing this scenario is by assuming that the extra dimensions form a compact space of very small volume. Such models are known as Kaluza–Klein theories, on account of the pioneering work of Kaluza [53] and Klein [54].

One motivation behind Kaluza–Klein theories is that the “internal” gauge symmetries of the standard model of particle physics might simply be the manifestation of spacetime symmetries in extra dimensions. The fact that the internal gauge transformations are physically distinguishable from ordinary (four-dimensional) spacetime coordinate transformations is due to the fact that the vacuum of the theory is $\mathcal{M}^4 \times \mathcal{B}^{D-4}$, where \mathcal{B}^n is a compact space of dimension n , rather than \mathcal{M}^D . Since there is no evidence for extra dimensions yet at the microscopic level the space \mathcal{B}^n must have a characteristic radius so small that it cannot be probed at the energies which have been available in particle accelerators to date. The process of going from the manifold \mathcal{M}^D to $\mathcal{M}^4 \times \mathcal{B}^{D-4}$ is called “spontaneous compactification” if the process is induced by the structure of the vacuum, in analogy to spontaneous symmetry breaking.

The concepts of Kaluza–Klein theory can be readily understood by considering the original 5-dimensional theory [53, 54]. Kaluza’s idea was to suppose that the physical world is described by the standard Einstein action in five dimensions

$$S_{(5)} = \frac{1}{4\bar{\kappa}^2} \int d^5x \sqrt{g} R. \quad (1.29)$$

Here $g \equiv |\det g_{AB}|$ and $\bar{\kappa}^2 = 4\pi\bar{G}$, where \bar{G} is Newton’s constant in five dimensions. The 5-metric may be conveniently parameterized in terms of a real scalar field σ , a

4-vector A_μ and a 4-metric ${}^4g_{\mu\nu}(x^\lambda)$ as follows:

$$ds^2 = \exp\left(\frac{4\kappa\sigma}{\sqrt{3}}\right) (dx^5 + 2\kappa A_\mu dx^\mu)^2 + \exp\left(\frac{-2\kappa\sigma}{\sqrt{3}}\right) {}^4g_{\mu\nu} dx^\mu dx^\nu, \quad (1.30)$$

where x^5 denotes the single extra spatial dimension, the index μ runs from 0 to 3 and $\kappa^2 = 4\pi G$ is the standard gravitational constant in four dimensions.

Compactification is achieved by taking the internal manifold to be S^1 so that x^5 is periodic, being identified modulo $2\pi R_\kappa$. Since the internal manifold is a circle one may expand the components of σ , A_μ and ${}^4g_{\mu\nu}$ as Fourier series in x^5 :

$$\begin{aligned} \sigma(x^A) &= \sum_{n=-\infty}^{\infty} \sigma^{(n)}(x^\lambda) e^{inx^5/R_\kappa}, A_\mu(x^A) \\ &= \sum_{n=-\infty}^{\infty} A_\mu^{(n)}(x^\lambda) e^{inx^5/R_\kappa}, {}^4g_{\mu\nu}(x^A) \\ &= \sum_{n=-\infty}^{\infty} {}^4g_{\mu\nu}^{(n)}(x^\lambda) e^{inx^5/R_\kappa}. \end{aligned} \quad (1.31)$$

One now makes the ansatz that ${}^4g_{\mu\nu}$ is independent of x^5 , i.e., that $\partial/\partial x^5$ is a Killing vector. This is equivalent to considering only the zero modes in (1.31) – the low-energy limit of the full theory. The restricted 5-dimensional Einstein equations may then be obtained from the effective 4-dimensional action

$$S_{(4)} = \int d^4x \sqrt{-{}^4g} \left(\frac{-R}{4\kappa^2} - \frac{1}{4} \exp(2\sqrt{3}\kappa\sigma) F_{\mu\nu} F^{\mu\nu} + \frac{1}{2} {}^4g^{\mu\nu} \partial_\mu \sigma \partial_\nu \sigma \right). \quad (1.32)$$

If one wishes to identify the actions (1.29) and (1.32) then the 4-dimensional and 5-dimensional gravitational constants must be related by

$$\bar{G} = 2\pi R_\kappa G. \quad (1.33)$$

However, such an identification is not required at the level of the classical equations. Coordinate transformations in five dimensions which preserve the symmetry of the ground state, namely

$$x^\mu \rightarrow \bar{x}^\mu(x^\lambda), \quad x^5 \rightarrow x^5 + \Lambda(x^\lambda), \quad (1.34)$$

give rise to 4-dimensional coordinate transformations and $U(1)$ gauge transformations,

$$A_\mu \rightarrow \bar{A}_\mu = A_\mu + \frac{1}{2\kappa} \partial_\mu \Lambda, \quad (1.35)$$

in the effective 4-dimensional theory.

To determine the order of magnitude of the radius R_κ that one could expect in a realistic theory one can consider coupling a complex scalar field ϕ to the 5-dimensional theory. If ϕ is expressed by a Fourier series similarly to (1.31) then the 5-dimensional scalar Lagrangian

$$\mathcal{L}_{(5)\phi} = \sqrt{g}g^{AB}\partial_A\phi^*\partial_B\phi \quad (1.36)$$

reduces to an effective 4-dimensional Lagrangian

$$\mathcal{L}_{(4)\phi} = \sum_{n=-\infty}^{\infty} \sqrt{-{}^4g} \left\{ (D^\mu\phi^{(n)})^* D_\mu\phi^{(n)} - n^2\phi^{(n)*}\phi^{(n)} \exp\left(\frac{-2\kappa\sigma}{\sqrt{3}}\right) \right\}, \quad (1.37)$$

where

$$D_\mu = \partial_\mu - \frac{2i\kappa n}{R_\kappa} A_\mu. \quad (1.38)$$

It follows that the 4-dimensional electric charge is quantised in units of

$$e = \frac{2\kappa}{R_\kappa}, \quad (1.39)$$

and consequently $R_\kappa \simeq 3.78 \times 10^{-34} m \simeq 23.4 \ell_{\text{Planck}}$, which certainly makes it too small to be observed experimentally.

One can see from (1.37) that the non-zero modes correspond to massive charged particles when viewed from four dimensions. The particles have masses,

$$m_n = \frac{n^2}{R_\kappa} \exp\left(\frac{-2\kappa\sigma}{\sqrt{3}}\right), \quad (1.40)$$

which are of course related to their charges because of (1.39). The coupling to the dilaton means that the “mass” terms are position dependent. One has in effect an infinite tower of states with charges and masses which are integer multiples of e and $m_0 = 2\kappa e$ respectively. These states have been named “Kaluza–Klein excitations”. Similar massive states will be present in the theory if the non-zero modes of (1.31) are included. One finds, in fact, that the massive states of the free 5-dimensional theory are pure spin two [55]. Of course the 5-dimensional model is by no means realistic. However, many of its features, such as the presence of Kaluza–Klein excitations, remain in more sophisticated unified models. If Kaluza–Klein excitations are stable, which seems reasonable [56, 57], then they should be present in the universe today as “remnants” from the compactification era. Thus on one hand Kaluza–Klein excitations are possible

candidates for the dark matter in the universe, while on the other hand cosmological arguments could be used to place constraints on Kaluza–Klein excitation masses [56].

The above example is a very simple case of the dimensional reduction procedure. The 5-dimensional theory may be generalised in a straightforward manner to models in higher dimensions which yield an effective 4-dimensional action with non-Abelian Yang-Mills fields when dimensionally reduced [58]–[62]. The D -dimensional spacetime is taken to be the product of \mathcal{M}^4 and a compact manifold \mathcal{B}^{D-4} , where \mathcal{B}^{D-4} admits the Killing vectors $\xi_1^a, \dots, \xi_{D-4}^a$ which generate the Lie algebra of the required Yang-Mills gauge group. In analogy to (1.34) the coordinate transformation

$$x^\mu \rightarrow \bar{x}^\mu(x), \quad y^a \rightarrow \bar{y}^a(y) + \theta^\alpha(x)\xi_\alpha^a, \quad (1.41)$$

induce the appropriate non-Abelian gauge transformations. (Here x^μ and y^a are physical and internal space coordinates respectively.) The dimensional reduction procedure may be further generalised to include supersymmetry [63]–[66].

In general, one must take care in applying the “Kaluza-Klein ansatz”. In particular, one must make sure that removal of the massive modes from the higher-dimensional field equations can be performed consistently, rather than naïvely setting the massive modes to zero in the higher-dimensional action and then deriving field equations from the dimensionally-reduced action. If one takes the second approach then it is possible that solutions of the truncated theory are not solutions of the full theory. The 5-dimensional theory is consistent (provided the scalar field σ is included) but one cannot be sure that there is a consistent truncation for an arbitrary Kaluza-Klein theory [67]. This is something which must be checked model by model, although certain criteria guarantee consistency in some cases [68].

Ideally one would like to have some sort of dynamical mechanism to explain how compactification took place: there should be some criterion such as a conserved energy-like quantity, with which different vacua of the theory could be graded. However, it would require quite a considerable extension of physical concepts to achieve this. As things stand, one cannot compare the magnitude of physical quantities calculated in one spacetime with those calculated in another [69]. For example, the definition of energy in general relativity depends on boundary conditions, which will differ for spacetimes

of different geometry.

1.3.3 Analysis of Higher Dimensional Black Holes

While the four dimensional Kerr-(A)dS solution is thermodynamically stable [70]–[72], and gravitational stability has been studied in ref [73], the thermodynamic and gravitational stability of higher dimensional Kerr–(A)dS black holes has yet to fully studied. We would like to know how the thermodynamic and gravitational stability of Kerr-(A)dS spacetimes varies with dimension. Specifically, we are very interested in modes of instability which are intrinsically higher dimensional in that they do not exist in four dimensional spacetimes. For example, four dimensional Kerr black holes can have one rotation parameter, but in higher dimensions they can have more. We investigate the thermodynamic and gravitational stability properties of these higher dimensional spacetimes in chapter 2.

1.4 Brane Worlds

Theorists have questioned whether there may be other possibilities for treating the extra dimensions of unified theories other than in the original Kaluza–Klein scenario, with the possibility of making testable predictions at energy scales lower than the Planck scale. For example, one possibility naturally arising in an M-theory context is that our universe is a 3-(mem)brane⁴, embedded in a higher 11-dimensional geometry.

Early attempts at describing the universe as a brane embedded in a higher dimensional geometry were not entirely successful [75]-[78]. Some of the problems encountered were the possibility of processes like electron–positron annihilation with no visible decay products at high energies, due to the high energy particles ability to penetrate into the extra dimensions [75], or the lack of a well-defined graviton zero mode that would produce an effective four dimensional Newtons law of gravity on the brane [78].

⁴A membrane, or “brane” [74] is a hypersurface embedded in a higher dimensional “bulk” space-time.

1.4.1 Large Extra (Compact) Dimensions

Interest in alternatives to the original Kaluza–Klein scenario took off when Arkani–Hamed, Dimopolous and Dvali (ADD) introduced the phenomenological idea ⁵ that there may be large compact extra dimensions [80]–[82] – potentially as large as 0.1mm. Since then these bounds have been improved, e.g. see [83]. In order to evade the Kaluza–Klein bound on electromagnetism, it was suggested that Standard Model particles were confined to a three–brane, while gravity was free to probe the extra dimensions. This picture is known as the “brane world” scenario; see [84] for a review.

Given that branes are an intrinsic feature of M-theory, studying brane worlds in the context of M-theory seems natural. In particular, there are a certain type of branes predicted by M-theory: Dirichlet–branes [85]. D–Branes have the interesting property that standard model gauge fields are confined to the brane, as those gauge fields are modelled as open strings whose ends must terminate on a D–brane. Gravity on the other hand is modelled as closed loops of string which are not confined to D–branes. D–branes and M–theory therefore provide a natural setting for the ADD brane world scenario.

The vast difference in energy between the electroweak and Planck scale is difficult to understand from the viewpoint of theoretical particle physics, and is called the hierarchy problem. The standard model of particle physics predicts a Higgs boson (which gives masses to the weak interaction gauge bosons) from electroweak symmetry breaking. The mass of the Higgs is expected to be near the electroweak symmetry breaking scale ~ 1 TeV at the 95% confidence level, given the non-observation of the Higgs and precision measurements of the top quark mass. Perturbation theory in the standard model suggests that the masses of scalar bosons should be of the order of the cutoff scale⁶ used when computing quantum corrections. The Planck scale, the scale at which gravitational interactions become non-negligible, has already been identified as an obvious potential cutoff scale. Unfortunately since the electroweak and Planck

⁵An almost identical scenario was proposed earlier by Antoniadis [79].

⁶The cutoff scale is the proposed energy scale which provides an upper bound for the validity of the standard model of particle physics. After this the standard model should be replaced by some more fundamental theory, for example, a model incorporating supersymmetry.

energy scales differ in magnitude by about 15 orders of magnitude, picking a Planck cutoff scale implies that the Higgs boson will have a mass comparable to the Planck scale, which is much in excess of experimental bounds. This is known as the *technical* hierarchy problem.

One resolution of the technical hierarchy problem is supersymmetry. While supersymmetry can solve the technical hierarchy problem, it does so by introducing a massive superpartner for each boson and fermion. The superpartners give quantum contributions to the mass of the Higgs boson which precisely cancel the contributions of their partners. Because these superpartners are not observed, supersymmetry is broken at some scale (the cutoff scale for the standard model of particle physics). Making that cutoff scale in the TeV range protects the Higgs mass (and other scalar bosons masses) from quantum corrections above TeV range.

An alternative resolution to the hierarchy problem is that the electroweak scale *is* the Planck scale. This can be accomplished by introducing extra dimensions and increasing the fundamental strength of gravity, thereby lowering the Planck scale to that of the electroweak scale. This idea is naturally accommodated within the brane world scenario, as can be seen by the following simple estimate. Ignoring the back reaction of the brane tension on the curvature of the embedding spacetime, the basic idea is to integrate out the extra dimensions in the D dimensional action, leaving an effective four dimensional theory with action,

$$S = \frac{1}{16\pi G_D} \int d^D X \sqrt{g_D} (\mathcal{R}_D), \quad (1.42)$$

$$= \frac{V_{D-4}}{16\pi G_D} \int d^4 \sqrt{g_4} (\mathcal{R}_4 + \mathcal{L}_m), \quad (1.43)$$

where $G_D = M_D^{2-D}$ and M_D is the “real” Planck mass. Therefore

$$\frac{V_{D-4}}{16\pi G_D} = \frac{1}{16\pi G_4}, \quad (1.44)$$

$$V_{D-4} M_D^{D-2} = M_4^2. \quad (1.45)$$

Taking a toroidal compactification where all the extra dimensions have the same radius, R , we find $V_{D-4} = (2\pi R)^{D-4}$. Therefore we can pick $M_4 = 10^{15} M_D$, and choose the number of extra dimensions to find the size of the extra dimensions. This is no different to the standard Kaluza–Klein scenario, except that now it has been posited

that standard model fields do not propagate in the extra dimensions, thereby leading to a modification of the calculations involved in determining the spectrum of Kaluza–Klein excitations.

The mechanical stability of a five dimensional electrostatic spherically symmetric spacetimes with one toroidally compactified dimension has been most thoroughly considered in [86], generalising and unifying a number of earlier works. It was found that black hole solutions are generically stable while regular solutions lead to a stability condition formulated in terms of an eigenvalue problem.

By introducing more interesting geometries, for example, warped bulk dimensions [87], one can obtain a finite volume for the bulk even if the extra dimensions are non-compact [88], leading to new and interesting behaviours for gravity at small scales. Equivalently, this gives new spectra for the Kaluza–Klein excitations of gravity in place of the standard Kaluza–Klein excitations. An exciting new possibility in the brane world scenario is that if extra dimensions exist, and the volume they enclose is sufficiently large, then due to the changes to the fundamental strength of the gravitational force on small scales, it will be possible to produce “Kaluza–Klein excitations” of the graviton in particle collider experiments and black holes whose radii are much smaller than the length scale of the extra dimensions [89]. It is hoped that the Large Hadron Collider, with TeV (Electroweak) scale events, will be able to probe such extra dimensions [90]. Additionally, if one were to observe non-conservation of energy, momentum, charge, etc in future collider events, a brane world scenario would be the natural explanation, as one would still be able to conserve these quantities in the bulk.

1.4.2 Warped extra dimensions

While one expects a brane to have a non-zero thickness, a huge amount of theoretical work has proceeded by considering distance scales much larger than that of the thickness of the brane and modelling the brane as a delta-function distribution. The two most important papers in this scenario were proposed by Randall and Sundrum; the Randall–Sundrum I [87] and Randall–Sundrum II [88] models. For an extensive reference list and review of the Randall–Sundrum models and further developments

see ref. [89]. The Randall–Sundrum I model introduces two branes with a warped AdS space in between which acts as a concrete example of the ADD scenario. It additionally takes into account the tension of the thin branes via the Israel–Lanczos–Sen junctions conditions, so that the model is gravitationally consistent in the bulk.

The brane we live on in the Randall–Sundrum I model is necessarily negative tension, in order to solve the hierarchy problem [89]. Negative tension branes are inherently unstable [91], a feature which is associated with the violation of particular energy conditions [92, 93]. As a consequence, six-dimensional brane world models have attracted interest as they are able to naturally incorporate positive tension branes [94]. In the Randall–Sundrum I model, a careful analysis of the effective gravitational equations on the negative tension brane shows that anti-gravitational general relativity is recovered in the low energy limit [95] and that it is the positive tension brane which recovers attractive gravity. Since the extra dimension is compact, one finds a discrete spectrum of Kaluza–Klein excitations. In order to recover four dimensional general relativity at low energies, a mechanism is required to stabilise the inter-brane distance, which corresponds to a scalar field degree of freedom known as the radion [89].

The Randall–Sundrum II model removes the second brane (by moving its position parameter in the extra dimension to infinity), leaving a single codimension–one brane with AdS warped space mirrored on either side. Remarkably, even though the extra dimension is now non-compact and hence the positive Kaluza–Klein mass spectrum is continuous on the half line, the model gives rise to Newton’s law of gravity with polynomial corrections on the brane [96]. Unfortunately, the bulk has an AdS Killing horizon on either side of the brane. This horizon tends to develop curvature singularities upon addition of perturbations, as has been found with black holes [97, 98] and gravitational waves [99, 100]. This raises questions about boundary conditions that may need to be imposed in the bulk and about their consequences on the brane. For example, in the higher-codimension brane world scenarios of [101, 102], the treatment of a bulk singularity affects the corrections to Newton’s law on the brane [103].

1.4.3 Hybrid Brane world Models

Louko and Wiltshire [104] proposed a hybrid brane world construction which combines elements of both the Kaluza–Klein and the Randall–Sundrum II models. The construction works in six dimensions or higher and includes a co-dimension one brane in addition to a regular Kaluza–Klein direction. Whereas the Randall–Sundrum II models bulk geometry is closed by an unstable anti–de Sitter horizon, in the Louko–Whiltshire model the geometry closes at bolts [105]: totally geodesic codimension two submanifolds at which a rotational Killing vector field vanishes. This provides a topological, singularity-free boundary condition for gravitational waves or any other perturbations one may wish to consider. Their model also reproduced Newton’s law of gravity on the brane, with exponential corrections. However, it did not lead to a solution of the hierarchy problem since due to parameter restrictions one could not keep the size of the Kaluza–Klein directions small while simultaneously making the bulk large enough to accommodate TeV scale gravity.

Brane worlds are most naturally framed within the context of M-theory or one of its low energy limits. Eleven dimensional supergravity is expected to be the low energy limit of 11–dimensional M-theory and 6–dimensional Salam-Sezgin supergravity is a low energy limit of 10–dimensional supergravity. As such, 6–dimensional Salam-Sezgin supergravity appears to provide a most reasonable framework in which to construct a 6–dimensional brane world model.

It would be desirable to construct a brane world scenario as some low energy limit of M-theory, in which the hierarchy problem is solved, general relativity/Newton’s law of gravity is recovered on the brane for large distance scales, and the entire brane world construction is stable to perturbations. In chapter 4 we present a generalisation of the Louko–Wiltshire model which appears to have these features.

1.5 Overview of Thesis

In chapter 2 we study the thermodynamic stability of Kerr–AdS black holes in five and higher dimensions. We also investigate the higher dimensional gravitational stability

of a background Kerr-(A)dS spacetime under metric perturbations.

In chapter 3 we take the method as outlined by Visser and Wiltshire and analyse the stability of gravastars that have a Schwarzschild-(anti)-de Sitter or Reissner–Nordström exterior. Given our current understanding, we pick these two types of exterior metrics as they are physically reasonable, spherically symmetric and static.

In chapter 4 we generalise the hybrid (Kaluza–Klein Randall–Sundrum) brane world model of Louko and Wiltshire to include a minimally coupled scalar field and an associated exponential potential as the low energy limit effective action for Salam–Sezgin six dimensional supergravity.

Chapter 2

Stability of Higher Dimensional Rotating (Kerr) AdS Black Holes

2.1 Higher Dimensional Black Holes and String-Theory

Recently, the study of black holes in a background anti-de Sitter (AdS) spacetime has been motivated from developments in string/M-theory, which naturally incorporate black holes as solitonic D-branes, or simply branes as the higher-dimensional progenitors of black holes. An intriguing example of this is the conjectured anti-de Sitter/conformal field theory (AdS/CFT) duality [106] between string theory on $AdS_5 \times S^5$ background and $\mathcal{N} = 2$ Super Yang-Mills theory in four dimensions. More formally, the conjectured AdS/CFT correspondence states that a string/M-theory on a manifold which can be decomposed into $AdS_d \times \mathcal{M}_{D-d}$ is mathematically equivalent to a conformal field theory (CFT) on the conformal boundary of AdS_d .

A particularly interesting application of the AdS/CFT conjecture is Witten's interpretation [107] of the Hawking-Page phase transition between thermal AdS and an AdS black hole [108] as the confinement-deconfinement phases of the dual gauge theory defined on the asymptotic boundaries of the AdS space. Much effort has been put into the weak AdS gravity regime, analyzing the implications of AdS black holes on dual (gauge) theories at non-zero temperature, using the conjectured AdS/CFT

correspondence. In this context, the most interesting black hole solutions are presumably the five dimensional Kerr-AdS solutions for a stationary black hole [71]. The thermodynamics of AdS quantum gravity has been extensively used to infer the thermodynamics of quantum field theory in the large N (or weak field) limits, with an AdS gravity dual, such as Schwarzschild-AdS [107], Kerr-Newman-AdS [109]–[112] and hyperbolic-AdS [113]–[115] black holes.

As noted in the introduction, the generalisation of the arbitrary dimensional Kerr solution [8] of Myers and Perry [47] to include a cosmological constant has only recently been given by Hawking *et al.* [71] and Gibbons *et al.* [116, 117]. There has also been recent interest in constructing the analogous charged rotating solutions in gauged supergravity in four, five and seven dimensions [119], and also on non-uniqueness [120] of those solutions in five and higher dimensions.

The layout of the chapter is as follows. We begin in section two by outlining the (anti)-de Sitter background metrics in d dimensions and their generalizations to Kerr-AdS solutions. In section three we pay special attention to the thermodynamic stability of Kerr-AdS black holes by studying the behavior of Hawking temperature, free energy and specific heat in various dimensions. In section four we study the gravitational stability of background Kerr-(A)dS metrics under linear tensor perturbations. Separability of Hamilton-Jacobi and Klein-Gordon equations in the Kerr (anti)-de Sitter backgrounds was discussed in [121], especially in the limit when all rotation parameters take the same value, see [122] for a discussion in five dimensions. An earlier work on separability of the Hamilton-Jacobi equation and quantum radiation from a five dimensional Kerr black hole with two rotation parameters, but in an asymptotically flat background, can be found in [123]. However, our analysis in section four is different. It corresponds not to a separability of the wave equations for a particle but rather to a separability of radial and angular wave equations under linear tensor perturbations of the metric.

2.2 AdS and Kerr-AdS metrics

One of the interesting features of the Kerr metric in (anti)-de Sitter spaces is that it can be written in the Kerr-Schild form, where the metric g_{ab} is given exactly by its linear approximation around the (anti)-de Sitter metric \tilde{g}_{ab} as follows [116, 121]:

$$ds^2 = g_{ab} dx^a dx^b = \tilde{g}_{ab} dx^a dx^b + \frac{2m}{U} (k_a dx^a)^2, \quad (2.1)$$

where k_a is a null geodesic with respect to both the full metric g_{ab} and the (A)dS metric \tilde{g}_{ab} . Moreover, the Ricci tensor of g_{ab} is related to that of \tilde{g}_{ab} by

$$R_a{}^b = \tilde{R}_a{}^b - \tilde{R}_a{}^c h_c{}^b + \frac{1}{2} \left(\tilde{\nabla}_c \tilde{\nabla}_a h^{bc} + \tilde{\nabla}^c \tilde{\nabla}^b h_{ac} - \tilde{\nabla}^c \tilde{\nabla}_c h_a{}^b \right), \quad (2.2)$$

where $h_{ab} = \frac{2m}{U} k_a k_b$, with m and U being the parameters proportional to the mass and gravitational potential of a Kerr black hole respectively.

The generalized d -dimensional (anti)-de Sitter metric can be written in a very compact form:

$$\tilde{ds}^2 = -(1 + cy^2) dt^2 + \frac{dy^2}{1 + cy^2} + y^2 \sum_{k=1}^{N+\varepsilon} \left(d\hat{\mu}_k^2 + \hat{\mu}_k^2 d\hat{\phi}_k^2 \right) \quad (2.3)$$

satisfying

$$\sum_{i=1}^{N+\varepsilon} \hat{\mu}_i^2 = 1, \quad (2.4)$$

where $d = 2N + \varepsilon + 1 \geq 4$, $\varepsilon = 0$ when d is even or $\varepsilon = 1$ when d is odd. There are N azimuthal angles ϕ_i each with period 2π associated with N orthogonal 2-planes and $N + \varepsilon$ directional cosines μ_i where $0 \leq \mu_i \leq 1$ for $1 \leq i \leq N$ and (for even d) $-1 \leq \mu_{N+1} \leq 1$, associated with $N + \varepsilon$ spatial dimensions.

Here we provide parameterisations of n -spheres (with line-element $d\Omega_n^2$) for $n = 2, 3$:

- $d=4$: d is even so $\varepsilon = 1$. $\mu_1 = \sin \theta$, $\mu_2 = \cos \theta$, $0 \leq \theta \leq \pi$, while $\phi_1 = \phi$, $0 \leq \phi \leq 2\pi$. Then

$$\sum_{i=1}^{1+1} d\mu_i^2 + \mu_i^2 d\phi_i^2 = \cos^2 \theta d\theta^2 + \sin^2 \theta d\phi^2 + \sin^2 \theta d\theta^2 \quad (2.5)$$

$$= \underbrace{\frac{1}{2}S^1}_{\frac{1}{2}S^1 \ltimes S^1} \underbrace{\sin^2 \theta d\phi_1^2}_{S^1} \quad (2.6)$$

$$= \underbrace{d\Omega_2^2}_{S^2} \quad (2.7)$$

- d=5: d is even so $\varepsilon = 0$. $\mu_1 = \sin \theta$, $\mu_2 = \cos \theta$, $0 \leq \theta \leq \pi/2$, while $\phi_1 = \phi_1$, $\phi_2 = \phi_2$, $0 \leq \phi_1 \leq 2\pi$, $0 \leq \phi_2 \leq 2\pi$. Then

$$\sum_{i=1}^2 d\mu_i^2 + \mu_i^2 d\phi_i^2 = \cos^2 \theta d\theta^2 + \sin^2 \theta d\phi_1^2 + \sin^2 \theta d\theta^2 + \cos^2 \theta d\phi_2^2 \quad (2.8)$$

$$= \underbrace{\frac{1}{2}S^2}_{\frac{1}{2}S^2 \ltimes S^1} \underbrace{\cos^2 \theta d\phi_2^2}_{S^1} \quad (2.9)$$

$$= \underbrace{d\Omega_3^2}_{S^3} \quad (2.10)$$

In AdS_d spaces the rotation group is $SO(d-1)$ and the number of independent rotation parameters for a localized object is equal to the number of Casimir operators, which is the integer part of $(d-1)/2$. Thus in four dimensions the metric of a Kerr black hole can have only one Casimir invariant of the rotation group $SO(3)$, which is uniquely defined by an axis of rotation, while in five dimensions it can have two independent rotation parameters associated with two possible planes of rotation.

One may introduce to (2.3) N rotation parameters, for example, by using the following coordinate transformation:

$$y^2 = \sum_{i=1}^N \frac{(r^2 + a_i^2)\mu_i^2}{1 - ca_i^2}, \quad (2.11)$$

where $\sum_{i=1}^{N+\varepsilon} \mu_i^2 = 1$. The constants a_i which are introduced in (2.11) merely as parameters in a coordinate transformation may be interpreted as genuine rotation parameters after one adds to (2.3) the square of an appropriate null vector, as in (2.1).

Using the following coordinate transformations [71],

$$\begin{aligned} dt &= d\tau + \frac{2m}{V-2m} \frac{dr}{(1+cr^2)}, \\ d\hat{\phi}_i &= d\phi_i + ca_i d\tau + \frac{2m}{V-2m} \frac{a_i dr}{(r^2 + a_i^2)}, \end{aligned} \quad (2.12)$$

and combining the expressions (2.1), (2.3), (2.11), one can obtain the Kerr (A)dS metrics in Boyer-Lindquist coordinates. We will not go into details of this construction but refer the reader to Ref. [116] for an elegant discussion. In five dimensions, the metric of Kerr-AdS solution is

$$ds^2 = -W(1+cr^2)d\tau^2 + \frac{\rho^2 dr^2}{V-2m} + \frac{\rho^2}{\Delta_\theta} d\theta^2 + \sum_{i=1}^2 \frac{r^2 + a_i^2}{1-ca_i^2} \mu_i^2 (d\phi_i + ca_i d\tau)^2 + \frac{2m}{\rho^2} \left(d\tau - \sum_{i=1}^2 \frac{a_i \mu_i^2 d\phi_i}{1-ca_i^2} \right)^2, \quad (2.13)$$

where $\mu_1 = \cos \theta$, $\mu_2 = \sin \theta$,

$$\begin{aligned} \rho^2 &= r^2 + a_1^2 \cos^2 \theta + a_2^2 \sin^2 \theta, \\ \Delta_\theta &= 1 - ca_1^2 \cos^2 \theta - ca_2^2 \sin^2 \theta, \\ V &= \frac{1}{r^2} (1+cr^2)(r^2+a_1^2)(r^2+a_2^2), \\ W &= \frac{\Delta_\theta}{\Xi_1 \Xi_2}, \quad \Xi_i = 1 - ca_i^2. \end{aligned} \quad (2.14)$$

In the limit $a_i \rightarrow 0$, one recovers the standard Schwarzschild-AdS metric. As we will see shortly, black holes with non-zero rotation parameters, or, in general, Kerr-AdS black holes, enjoy many interesting properties distinct from Schwarzschild-AdS black holes.

2.3 Thermodynamics of Kerr AdS Solutions

Using the standard technique of background subtraction, Gibbons *et al.* [118] have recently calculated the regularized (Euclidean) actions for the Kerr-AdS black holes in arbitrary d (≥ 4) dimensions. The results are

$$\hat{I} = -\frac{\mathcal{A}_{d-2}}{8\pi G \prod_j \Xi_j} \frac{\beta}{l^2} \left(l^{2N} \prod_{i=1}^N (R^2 + \alpha_i^2) - ml^2 \right) \quad (2.15)$$

for odd d ($= 2N + 1$), and

$$\hat{I} = -\frac{\mathcal{A}_{d-2}}{8\pi G \prod_j \Xi_j} \frac{\beta}{l} \left(R l^{2N} \prod_{i=1}^N (R^2 + \alpha_i^2) - ml \right) \quad (2.16)$$

for even d ($= 2N + 2$), where

$$\mathcal{A}_{d-2} = \frac{2\pi^{(d-1)/2}}{\Gamma[(d-1)/2]}, \quad (2.17)$$

is the volume of the unit $(d-2)$ -sphere. In the above we have defined $c \equiv 1/l^2$, with l being the curvature radius of the (bulk) AdS space. The dimensionless parameters are: $\Xi_j \equiv 1 - \alpha_j^2$, $R \equiv r_+/l$ and $\alpha_i \equiv a_i/l$, where, as usual, r_+ is the radius of the horizon, which occurs at the largest root of $V - 2m = 0$. The Hawking temperature, which is the inverse of Euclidean period, $T \equiv 1/\beta$, is given by

$$T = \frac{R}{2\pi l} \left[(1 + R^2) \left(\sum_{i=1}^N \frac{1}{R^2 + \alpha_i^2} + \frac{\varepsilon}{2R^2} \right) - \frac{1}{R^2} \right], \quad (2.18)$$

where $\varepsilon = 0$ for odd d and $+1$ for even d .

The calculation of total energy in an asymptotically (A)dS background is somewhat trickier (see e.g. [118]), mainly because the analogous Komar integral for the relevant time-like Killing vector diverges, which then requires a regularization; see also Ref. [124], which presents a general analysis for the conserved charges and the first law of thermodynamics for the four dimensional Kerr-Newman-AdS and the five dimensional Kerr-AdS black holes. In this context, the conserved charges (energies) E and E' associated with different Killing vectors, respectively, ∂_t and $\partial_t + l^{-1}\alpha_i\partial_{\phi_i}$ are different. However, the calculation of free energy itself is unambiguous. In fact, one can always identify the free energy of a Kerr-AdS black hole as $F = \hat{I}/\beta$, and hence

$$F = \frac{\mathcal{A}_{d-2}}{16\pi G} (lR)^{d-3} (1 - R^2) \prod_j \Xi_j \prod_{i=1}^N \left(1 + \frac{\alpha_i^2}{R^2} \right). \quad (2.19)$$

This result is modified from that of a Schwarzschild-AdS black hole by certain terms in the product which are now functions of R and the rotation parameters α_i .

2.3.1 Thermal Phase Transition

Five dimensions

The issue of thermodynamic stability of four dimensional solutions has been well studied. However, the issue of thermodynamic stability may be raised in five and higher dimensions. The five-dimensional Kerr-AdS solutions are particularly interesting as these could be embedded into type IIB supergravity in ten dimensions.

From (2.19), it is readily seen that for $R < 1$ the free energy, F , of the background subtracted Kerr-AdS black hole is greater than zero, $F > 0$, while for $R > 1$, $F < 0$. In

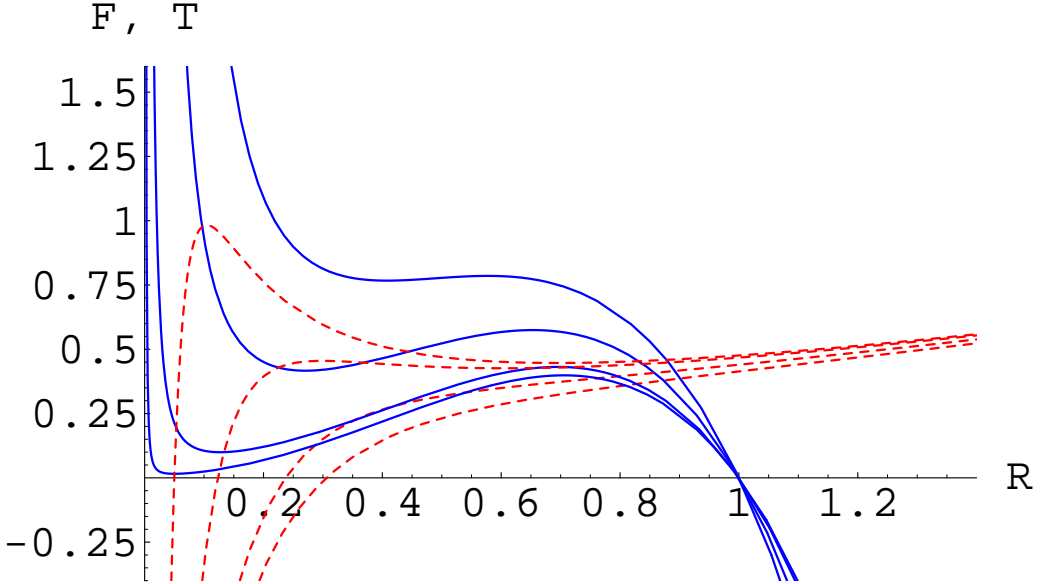


Figure 2.1: ($d = 5$) The free energy (solid lines) and temperature (dashed lines) as a function of horizon position, with $\alpha_1 = \alpha_2 \equiv \alpha$. From top to bottom (free energy) or bottom to top (temperature): $\alpha = 1/3, 0.25, 1/8, 0.05$. In all plots we have set $4G = 1$.

general, when the values of the rotation parameters α_i are decreased, the free energy lowers towards zero at low temperature. For $0 < \alpha \ll 1$, in the small R region, F nearly approaches but never touches the $F = 0$ axis (see Figs. 2.1 and 2.2). That is, the free energy curve crosses the $F = 0$ axis only once, namely when $R = 1$.

In five dimensions, with $\alpha_1 = \alpha_2 \equiv \alpha > 0$, for each non-zero α there is a minimum R below which the temperature is negative and diverges to negative infinity as $R \rightarrow 0$ (see Fig. 2.1). This should be contrasted with (small) Schwarzschild–AdS black holes in five dimensions, whose temperature diverges to positive infinity as $R \rightarrow 0$ which signals a thermodynamic instability. In fact when $T = 0$ a Kerr–AdS black hole simply ceases to radiate and as such is unable to attain a smaller horizon radius so the limit of $R \rightarrow 0$ is physically irrelevant. The minimum radius associated with this freezing can be read off Fig. 2.1 for a variety of angular momenta. Since the temperature decreases as the black hole becomes smaller, it can in principle come into thermal equilibrium with any surrounding thermal radiation. Hence there is a qualitative difference between the thermodynamic behaviours of Schwarzschild–AdS and Kerr–AdS as $R \rightarrow 0$. One can

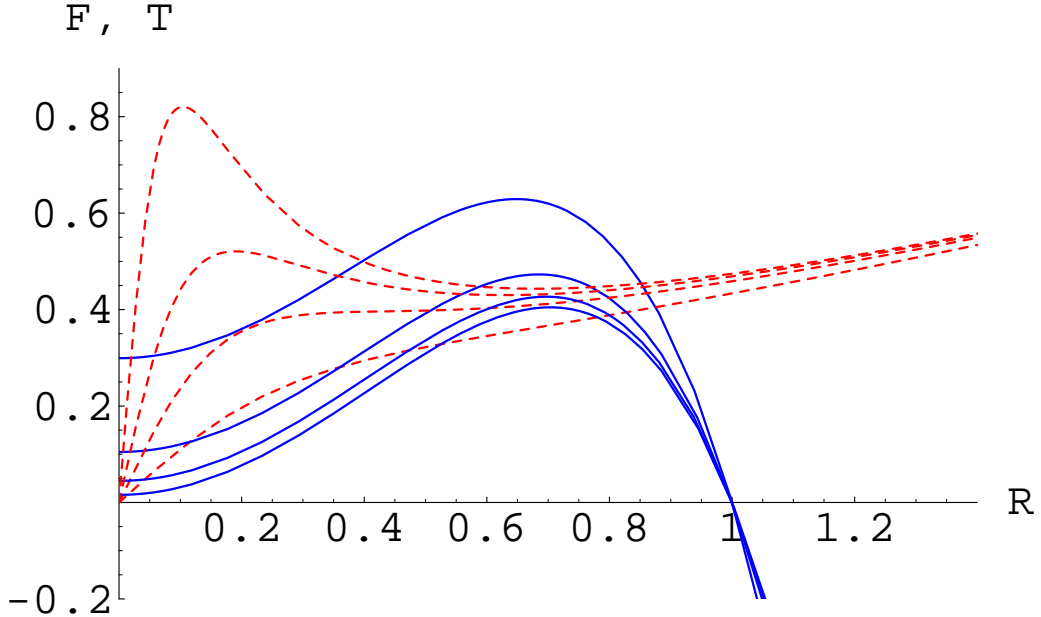


Figure 2.2: ($d = 5$) The free energy (solid lines) and temperature (dashed lines) vs horizon position, with $\alpha_1 \equiv \alpha$, $\alpha_2 = 0$. From top to bottom (free energy) or bottom to top (temperature): $\alpha = 0.4, 0.25, 1/6, 0.1$.

see that as $\alpha \rightarrow 0$ the Kerr–AdS case approximates the Schwarzschild–AdS case for non–zero R , but in the limit $R \rightarrow 0$ there is no smooth transition between the two behaviours. This is possibly not an issue, as quantum effects may become significant at such small scales and hence due to the discrete nature of the emitted and absorbed quanta a smooth transition might not be physically plausible. Additionally, our exterior vacuum approximation almost certainly breaks down.

We note that the limit of $R \rightarrow 0$ is equivalent to fixing r_+ and sending $l \rightarrow \infty$. This corresponds to reducing the cosmological constant, where the limit $R = 0$ corresponds to zero cosmological constant, i.e. we are left with a Myers–Perry higher dimensional Kerr black hole.

In Fig. 2.3 we show parametric plots of F vs T for $T > 0$. This means that the limit $R \rightarrow 0$ is not shown. However, as can be seen in Fig. 2.1 the physically irrelevant region in Fig. 2.3 would be characterised by $F \rightarrow \infty$, $T \rightarrow -\infty$. We also note that the specific heat is a monotonically increasing function of temperature when $\alpha \geq 0.15$, i.e., five dimensional Kerr–AdS black holes which rotate sufficiently fast with equal rotation

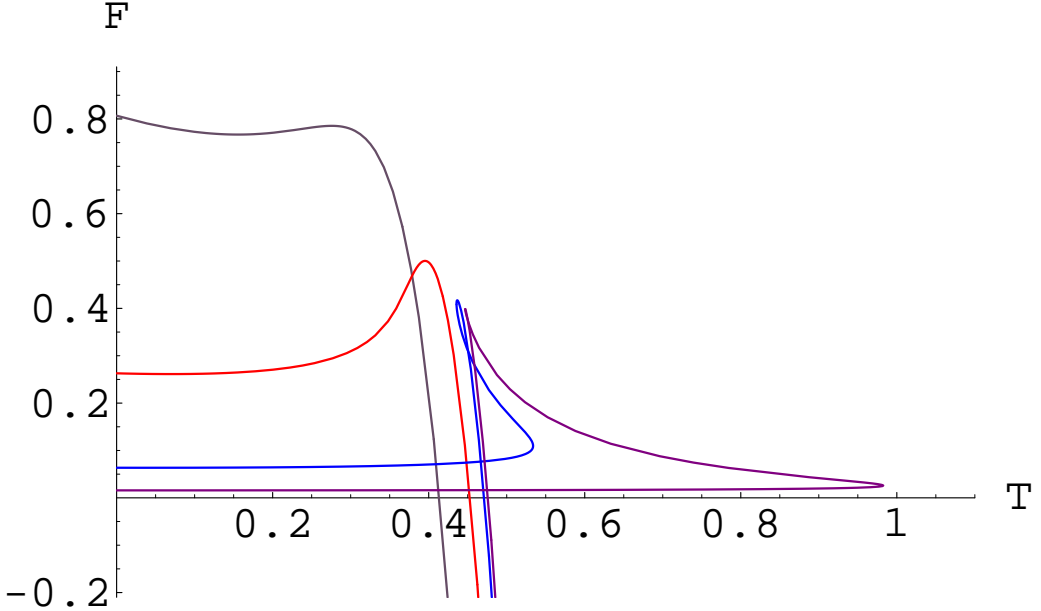


Figure 2.3: ($d = 5$) The free energy, $F(R)$, vs temperature, $T(R)$, with $\alpha_1 = \alpha_2 \equiv \alpha$ plotted parametrically as functions of R with fixed α . From top to bottom: $\alpha = 1/3, 0.2, 0.1, 0.05$. For all α , $F(1) = 0$ as in Fig. 2.1.

parameters are thermodynamically stable at all horizon radii.

The Hawking temperature of a Kerr-AdS black hole with one non-vanishing rotation parameter approaches zero as R goes to zero. The free energy is still a smooth relation of both the horizon size and the temperature (see Figs. 2.2 and 2.4). These imply thermodynamic stability for a small Kerr black hole which conserves its angular momentum in AdS_5 space with either one non-zero or two equal rotation parameters.

It should also be noted that while the behaviour of the temperature and free energy as functions of R appear qualitatively quite different between the one non-zero and two equal rotation parameter cases, when F and T are plotted parametrically against each other the qualitative behaviours of the two cases are identical and as such the different cases should not be thought of as having radically different thermodynamic behaviour.

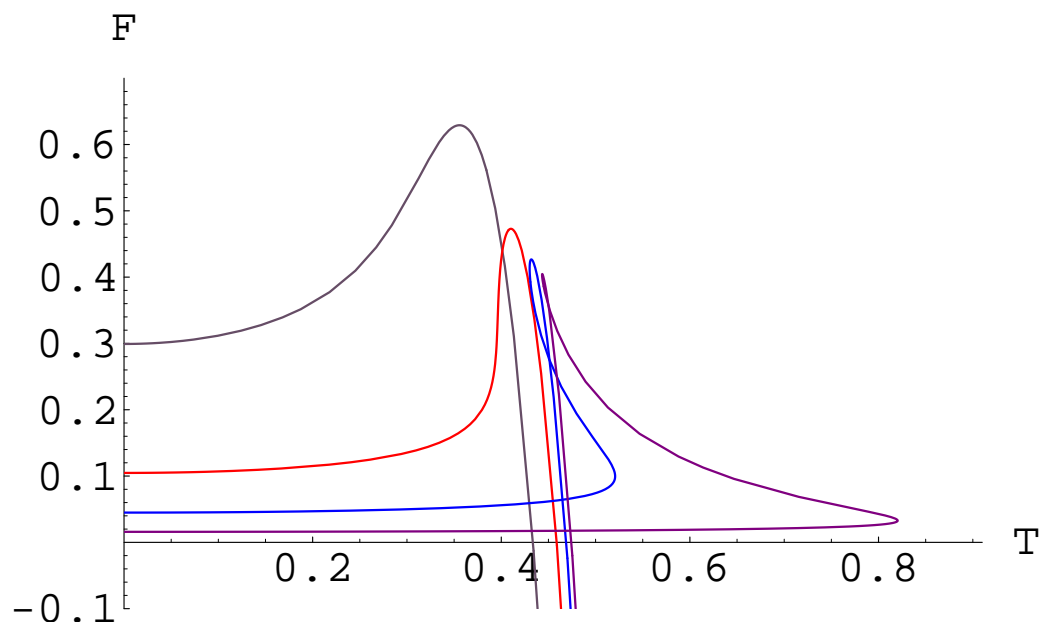


Figure 2.4: ($d = 5$) The free energy vs temperature plotted parametrically as functions of R with $\alpha_1 \equiv \alpha$, $\alpha_2 = 0$. From top to bottom: $\alpha = 0.4, 0.25, 1/6, 0.1$

Six dimensions

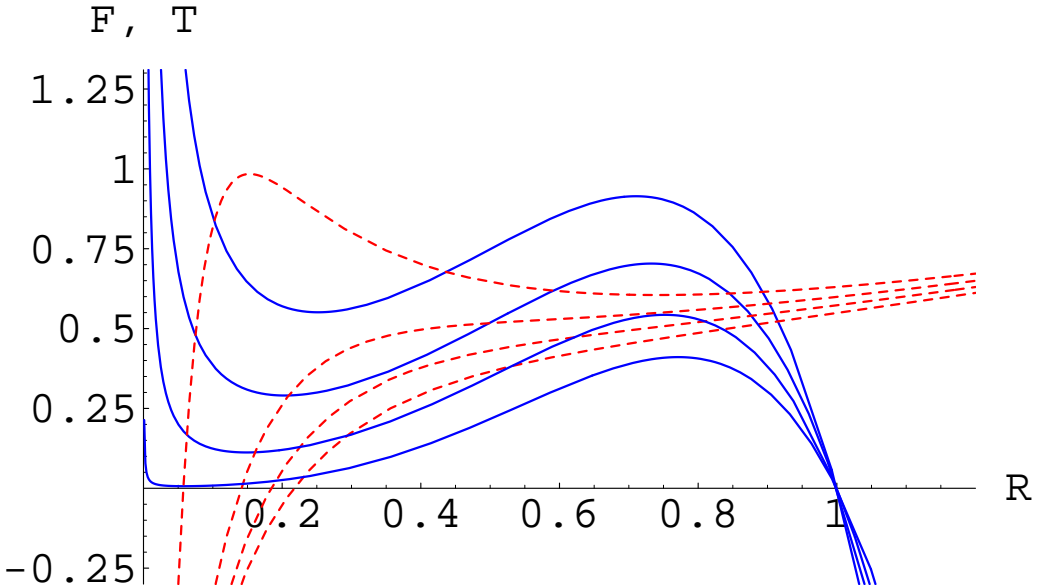


Figure 2.5: ($d = 6$) The free energy and temperature vs horizon position, with $\alpha_1 = \alpha_2 = \alpha$. From top to bottom: $\alpha = 0.4, 1/3, 0.25, 0.1$.

The thermodynamic behavior found in six–dimensions is similar to that in five dimensions in the case of two equal rotation parameters as can be seen by comparing Fig. 2.1 and Fig. 2.5.

As the plots in Figs. 2.5–2.8 show the thermodynamics of single parameter solutions are quite different from those with equal rotation parameters. Not only do the free energy and temperature as functions of R behave differently, but when F and T are plotted parametrically against each other, the case of one non–zero rotation parameter behaves quite differently to that of two equal rotation parameters.

We see that the equal rotation parameter case leaves small stable Kerr–AdS black holes, while the case with one non–zero rotation parameter behaves similarly to the Schwarzschild–AdS case, in that if the black hole has a radius smaller than l it is thermodynamically unstable, and according to this analysis will completely evaporate leaving an equilibrium solution of thermal–anti de–Sitter space.

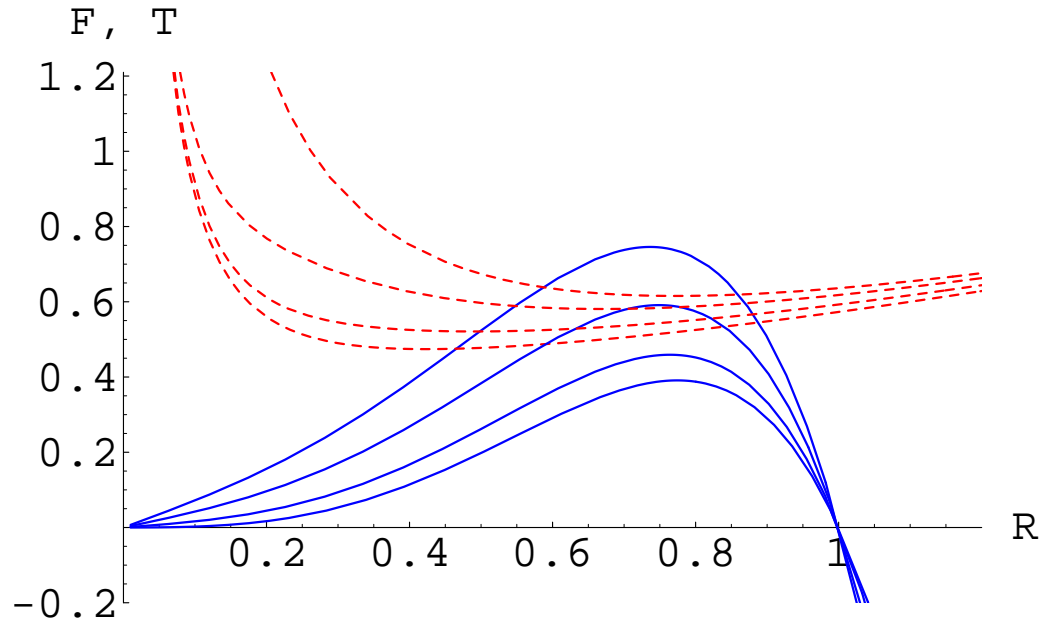


Figure 2.6: ($d = 6$) The free energy and temperature vs horizon position, with $\alpha_1 \equiv \alpha$, $\alpha_2 = 0$. From top to bottom: $\alpha = 0.5, 0.4, 0.25, 0.04$.

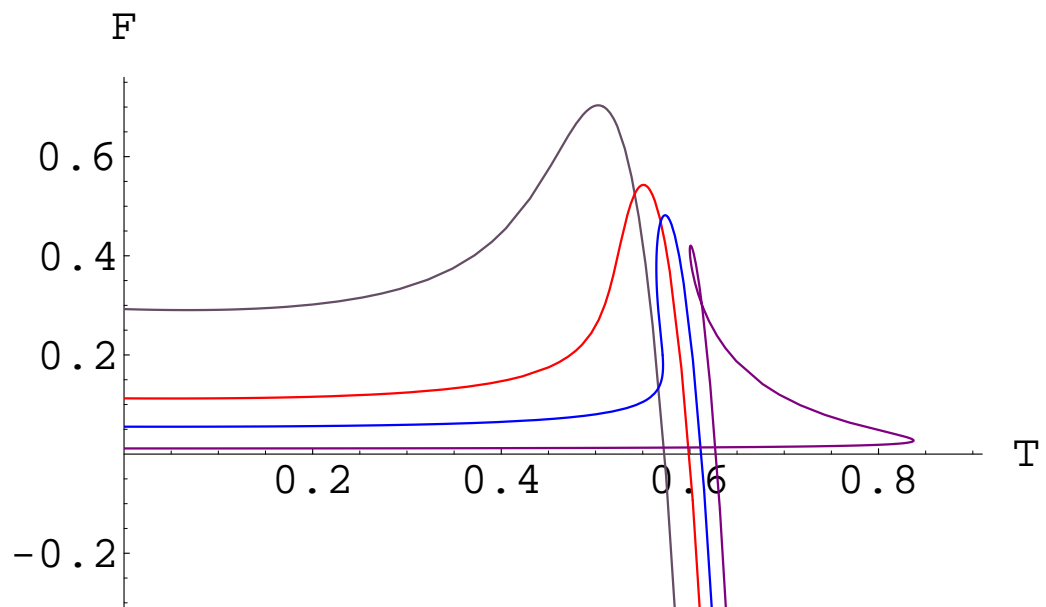


Figure 2.7: ($d = 6$) The free energy vs temperature plotted parametrically as functions of R with $\alpha_1 = \alpha_2 \equiv \alpha$. From top to bottom: $\alpha = 1/3, 0.25, 0.2, 0.12$.

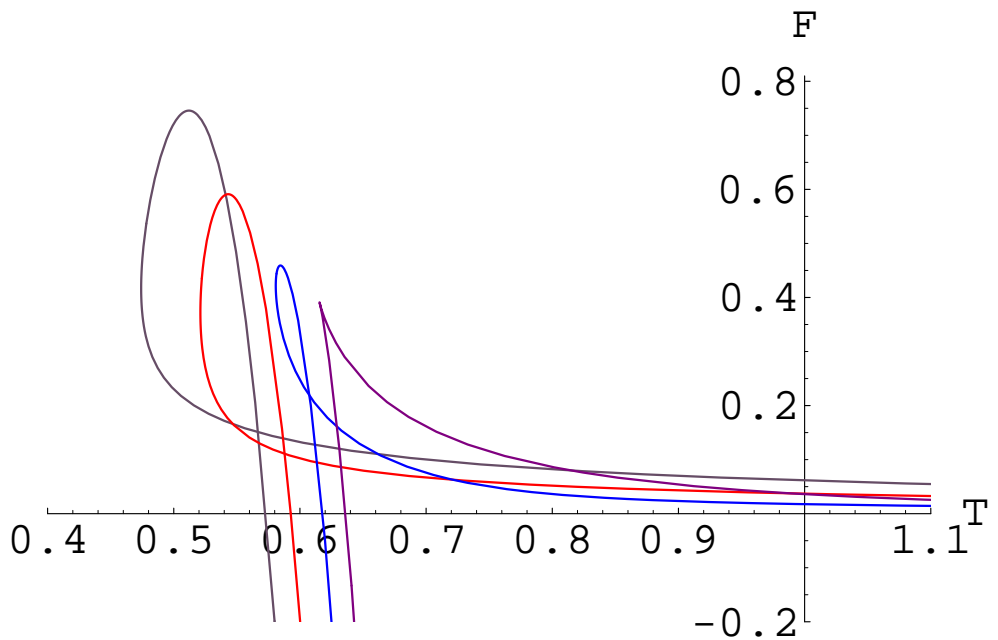


Figure 2.8: ($d = 6$) The free energy vs temperature plotted parametrically as functions of R with $\alpha_1 = \alpha$, $\alpha_2 = 0$. From left to right: $\alpha = 0.5, 0.35, 0.2, 0.05$

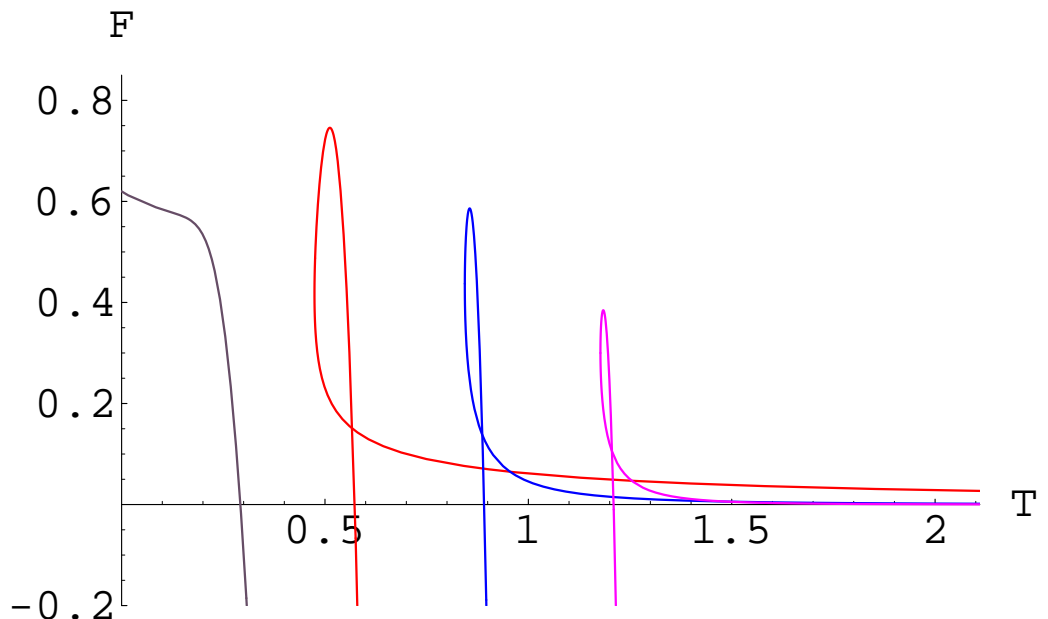


Figure 2.9: The free energy vs temperature with a single non-vanishing rotation parameter α . From left to right $d = 4$ (with $\alpha = 0.3$) and $d = 6, 8, 10$ (with $\alpha = 0.5$).

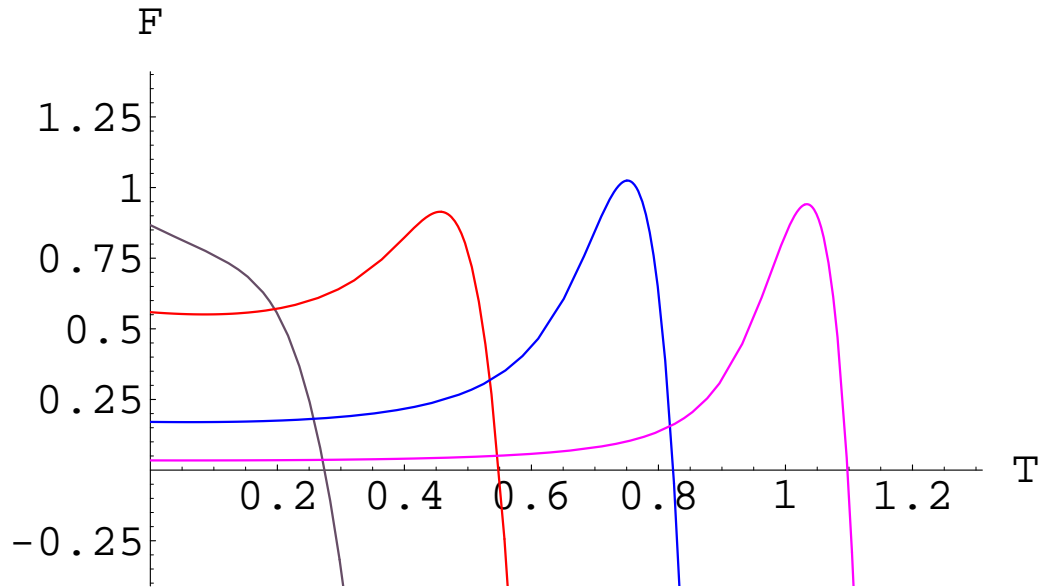


Figure 2.10: The free energy vs temperature with equal rotation parameters, $\alpha_i = \alpha = 0.4$. From left to right $d = 6, 8, 10$. Note that on the far left $d = 4$ has been displayed for comparison purposes, even though it has only one rotation parameter.

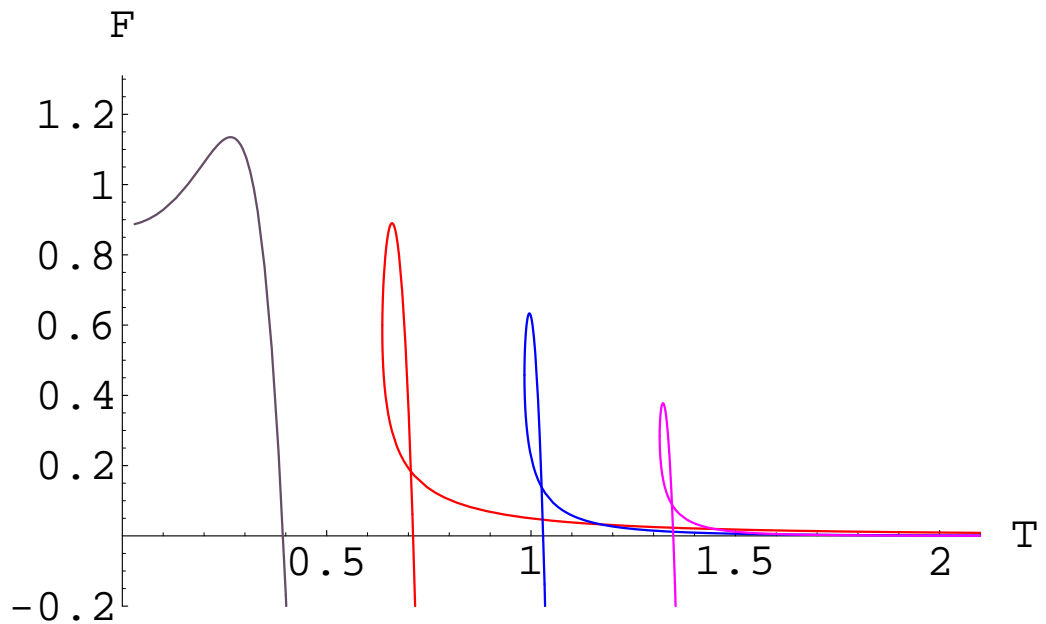


Figure 2.11: The free energy vs temperature plotted parametrically as functions of R with a single non-vanishing rotation parameter α . From left to right: $d = 5, 7, 9, 11$ (with $\alpha = 0.6$).

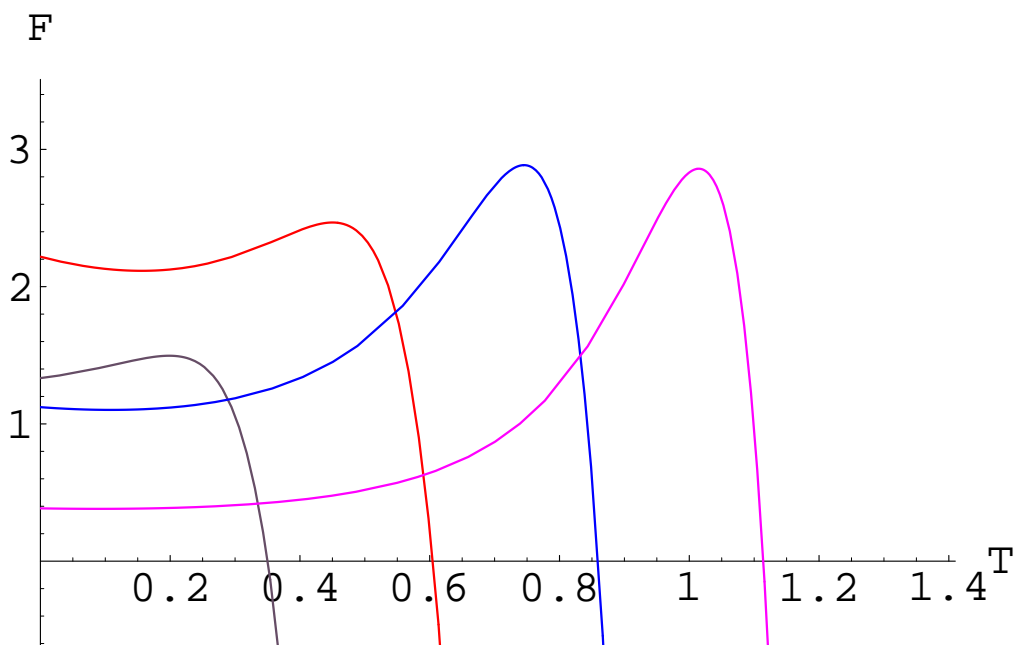


Figure 2.12: The free energy vs temperature plotted parametrically as functions of R with equal rotation parameters, $\alpha_i = \alpha = 0.5$. From left to right $d = 5, 7, 9, 11$.

2.3.2 The first law of AdS bulk thermodynamics

One of the simplest ways of calculating the energy in an asymptotically AdS background is to integrate the first law of (bulk) thermodynamics:

$$dE = T dS + \sum_i \Omega_i J^i. \quad (2.20)$$

where the entropy S and angular momenta (of a rotating black hole) J_i are defined via

$$S = \beta \frac{\partial \hat{I}}{\partial \beta} - \hat{I}, \quad J^i = -\frac{\partial F}{\partial \Omega_i}, \quad (2.21)$$

where

$$\Omega_i \equiv \frac{\alpha_i(1+R^2)l}{R^2 + \alpha_i^2}. \quad (2.22)$$

In Ref. [118], the mass (energy) of Kerr AdS black hole was evaluated, by demanding *as a priori* that entropy of the black hole is one-quarter the area, $S = A/4$, in order to satisfy (2.20). The results are, for $d = 2N + 1 \geq 5$,

$$\begin{aligned} E &= \frac{m\mathcal{A}_{d-2}}{4\pi \prod_j \Xi_j} \left(\sum_{i=1}^N \frac{1}{\Xi_i} - \frac{1}{2} \right), \\ S &= \frac{\mathcal{A}_{d-2}}{4} (l R)^{2N-1} \prod_{i=1}^N \left(1 + \frac{\alpha_i^2}{R^2} \right) \frac{1}{\Xi_i}, \end{aligned} \quad (2.23)$$

and for $d = 2N + 2 \geq 4$,

$$\begin{aligned} E &= \frac{m\mathcal{A}_{d-2}}{4\pi \prod_j \Xi_j} \sum_{i=1}^N \frac{1}{\Xi_i}, \\ S &= \frac{\mathcal{A}_{d-2}}{4} (l R)^{2N} \prod_{i=1}^N \left(1 + \frac{\alpha_i^2}{R^2} \right) \frac{1}{\Xi_i}. \end{aligned} \quad (2.24)$$

This result differs from the expression of energy suggested by Hawking *et al.* in [71], both in odd and even dimensions,

$$E' = \frac{m\mathcal{A}_{d-2}}{4\pi \prod_{j=1}^N \Xi_j} \frac{(d-2)}{2}. \quad (2.25)$$

The reason for this is that the energy (2.25) is measured in a frame rotating at infinity with the angular velocities:

$$\Omega'_i = \frac{\alpha_i \Xi_i l}{R^2 + \alpha_i^2}, \quad (2.26)$$

instead of (2.22). Since the angular velocities differ by $\Omega_i - \Omega'_i = \alpha_i l$, the two results above, (2.23) or (2.24), (2.25), agree only in the limit $\alpha_i \rightarrow 0$ (i.e. $\Sigma_i \rightarrow 1$).

It should be noted that in the limit of $r_+ \rightarrow 0$, $E \rightarrow 0$. This is expected, as the infinite energy due to the non-zero value of the cosmological constant has been subtracted out in the background subtraction procedure.

2.3.3 The specific heat and thermodynamic stability

A black hole as a thermodynamic system is semiclassically unstable if it has negative specific heat. As is known, small Schwarzschild-AdS black holes (i.e. with $a_i = 0$) have negative specific heat but large black holes have positive specific heat. There also exists a discontinuity of the specific heat as a function of temperature at $R = 1/\sqrt{2}$, and so small and large black holes are found to have different thermodynamic behaviour. However, this is not the case when some of the a_i are non-trivial. For example, we shall find that a small Kerr black hole in AdS_5 space has positive specific heat if its horizon radius is sufficiently small with respect to the AdS length scale l .

Five dimensions

We shall study the thermodynamic stability of a Kerr-AdS black hole by evaluating its specific heat, which is given by

$$C_v = \frac{\partial E}{\partial T}. \quad (2.27)$$

Figures 2.13 and 2.14 show the plots of energy and temperature differentials as functions of the horizon size R with fixed angular momenta. In the case of one non-zero rotation parameter, Fig. 2.13, $dT = 0$ can have two roots for $\alpha < 1/\sqrt{17}$, a repeated root at $\alpha = 1/\sqrt{17}$ and no roots for $\alpha > 1/\sqrt{17}$. The roots are exactly given by

$$R_{\pm} = \frac{\sqrt{1 - 5a^2 \pm \sqrt{17a^4 - 18a^2 + 1}}}{2} \quad (2.28)$$

and the repeated root occurs at $R = \sqrt{3/17} \approx 0.42$. As $dE > 0$ for all α in the one non-zero rotation parameter case, $dE/dT < 0$ between the roots in R which means that the specific heat is negative there and the Kerr-AdS black hole will be locally thermodynamically unstable. It becomes stable again if it can radiate while conserving

dE, dT

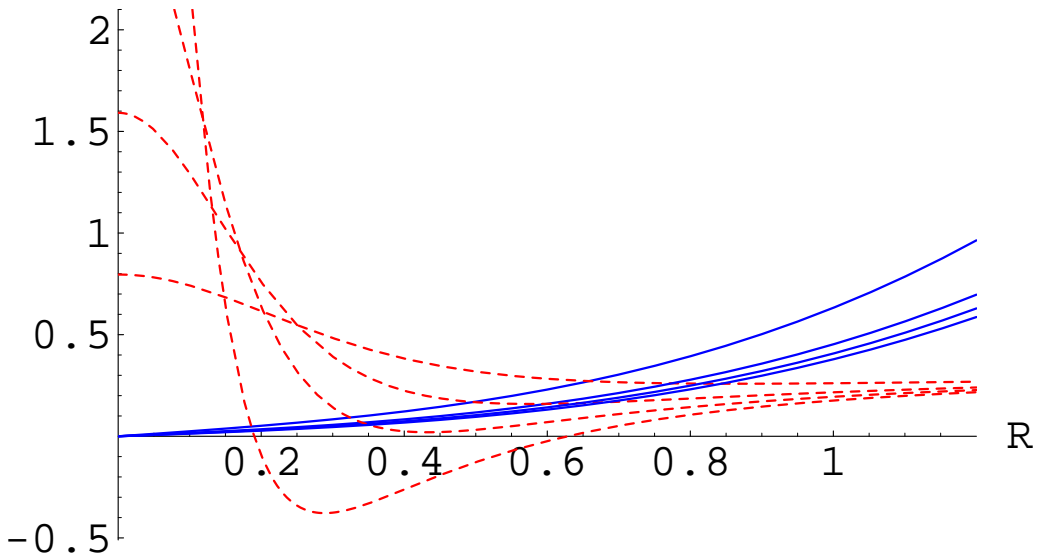


Figure 2.13: ($d = 5$) The energy and temperature differentials w.r.t. R vs horizon position, with $\alpha_1 = \alpha$, $\alpha_2 = 0$. As $R \rightarrow 0$, $dE \rightarrow 0$ and $dT > 0$. From top to bottom (free energy) or bottom to top (temperature) $\alpha = 0.5, 1/3, 0.25, 1/6$. It is possible for there to exist an interval of R where $dT < 0$ for values of $\alpha < 1/\sqrt{17}$.

angular momentum, thereby dropping its horizon radius enough to gain a positive specific heat, which would eventually allow it to come into thermal equilibrium with the surrounding thermal radiation. However, it is well known that Kerr black holes can shed angular momentum while radiating. As such it is plausible that the black hole will transfer its angular momentum into its radiation, thereby remaining unstable long enough to eventually become Schwarzschild–AdS and hence evaporate completely. However, it is also plausible that the black hole can be “spun up” by absorbing radiation with angular momentum, potentially not only coming into thermal equilibrium, but also coming into “rotational equilibrium” with the surrounding radiation, making it semiclassically stable. Further detailed work on the exact evolution of such black holes in thermal equilibrium with a surrounding radiation fluid would be required to settle this issue definitively and remains outside the scope of the current work.

As seen in Fig. 2.14, the case of equal rotation parameters in five dimensions $dT = 0$ has two roots for $\alpha \lesssim 0.15$, a repeated root for $\alpha \approx 0.15$, at $R \approx 0.4$, and no roots

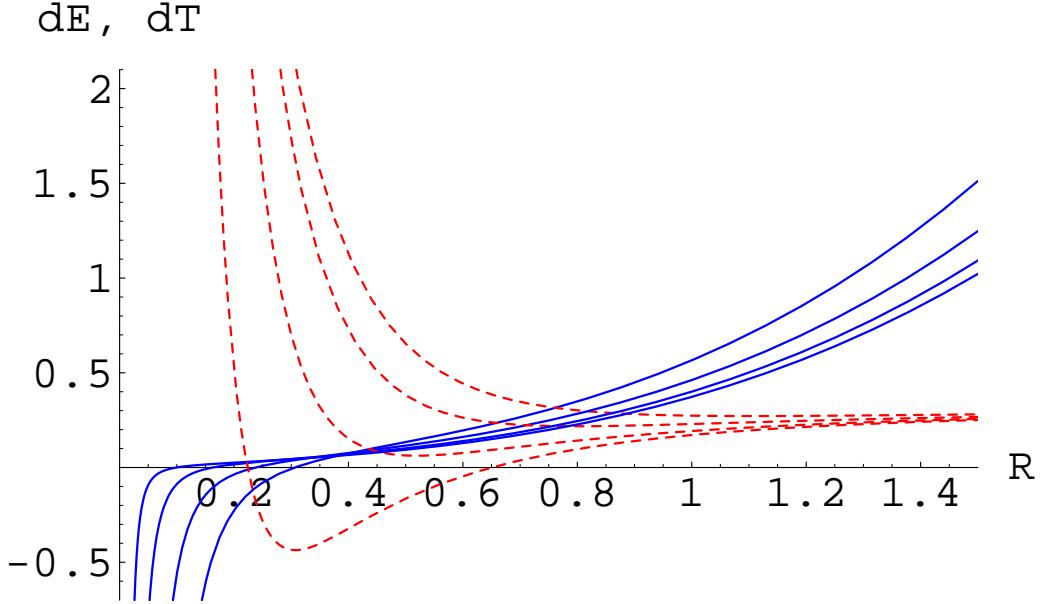


Figure 2.14: ($d = 5$) The energy and temperature differentials vs horizon position, with $\alpha_1 = \alpha_2 \equiv \alpha$. As $R \rightarrow 0$, $dE \rightarrow +\infty$ and $dT \rightarrow -\infty$. From left to right: $\alpha = 0.1, 1/6, 0.25, 1/3$.

for $\alpha \gtrsim 0.15$. However, in this case dE becomes negative for sufficiently small R and as such the specific heat becomes negative, implying a thermodynamic instability. However, it should be noted that this limit cannot be reached by an evaporating black hole as the temperature also heads towards zero, in a positive specific heat region of R . That is, the end point of gravitational evaporation in this scenario is a black hole with zero specific heat and zero temperature of finite size – before this occurs the black hole will come into thermal equilibrium with its surrounding radiation, subject to the assumption of it conserving its angular momenta.

Once again, it is potentially plausible that the black hole can shed its angular momenta, but in doing so it will always have a positive specific heat. It might be subject to an instability in the form of eventually approximating Schwarzschild–AdS. It is also entirely plausible that this black hole can lose its angular momentum during the evaporation phase in such a way that it becomes well approximated by the single non-zero rotation parameter case, i.e., where it loses angular momentum roughly equally from both rotation parameters until one rotation parameter is exactly zero and the other is approximately zero due to an appreciable discrete loss of angular momentum.

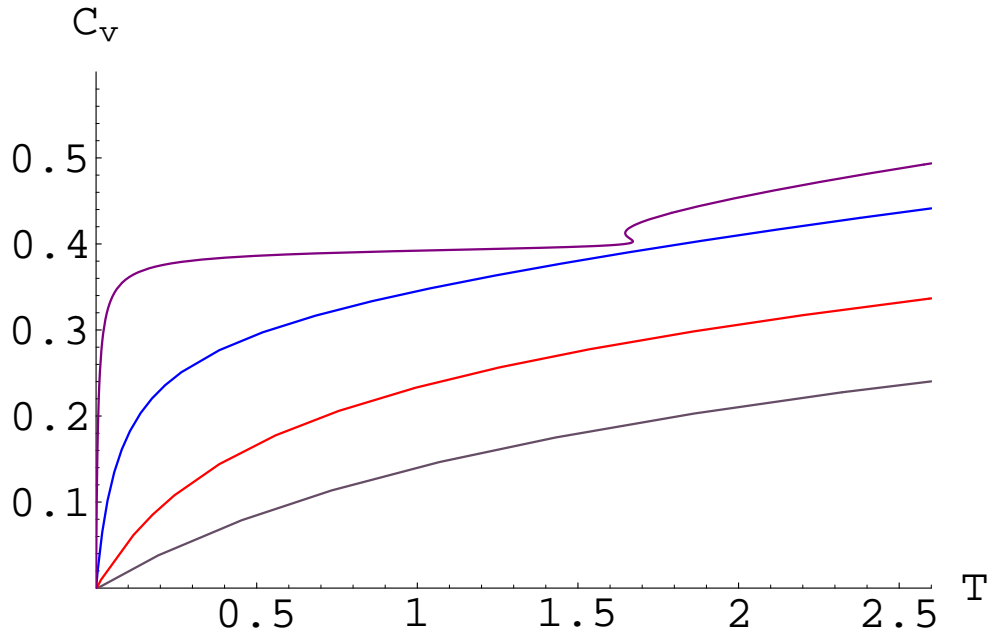


Figure 2.15: ($d = 5$) The specific heat vs temperature with $\alpha_1 = \alpha_2 = \alpha$; from top to bottom $\alpha = 0.17, 1/3, 0.5, 0.6$. When α is $\lesssim 1/6$, then there would appear a new branch with almost constant specific heat at low temperature.

Via this process, if the single rotation parameter case is stable then the end point of the equal rotation parameter case would also be stable.

Six dimensions

Similarly, in $d \geq 6$ dimensions, the Kerr-AdS black holes become unstable for rotation parameters below some critical values, at which point a new branch appears. When $d = 6$, with equal rotation parameters, the critical value is $\alpha \approx 0.22$ (see Figs. 2.16–2.17); it is slightly higher in the case of a single rotation parameter.

However, in the case of equal rotation parameters the same behaviour as the five dimensional cases is observed, and it is uncertain whether or not the black holes can completely evaporate. The single rotation parameter case clearly shows an instability for small R , regardless of angular momentum. In that case the specific heat is negative for small enough R , and the temperature diverges to positive infinity. In this scenario it is almost certain that the small black holes will evaporate, leaving thermal AdS as

the equilibrium solution.

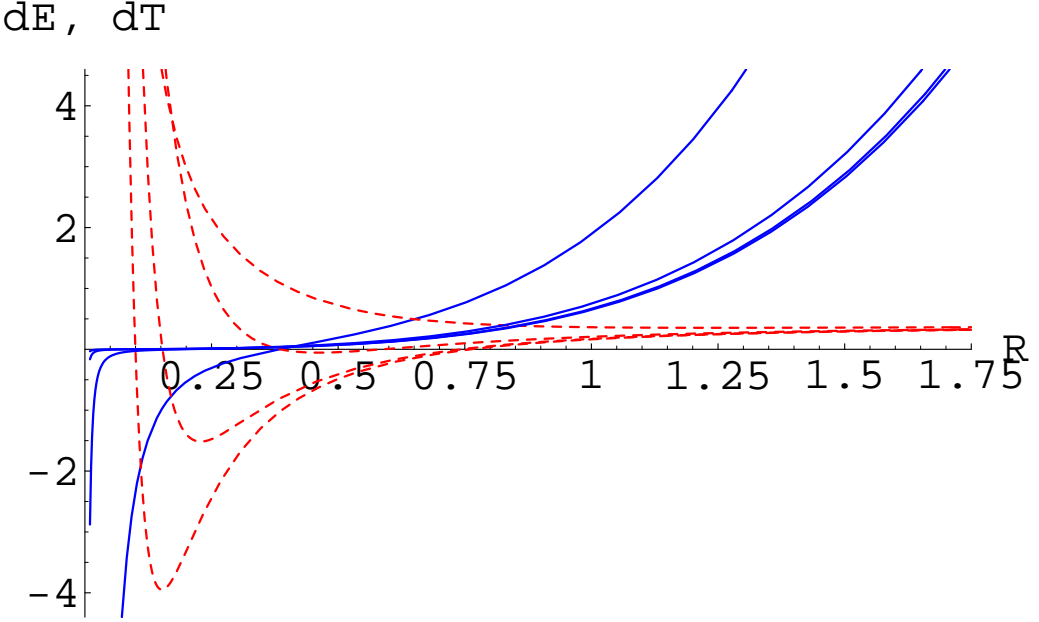


Figure 2.16: ($d = 6$) The energy differential (solid lines) and temperature differential (dashed lines) vs horizon position, with $\alpha_1 = \alpha_2 \equiv \alpha$. From left to right (dE in the $dE > 0$ region) or top to bottom (dT): $\alpha = 0.5, 0.2, 0.1, 1/15$

n dimensions

In all odd dimensions, the specific heat has a single branch at high rotation and two branches or more branches at low rotations: the critical value of α which distinguishes these two cases increases with the number dimensions, and also with number of non-trivial rotation parameters. A similar behavior is observed in all even dimensions $d \geq 6$, but in this case an interesting difference is that the specific heat can never be zero with $T > 0$.

It seems relevant to ask what happens at the critical angular velocity limit, $\alpha_i = 1$. Apparently, the action as well as the entropy is divergent in this limit. Nevertheless, as discussed in [71] (see also [125]), there exists a scaling of the mass parameter $m \rightarrow 0$ which makes the physical charges of the configuration finite. With equal rotation parameters, when $\alpha_i \rightarrow 1$, Kerr-AdS black holes are thermodynamically stable. On the other hand, in all even dimensions $d \geq 6$, small Kerr-AdS black holes with a single

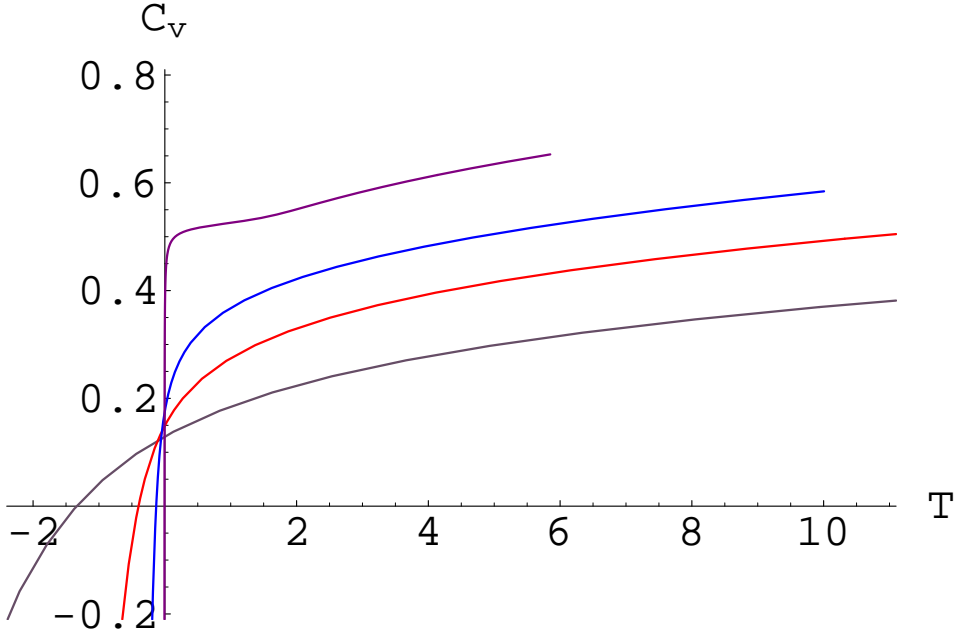


Figure 2.17: ($d = 6$) The specific heat vs temperature plotted parametrically as functions of R with $\alpha_1 = \alpha_2 = \alpha$. From top to bottom $\alpha = 0.25, 0.5, 0.6, 0.7$

non-vanishing rotation parameter are thermodynamically unstable.

In our plots we have used the energy expressions suggested by Gibbons *et al.* [118], which differ from those suggested by Hawking *et al.* [71] by some overall constant factors. This itself does not introduce any significant difference in the behavior of the specific heat and hence the thermodynamic stability of Kerr-AdS solutions. At any rate, the energy measured in a non-rotating frame can be derived using various other methods [126, 127, 128, 129, 130] and so is easier to work with; the energy (or total mass) expressions given in [128], however, disagree with those in [118] in odd spacetime dimensions.

2.3.4 The temperature bound for rotating black holes

It was recently shown in [131] that at fixed entropy, the temperature of a rotating black hole is bounded above by that of a non-rotating black hole in four and five dimensions, but not in six or more dimensions. We verify this claim by plotting temperature as a function of entropy, in various dimensions; some of the plots are depicted in Figs. 2.18–2.20. In six dimensions or more, the minimum of the entropy is not always the minimum of the temperature; the minimum of the entropy actually depends upon the choice of rotation parameters. This is precisely the case where the inequality $T_{\text{Kerr-AdS}} \geq T_{\text{S-AdS}}$ may be realized with a very small entropy. But in this limit the temperature actually diverges, so an effect like this might be absent in a physical picture. At fixed entropy, but $S \gg 0$, the Hawking temperature of a rotating black hole is always suppressed relative to that of a non-rotating black hole and the inequality $T_{\text{Kerr-AdS}} < T_{\text{S-AdS}}$ holds in all dimensions. This result, presumably, holds with various charges and classical matter fields (such as gauge fields, dilaton, etc) and is in accord with the earlier observation made by Visser while studying a static spherically symmetric case in four dimensions with no cosmological term [132].

A five dimensional Kerr-AdS black hole with a single non-vanishing rotation parameter possesses an interesting (and perhaps desirable) feature; in this case the entropy vanishes when the temperature becomes zero. A similar feature is present in seven dimensions, but with two equal rotation parameters: $\alpha_1 = \alpha_2 \sim 0.33$, $\alpha_3 = 0$.

In recent work [133] on the evolution of a five dimensional rotating black hole via scalar field radiation, Maeda *et al.* observed that in a flat background ($c = 0$), the asymptotic state of a five dimensional rotating black hole with a single non-vanishing parameter is described by $a \sim 0.11\sqrt{M}$. It would be interesting to know a similar result in an anti-de Sitter background, $c > 0$.

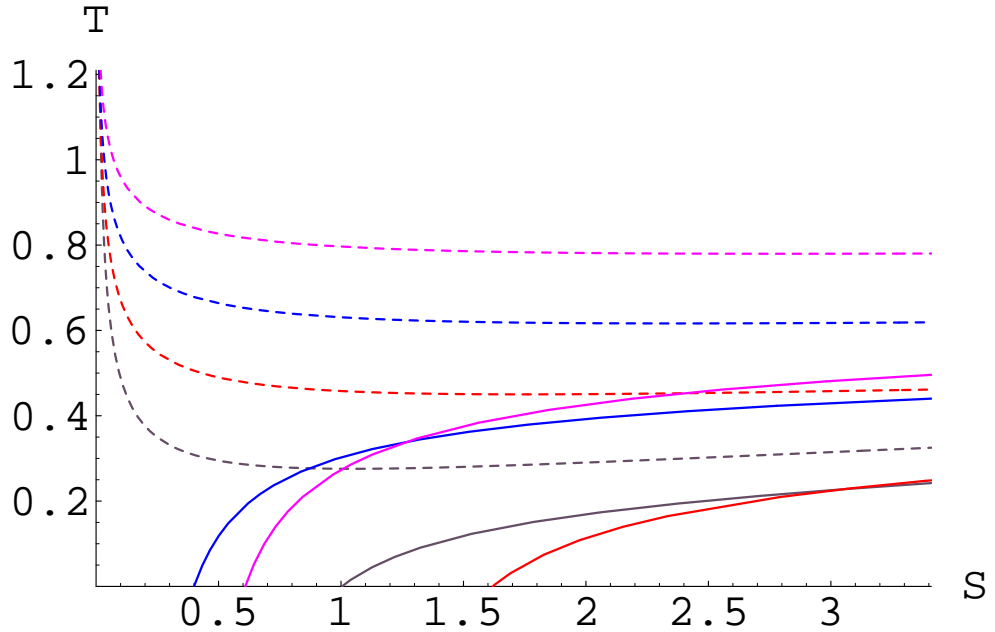


Figure 2.18: The temperature vs entropy plotted parametrically as functions of R , in various dimensions with equal rotation parameters, $\alpha_i \equiv \alpha$. From top to bottom: $d = 7, 6, 5, 4$ with all $\alpha_i = 0$ (dashed lines); from left to right: $d = 6, 7, 4, 5$ (solid lines) each with $\alpha = 0.4$.

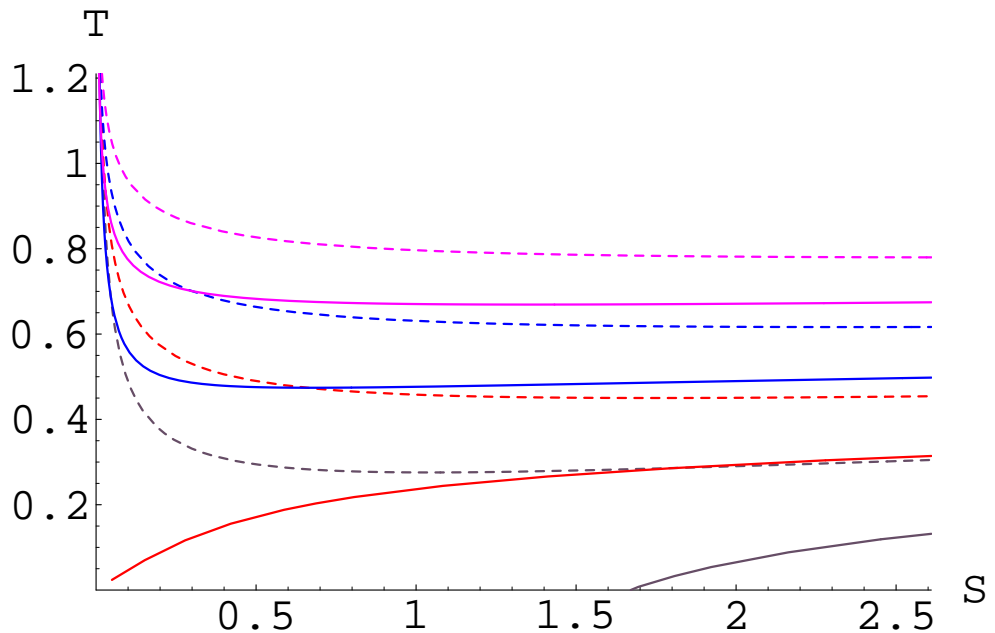


Figure 2.19: The temperature vs entropy plotted parametrically as functions of R with a single rotation parameter α . From top to bottom: $d = 7, 6, 5, 4$ each with $\alpha = 0.4$ (solid lines), and $\alpha_i = 0$ (dashed lines).

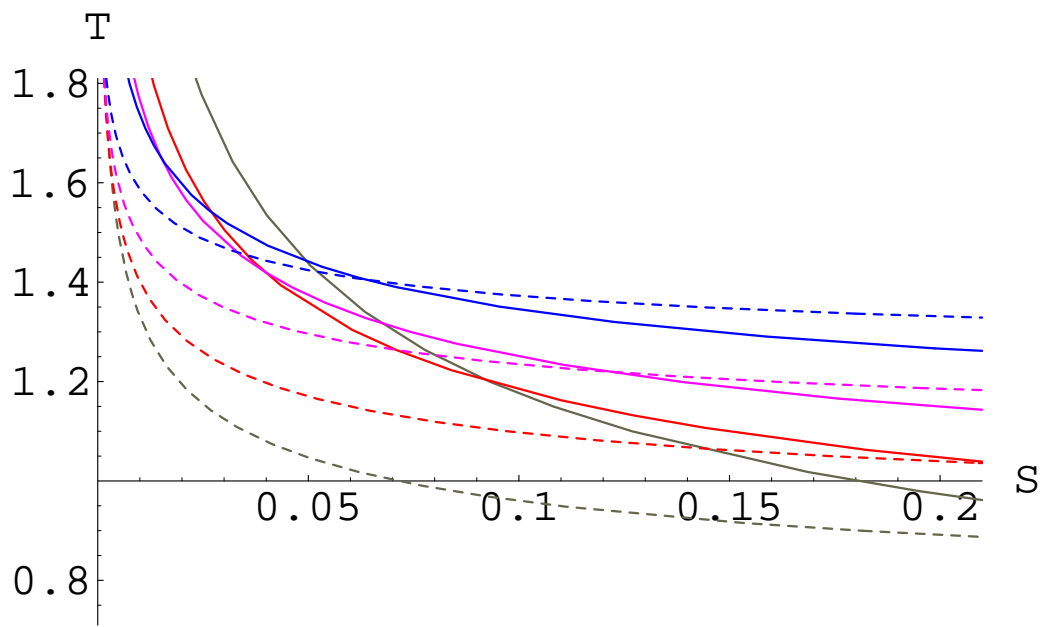


Figure 2.20: The temperature vs entropy plotted parametrically as functions of R , in the small entropy region. From top to bottom (in the region $S > 0.1$): $d = 10, 9, 8, 7$ with $\alpha_1 = \dots \alpha_{N-1} = 0.01, \alpha_N = 0.9$ (solid lines, Kerr-AdS) and $\alpha_i = 0$ (dashed lines, Schwarzschild-AdS).

2.3.5 Rotation and the AdS-CFT correspondence

Following [107, 71], one would expect the partition function of a Kerr-AdS black hole to be related to the partition function of a CFT in a rotating Einstein universe on the (conformal) boundary of the AdS space.

A curious observation in Ref. [134] is that the Cardy-Verlinde entropy formula works more naturally using the bulk thermodynamic variables defined by Hawking *et al.* [71]. This seems to indicate that the energy expression (2.25) is still relevant in a dual CFT. The Killing vector is then given by

$$\chi = \frac{\partial}{\partial \tau} + \Omega_i \frac{\partial}{\partial \phi_i}, \quad (2.29)$$

where ϕ_i are the angular coordinates. This property normally allows the thermal radiation to rotate with black hole's angular velocity all the way to conformal infinity.

One could ask whether or not the bulk thermodynamic variables suggested by Gibbons *et al.* [118], which were measured with respect to a frame that is non-rotating at infinity, can be mapped onto the boundary CFT variables by using the usual scaling argument. This does not seem to be the case as long as the CFT is assumed to be on a surface of large R in Boyer-Lindquist coordinates. However, such a mapping might exist when the CFT is assumed to be on a large spherical surface, that is one for which the coordinate $y = \text{constant}$ at large y . That is to say, it is possible that the set of bulk variables for Kerr-AdS black holes given by Gibbons *et al.* [118], in some (modified) form, match onto the boundary CFT variables that satisfy the first law of thermodynamics. This was indeed shown to be the case in [131].

Let us briefly discuss the role of non-trivial rotation parameters on the existence of an equilibrium between Kerr-AdS black hole and co-rotating thermal radiation around it. For this, the requirement of a positive specific heat is a necessary condition. In five dimensions, the specific heat is always positive and also a monotonically increasing function of temperature when one (or both) of the rotation parameters takes a value at least one-quarter the AdS length scale l . It should also be noted that for all values of the rotation parameters the specific heat is positive for sufficiently small Kerr-AdS black holes in five dimensions. This means that, unlike in Minkowski (infinite) space, rotating Kerr-AdS black holes (which conserve their angular momentum) can be in

equilibrium with their thermal radiation rotating around them, when $0 < \alpha_i \lesssim 1$.

2.4 The stability of the background of Kerr–AdS spacetime under gravitational perturbations

Gravitational (classical) stability of a spacetime is physically more important than thermodynamic stability. While it is possible to have a physically reasonable spacetime which is classically stable but thermodynamically unstable (e.g. 4–D Schwarzschild) it is more difficult to seriously consider solutions in general relativity as physical without classical stability.

The Schwarzschild solution has been shown to be stable against small metric perturbations by Vishveshwara [135], Zerilli [136, 137] and Chandrasekhar [138]. Similar efforts have been attempted with the Kerr solution by Press and Teukolsky [139, 140, 141], Hartle and Wilkins [142], Chandrasekhar and Detweiler [143]–[147] and others, but due to the huge increase in complications when setting up and solving the linearised perturbation equations, they were only able to provide plausibility or numerical arguments against exponentially growing modes on a Kerr background – no definitive proofs of gravitational stability are available. However, Press was able to show that all slowly rotating Kerr black holes are gravitationally stable, as expected since they are approximately Schwarzschild which is stable. Whiting [148] was able to prove that normal modes of the Kerr solution grow linearly at most in time. This is consistent with the study of massive scalar perturbations of Kerr which point to the existence of unstable modes with growth times similar to the age of the universe [149, 150, 151].

As a precursor to studying Kerr–AdS spacetimes in higher dimensions, in this section we study the stability of Kerr–AdS background metrics (with $M = 0$) in dimensions five and higher against linearised metric perturbations. For this purpose, it is sufficient to consider the following d -dimensional (time-independent) metric *ansatz*:

$$g_{ab}(X)dX^a dX^b = g_{\mu\nu}(x)dx^\mu dx^\nu + \gamma(x)^2 d\tilde{\Sigma}_{k,n}^2(\tilde{x}), \quad (2.30)$$

where the metric $g_{ab}(X)$ is effectively separated into two parts: a diagonal “bulk” line element and $d\tilde{\Sigma}_{k,n}^2$, which is the metric on an n -dimensional “base manifold”, $\tilde{\mathcal{M}}^n$,

whose curvature has not been specified, (so $k = 0$ or ± 1), and hence can be replaced by any Einstein-Kähler metric with the same scalar curvature. Tilded quantities refer to base manifold quantities. However, in the present work we study only the $k = +1$ case. The modes we will study do not exist in stability analyses of, for example, Schwarzschild, as no suitable restrictions of these modes exist on S^2 [152]. Hence the modes we study are intrinsically higher dimensional. A comprehensive classical stability analysis of metrics of the form (2.30) has been carried out in ref [153], but the work there does not specifically address modes of instability which are exclusively higher dimensional. We also note that the form of (2.30) is sufficiently general to encompass a variety of non-rotating massive black hole solutions, but we will restrict our attention to the AdS backgrounds of higher dimensional Kerr-AdS black holes.

It should be noted that the rotation parameters which parameterise the angular momenta of the spacetime become coordinate transformations when the mass parameter is zero. This can be seen most simply by considering the Kerr-Schild form of Kerr-AdS:

$$g_{ab} = \tilde{g}_{ab} + \frac{2M}{U} k_a k_b dx^a dx^b. \quad (2.31)$$

Setting $M = 0$, the geometry reduces to that of the AdS base space, with whatever non-trivial topologies one assigns to it. The higher dimensional tensor perturbations of AdS with non-trivial topologies have already been studied by Gibbons and Hartnoll [154]. Here we perform the same analysis as in [154] but in a set of coordinates adapted to a Kerr-AdS spacetime in the hope that some previously unrecognised behaviour, potentially related to higher dimensional Kerr-AdS spacetimes, becomes apparent.

2.4.1 The Lichnerowicz operator

To study the inherently higher dimension tensor modes of the base manifolds of spacetimes of the form 2.30, we will use the Lichnerowicz operator [154]. Under a small linear metric perturbation,

$$g_{ab}(X) \rightarrow g_{ab}(X) + h_{ab}(X), \quad (2.32)$$

where h is symmetric and $|h_a^b| \ll 1$, the variation in the Ricci tensor is given by,

$$\delta R_{ab} = \frac{1}{2} \Delta_L h_{ab} - \frac{1}{2} \nabla_a \nabla_b h_c^c + \nabla_{(a} \nabla^c h_{b)c}, \quad (2.33)$$

where the spin-2 Lichnerowicz operator Δ_L acting on a rank two symmetric tensor is defined by (see, for example, [155])

$$\Delta_L h_{ab} = -\nabla^2 h_{ab} - 2R_{cadb}h^{cd} + 2R_{c(a}h_{b)}^c. \quad (2.34)$$

The stability of background metrics of the form (2.30) with $n > 2$, under certain metric perturbations, is expected to be specific to tensor perturbations [154]. We therefore would like to restrict our analysis here to the tensor mode fluctuations that satisfy

$$h_{ab}(X) = 0 \quad (2.35)$$

unless $(a, b) = (i, j)$, where the indices a, b, \dots run from $0 \dots (d-1)$ and the indices i, j, \dots will run from $(d-n) \dots (d-1)$ for the n -dimensional base manifold. The above choice of the form of the perturbation tensor does *not* correspond to a gauge choice, but instead has the effect of removing the scalar and vector modes of the perturbation leaving one with just the higher dimensional tensor modes on the base manifold [154].

The Lichnerowicz operator Δ_L is compatible with the transverse, trace-free (de Donder) gauge for h_{ab} : $h_a^a = 0 = h_{b;a}^a$. Applying the transverse tracefree gauge, the variation of the Ricci tensor with coordinates restricted to the base manifold satisfies

$$\delta R_{ij} = \frac{1}{2}(\Delta_L h)_{ij} = -c(d-1)h_{ij}, \quad (2.36)$$

where c is the d -dimensional cosmological constant and

$$\begin{aligned} \Delta_L h_{ij} &= \frac{1}{\gamma^2} \tilde{\Delta}_L h_{ij} + [-g^{\mu\nu} \partial_\mu \partial_\nu] h_{ij} + \sum_{\nu=1}^{d-n} \left[\partial^\sigma g_{\sigma\nu} - \frac{1}{2} g^{\sigma\rho} \partial_\nu g_{\sigma\rho} + (4-n) \frac{\partial_\nu \gamma}{\gamma} \right] \partial^\nu h_{ij} \\ &- \frac{4}{\gamma^2} [g^{\mu\nu} \partial_\mu \gamma(x) \partial_\nu \gamma(x)] h_{ij}, \end{aligned} \quad (2.37)$$

where $\tilde{\Delta}_L h_{ij}$ is the spin-2 Lichnerowicz operator acting on the base manifold $\widetilde{\mathcal{M}}^n$. It should be noted that this expression generalises other results in the literature and is applicable to a wide range of spacetimes satisfying 2.30.

2.4.2 Dependence on radial coordinate only

Let us first consider a background spacetime where $d = n + 2$, such that we can write the metric as

$$ds^2 = -\alpha(r)^2 dt^2 + \beta(r)^2 dr^2 + \gamma(r)^2 d\widetilde{\Sigma}_n^2. \quad (2.38)$$

We can write the Lichnerowicz operator as

$$\Delta_L h_{ij} = \left[\frac{1}{\gamma^2} \tilde{\Delta}_L + \left[\frac{\partial_t^2}{\alpha^2} - \frac{\partial_r^2}{\beta^2} \right] + \left[\frac{\beta_r}{\beta} - \frac{\alpha_r}{\alpha} + (4-n) \frac{\gamma_r}{\gamma} \right] \frac{\partial_r}{\beta^2} - \frac{4}{\gamma^2} \frac{\gamma_r^2}{\beta^2} \right] h_{ij} \quad (2.39)$$

where the subscripts t, r denote derivatives w.r.t. t, r respectively. In this case we find it convenient to choose metric perturbations of the form

$$h_{ij} = \Psi(r) e^{\omega t} \tilde{h}_{ij}(\tilde{x}), \quad (2.40)$$

such that

$$(\tilde{\Delta}_L \tilde{h})_{ij} = \lambda \tilde{h}_{ij}, \quad (2.41)$$

where \tilde{x} are coordinates on $\tilde{\mathcal{M}}^n$ and λ is the eigenvalue of the Lichnerowicz operator on $\tilde{\mathcal{M}}^n$. We wish to write the perturbed equations

$$(\Delta_L h)_{ij} + 2c(d-1)h_{ij} = 0, \quad (2.42)$$

in the form

$$(\partial_{r_*}^2 - V(r_*)) \Phi(r_*) = \omega^2 \Phi(r_*). \quad (2.43)$$

To do so, consider a second order differential equation of the form

$$(A\partial_r^2 + B\partial_r + C + D\partial_t^2 + E\tilde{\Delta}_L)h = 0, \quad (2.44)$$

where A, B, C are functions of r only. We find it is convenient to choose $h \equiv \Psi(r) e^{\omega t} \tilde{h}$, such that $\tilde{\Delta}_L \tilde{h} = \lambda \tilde{h}$. We then have

$$(A\partial_r^2 + B\partial_r + C + D\omega^2 + E\lambda) \Psi(r) e^{\omega t} \tilde{h} = 0. \quad (2.45)$$

For non-zero fluctuations, $e^{\omega t} \tilde{h} \neq 0$, this implies that

$$(A\partial_r^2 + B\partial_r + \tilde{C}) \Psi(r) = 0, \quad (2.46)$$

where $\tilde{C} \equiv C + D\omega^2 + E\lambda$. We would like to write this in the form

$$[\partial_x^2 - V(x(r))] \varphi = \omega^2 \varphi. \quad (2.47)$$

To facilitate this we introduce two transformations:

$$dr = \frac{\partial r}{\partial x} dx, \quad \Psi = \chi \varphi. \quad (2.48)$$

The differential equation then takes the form

$$\frac{A}{r_x^2} \varphi'' + \left[\frac{2A}{r_x^2} \frac{\chi'}{\chi} + \frac{B}{r_x} - \frac{A r_{xx}}{r_x^3} \right] \varphi' + \left[\frac{A}{r_x^2} \frac{\chi''}{\chi} + \left(\frac{B}{r_x} - \frac{A r_{xx}}{r_x^3} \right) \frac{\chi'}{\chi} + \tilde{C} \right] \varphi = 0, \quad (2.49)$$

where $r_x \equiv r' = (\partial r / \partial x)$. Let us define

$$r_x^2 = -\frac{A}{D}, \quad \frac{\chi'}{\chi} = \frac{B}{2Dr_x} + \frac{r_{xx}}{2r_x}. \quad (2.50)$$

This implies

$$\frac{r_{xx}}{r_x} = \frac{1}{2} \left(\frac{A_x}{A} + \frac{D_x}{D} \right). \quad (2.51)$$

The differential equation then takes the standard form:

$$\partial_x^2 \varphi - V \varphi = \omega^2 \varphi, \quad (2.52)$$

where

$$V = -\left(\frac{\chi'}{\chi} \right)' + \left(\frac{\chi'}{\chi} \right)^2 + \frac{\bar{C}}{D}, \quad (2.53)$$

where $\bar{C} \equiv C + E\lambda$.

Therefore to facilitate the transformation of (2.42) to (2.43) we introduce two transformations:

$$dr = \frac{\partial r}{\partial r_*} dr_*, \quad \Psi(r) = \chi(r) \Phi(r), \quad (2.54)$$

with

$$\chi(r) = C_1 \gamma^{(4-n)/2}. \quad (2.55)$$

We then find

$$V(r(r_*)) = \frac{\lambda \alpha^2}{\gamma^2} + \frac{n^2 - 10n + 8}{4} \left(\frac{\gamma_{r_*}}{\gamma} \right)^2 + \frac{(n-4)}{2} \frac{\gamma_{r_* r_*}}{\gamma} + 2(n+1)c\alpha^2, \quad (2.56)$$

where

$$\begin{aligned} \gamma_{r_*} &\equiv \frac{\partial r}{\partial r_*} \frac{\partial \gamma}{\partial r} = \frac{\alpha}{\beta} \gamma_r, \\ \gamma_{r_* r_*} &= \frac{\alpha^2}{\beta^2} \left[\gamma_{rr} + \left(\frac{\alpha_r}{\alpha} - \frac{\beta_r}{\beta} \right) \gamma_r \right]. \end{aligned} \quad (2.57)$$

The above potential correctly reproduces the result in ref [115] (cf. Eq. (41) with $\alpha^2 = f(r)$ and $\gamma^2 = r^2$), see also [154, 156]. Apparently, the case $n = 4$ is special.

2.4.3 Anti de-Sitter spacetime in odd dimensions

In the case of an odd number of spacetime dimensions $d = 2N + 1 = n + 2 \geq 5$, the AdS background metric may be given in rotating coordinates by

$$ds^2 = -\frac{(1+cr^2)dt^2}{(1-ca^2)} + \frac{r^2 dr^2}{(1+cr^2)(r^2+a^2)} + \frac{r^2+a^2}{1-ca^2} ds^2(\widetilde{\mathcal{M}}^n), \quad (2.58)$$

where the rotation parameters are set equal (i.e., $a_1 = a_2 = a$). The base space $\widetilde{\mathcal{M}}^n$, which is topologically S^{2N-1} , may be parameterized by the metric

$$\sum_{k=1}^N \left(d\hat{\mu}_k^2 + \hat{\mu}_k^2 d\hat{\phi}_k^2 \right) \quad (2.59)$$

satisfying

$$\sum_{i=1}^N \hat{\mu}_i^2 = 1. \quad (2.60)$$

There are N azimuthal angles ϕ_i each with period 2π associated with N orthogonal 2-planes and N directional cosines μ_i where $0 \leq \mu_i \leq 1$ for $1 \leq i \leq N$ associated with N spatial dimensions. For example, in five dimensions, the metric on base \mathcal{M}^3 is $ds^2(\mathcal{M}^3) = d\theta^2 + \sin^2 \theta d\phi_1^2 + \cos^2 \theta d\phi_2^2$.

In the above background, the linear tensor perturbations satisfy

$$\Delta_L h_{ij} = -2c(n+1)h_{ij}, \quad (2.61)$$

where

$$\begin{aligned} \Delta_L h_{ij} &= \left[-\frac{(r^2+a^2)(1+cr^2)}{r^2} \left(\frac{\partial^2}{\partial r^2} + \frac{4r^2}{(r^2+a^2)^2} \right) + \frac{1-ca^2}{1+cr^2} \frac{\partial^2}{\partial t^2} \right] h_{ij} \\ &- \left((n-2)cr + \frac{n-4}{r} - \frac{a^2(1-cr^2)}{r^3} \right) \frac{\partial h_{ij}}{\partial r} + \frac{1-ca^2}{r^2+a^2} (\tilde{\Delta}_L h)_{ij}. \end{aligned} \quad (2.62)$$

In terms of the Regge-Wheeler type coordinate r_* , which may be defined by

$$dr = \frac{(1+cr^2)\sqrt{r^2+a^2}}{r\sqrt{1-ca^2}} dr_*, \quad (2.63)$$

and using Eqs. (2.40),(2.54) the differential equation is cast in the standard form:

$$-\frac{d^2\Phi}{dr_*^2} + V(r(r_*))\Phi = -\omega^2\Phi \equiv E\Phi, \quad (2.64)$$

where the potential is

$$V(r(r_*)) = \frac{\lambda(1+cr^2)}{r^2+a^2} + \frac{(n^2-10n+8)(1+cr^2)^2}{4(1-ca^2)(r^2+a^2)} + \frac{(3n-2)c(1+cr^2)}{1-ca^2}. \quad (2.65)$$

This potential is well behaved around $r = 0$ due to the coordinate transformation with $a \neq 0$. Note that one is able to reproduce the relevant result in [154] by making the substitution

$$\frac{r^2 + a^2}{1 - ca^2} \rightarrow y^2. \quad (2.66)$$

There exists a criterion for stability against exponentially growing modes of the perturbations in terms of the minimum Lichnerowicz eigenvalue, λ_{min} , on the base manifold $\widetilde{\mathcal{M}}^n$. In the case of a vanishing cosmological constant ($c = 0$), this criterion is the same as that for a Schwarzschild-AdS background [154]:

$$\lambda_{min} \geq \lambda_c = -\frac{n^2 - 10n + 8}{4} \Leftrightarrow \text{stability}. \quad (2.67)$$

A requirement that $\lambda_c \geq 0$ constrains the spacetime dimensions to $n \leq 9$ (or $d \leq 11$). The stability of the potential depends on the eigenvalue λ , ensuring that the potential is positive everywhere and bounded from below. Taking the limit $r \rightarrow 0$ in (2.65) and defining $\mu \equiv ca^2$ where $a > 0$ we find the criteria for stability,

$$\lambda \geq \bar{\lambda}_c = -\frac{n^2 - 10n + 8 + 4(3n - 2)\mu}{4(1 - \mu)}. \quad (2.68)$$

where $\mu < 1$. Setting $\tilde{\lambda}_c \geq 0$ provides an upper bound on μ for each n . Specifically,

$$\mu_{max} = -\frac{n^2 - 10n + 8 + 4\bar{\lambda}_c}{4(3n - 2 - \bar{\lambda}_c)}. \quad (2.69)$$

Increasing n pushes the maximum value of μ down, and for $n > 9$, $\mu_{max} < 0$. Note that for $\mu < 0$, $c < 0$, which corresponds to de-Sitter spacetime.

Instead of solving the Schrödinger-like equation directly in terms of r_* , one can solve the radial part of equation (2.61) by expressing it as a hypergeometric equation, whose solution is given by linear combinations of

$$\begin{aligned} \Psi_{\pm}(x, \mu) &= \left(\frac{x + \mu}{c}\right)^{(5-n \pm 2\nu)/4} (1 + \mu)^{i\omega/2\sqrt{c}} \times \\ &{}_2F_1\left(\frac{\pm 2\nu - (n - 1)}{4} + \frac{i\omega}{2\sqrt{c}}, \frac{\pm 2\nu + (n + 3)}{4} + \frac{i\omega}{2\sqrt{c}}, \pm\nu + 1; -\frac{x + \mu}{1 - \mu}\right), \end{aligned} \quad (2.70)$$

where $x \equiv cr^2$, and

$$\nu = \frac{1}{2} \sqrt{4\lambda + (5 - n)^2 - 16}. \quad (2.71)$$

We note that reality of ν immediately implies the stability condition (2.67) as it provides a (slightly) more stringent bound on λ_c . Reality of the solution also requires $\omega = i\tilde{\omega}$

which implies that there are no exponentially growing (unstable) modes. Requiring the solution to be bounded as $r \rightarrow \infty$ fixes one arbitrary constant which leaves Ψ decaying as r^{1-n} . Given that $\Psi = \chi\Phi$ we find that Φ decays as $r^{-(n+2)/2}$. By considering the large r limit of potential (2.65) we also see that $n \geq 2$ so that eq. (2.64) remains bounded as required to ensure that the total energy is finite; this is automatically satisfied as $n \geq 3$ by construction.

2.4.4 AdS spacetime in even dimensions

Consider a background spacetime where $d = n + 3$, such that we can write the metric as

$$\begin{aligned} ds^2 = & -\alpha(r, \theta)^2 dt^2 + \beta(r, \theta)^2 dr^2 + \sigma(r, \theta)^2 d\theta^2 \\ & + \gamma(r, \theta)^2 d\Sigma_n^2. \end{aligned} \quad (2.72)$$

We can write the Lichnerowicz operator as

$$\begin{aligned} \Delta_L h_{ij} = & \frac{1}{\gamma^2} \tilde{\Delta}_L h_{ij} + \left[\frac{\partial_t^2}{\alpha^2} - \frac{\partial_r^2}{\beta^2} - \frac{\partial_\theta^2}{\sigma^2} \right] h_{ij} + \left[-\frac{\alpha_r}{\alpha} + \frac{\beta_r}{\beta} - \frac{\sigma_r}{\sigma} + (4-n) \frac{\gamma_r}{\gamma} \right] \frac{\partial_r h_{ij}}{\beta^2} \\ & + \left[-\frac{\alpha_\theta}{\alpha} - \frac{\beta_\theta}{\beta} + \frac{\sigma_\theta}{\sigma} + (4-n) \frac{\gamma_\theta}{\gamma} \right] \frac{\partial_\theta h_{ij}}{\sigma^2} - \frac{4}{\gamma^2} \left[\frac{\gamma_r^2}{\beta^2} + \frac{\gamma_\theta^2}{\sigma^2} \right] h_{ij}, \end{aligned} \quad (2.73)$$

To this end, we shall consider a Kerr-AdS metric with $M = 0$ (i.e., AdS spacetime) in even dimensions, $n = 2N - 1$, by setting the N rotation parameters equal (i.e. $a_1 = \dots = a_N = a$). The background metric is [116]

$$\begin{aligned} ds^2 = & -\frac{(1+cr^2)\Delta_\theta}{1-ca^2} dt^2 + \frac{\rho^2}{(1+cr^2)(r^2+a^2)} dr^2 \\ & + \frac{\rho^2}{\Delta_\theta} d\theta^2 + \frac{(r^2+a^2)\sin^2\theta}{1-ca^2} d\widetilde{S}^2(\widetilde{\mathcal{M}}^n), \end{aligned} \quad (2.74)$$

where,

$$\rho^2 \equiv r^2 + a^2 \cos^2\theta, \quad \Delta_\theta = 1 - ca^2 \cos^2\theta. \quad (2.75)$$

The Lichnerowicz operator is

$$\begin{aligned} (\Delta_L h)_{ij} = & \left[\frac{1-ca^2}{(1+cr^2)\Delta_\theta} \frac{\partial^2}{\partial t^2} - \frac{(1+cr^2)(r^2+a^2)}{\rho^2} \frac{\partial^2}{\partial r^2} \right. \\ & \left. - \frac{\Delta_\theta}{\rho^2} \frac{\partial^2}{\partial\theta^2} - \frac{4}{\rho^2} \left(\frac{r^2(1+cr^2)}{r^2+a^2} + \frac{\Delta_\theta}{\tan^2\theta} \right) \right] h_{ij} \end{aligned}$$

$$\begin{aligned}
& + \frac{(1 - ca^2)}{(r^2 + a^2) \sin^2 \theta} \tilde{\Delta}_L h_{ij} \\
& + \frac{r}{\rho^2} (2(1 - ca^2) - (n - 1)(1 + cr^2)) \partial_r h_{ij} \\
& + \frac{1}{\rho^2 \tan \theta} (2(1 - ca^2) - (n - 2)\Delta_\theta) \partial_\theta h_{ij}.
\end{aligned} \tag{2.76}$$

Equation (2.76) may be separated by writing,

$$h_{ij} = \Psi(r) e^{\omega t} S(\theta) \tilde{h}_{ij}(\tilde{x}), \tag{2.77}$$

and taking the large r limit. Hence,

$$0 = \left(r^2 \frac{\partial^2}{\partial r^2} + (n - 1)r \frac{\partial}{\partial r} - 2n + \frac{p}{cr^2} \right) \Psi, \tag{2.78}$$

$$\begin{aligned}
0 &= \Delta_\theta \frac{\partial^2 S}{\partial \theta^2} - \frac{1}{\tan \theta} (2(1 - ca^2) - (n - 2)\Delta_\theta) \frac{\partial S}{\partial \theta} \\
&+ \left(\frac{4\Delta_\theta}{\tan^2 \theta} - \frac{\lambda(1 - ca^2)}{\sin^2 \theta} - \frac{\omega^2(1 - ca^2)}{c\Delta_\theta} - p \right) S,
\end{aligned} \tag{2.79}$$

where we have defined $(\tilde{\Delta}_L \tilde{h})_{ij} = \lambda \tilde{h}_{ij}$, so that λ is the eigenvalue of the Lichnerowicz operator on $\tilde{\mathcal{M}}^n$, and p is the separation constant.

The radial equation is easily solved to yield

$$\Psi = c_1 r^{(2-n)/2} J_1 \left(\frac{n+2}{2}, \sqrt{\frac{p}{cr^2}} \right) + c_2 r^{(2-n)/2} Y_1 \left(\frac{n+2}{2}, \sqrt{\frac{p}{cr^2}} \right). \tag{2.80}$$

However, regularity of the radial solution at $r = \infty$ requires $c_2 = 0$ and hence as $r \rightarrow \infty$ the radial solution behaves as

$$\Psi(r) \sim \frac{c_1}{r^n}. \tag{2.81}$$

Equation (2.79), together with boundary conditions of regularity at $\theta = 0$ and π , constitute an eigenvalue problem for the separation constant p . For $\sin \theta \approx \theta$, $\cos \theta \approx 1$, the solution is

$$S = \theta^{(5-n)/2} [c_1 J_m(z) + c_2 Y_m(z)], \tag{2.82}$$

where

$$\begin{aligned}
m &= \sqrt{\lambda - 4 + \frac{(5-n)^2}{4}}, \\
z &= \sqrt{-\frac{pc + \omega^2}{c(1 - ca^2)}} \theta.
\end{aligned} \tag{2.83}$$

The criterion for gravitational stability, in terms of the minimum Lichnerowicz eigenvalue λ_{min} on the base manifold $\widetilde{\mathcal{M}}^n$, namely $\lambda_{min} \geq \lambda_c = 4 - (5 - n)^2/4$, now translates into the requirement that $m \in \mathbf{R}$. However we note that $c \neq 0$ in this case. In AdS space, $c > 0$, for reality of the solution we also require,

$$0 < 1 - ca^2 < 1, \quad p < -\frac{\omega^2}{c}. \quad (2.84)$$

For real ω , $p < 0$ and hence $\sqrt{p/cr^2}$ is imaginary, but this is not allowed by the radial wave equation. Therefore there are no normalisable solutions with $\omega \in \mathbf{R}$ and hence unstable modes are not allowed. For $\omega \rightarrow i\tilde{\omega}$, one requires $p < \tilde{\omega}^2/c$. A useful inequality for stability of the background AdS metric (2.74) is therefore,

$$0 < p < \frac{\tilde{\omega}^2}{c}. \quad (2.85)$$

Instead of considering the large r limit in (2.76), let us now consider the special case where the angular velocity approaches the critical limit, $ca^2 = 1$ (or $a = l$). The eigenfunctions are then the associated Legendre polynomials $P_{\tilde{n}}^m(\cos \theta)$, $Q_{\tilde{n}}^m(\cos \theta)$, where,

$$\begin{aligned} m &= \frac{1}{2}\sqrt{4p - (7 - n)(n + 1)}, \\ \tilde{n} &= \frac{1}{2}\left(\sqrt{(n - 6)(n + 2)} - 1\right). \end{aligned} \quad (2.86)$$

An interesting case is $n = 7$, which allows one to study supergravity solutions in $d = 10$. It would be interesting to know what the limit $ca^2 \rightarrow 1$ corresponds to in a dual field theory. We leave this issue to future work.

Because of the form of the original metric, it is not possible to transform the results in this section into that of [154] via a coordinate transformation. Specifically, the base manifold studied here is *different* to the standard boundary of AdS spacetime, due to the way the AdS metric in this section has been decomposed into bulk and base spacetimes.

2.5 Conclusion

In chapter 2 the thermodynamics of higher-dimensional ($d \geq 5$) rotating black holes in a background (anti)-de Sitter spacetime were studied. The thermodynamic quan-

ties for Kerr-AdS black hole solutions suggested by Gibbons *et al.* [118] have been used to study the behavior of the free energy and specific heat (which are defined unambiguously in all spacetime dimensions $d \geq 4$) as functions of temperature and horizon positions. The two apparently different expressions of energy in the Kerr-AdS background suggested by Hawking *et al.* [71] and Gibbons *et al.* [118] do not introduce any significant difference in the behavior of bulk thermodynamic quantities (such as entropy, free energy, specific heat, etc) and therefore the thermodynamic stability of Kerr-AdS solutions. Nevertheless, the Gibbons *et al.* bulk variables are more useful as they map onto the boundary variables with the natural definition of boundary metric, that is the one for which the coordinate $y = \text{constant}$ for large y , and they satisfy the first law of thermodynamics.

As for thermodynamic stability, most rotating black holes are found to be stable for all non-zero values of the rotation parameters. The exception to this is for $2n$, $n \geq 3$ dimensions with one non-zero rotation parameter. Sufficiently small black holes in those spacetimes are thermodynamically unstable.

We have not attempted to tackle the extremely difficult calculations associated with the determination of the classical stability of higher dimensional Kerr-AdS black holes, even for special values of the rotation parameters. A study of the classical stability of the higher dimensional AdS background in coordinates adapted to the rotating case does not yield any new information above that already obtained by Gibbons and Hartnoll [154].

Chapter 3

Gravastars with generalised exteriors

3.1 Gravastars

Black holes are widely accepted as physical objects due to their mathematical elegance and the strong astronomical evidence for their existence. The study of the properties of black hole horizons is of fundamental importance as horizons appear to provide a strong link between gravitation, thermodynamics and quantum theory. However, these horizons when described semi-classically give rise to a number of seemingly paradoxical theoretical problems which have yet to be satisfactorily resolved (see [20] for a review). For example, one such topic of current interest is whether a pure quantum state which passes over the event horizon of a black hole can evolve into a mixed state during black hole evaporation. This has relevance in the scenario that matter (requiring much information to describe) can collapse into a black hole (requiring little information to describe, via a no hair theorem). As discussed in the introduction, this problem is known as the ‘black hole information paradox’. It is generally accepted that the final resolution of this issue, and other difficult theoretical problems (such as the ‘blue shift catastrophe’ [157]) caused by the current description of black hole horizons, will be achieved using quantum gravity. However, we do not yet have a full theory of quantum gravity, and therefore, other possible solutions to remove the paradoxes generated by

black hole horizons should be investigated.

Given the above, it has been suggested that alternative endpoints of gravitational collapse of a massive star, which do not involve horizons, should also be studied. The general idea is to prevent the possibility of a horizon forming, by stopping the collapse of matter at some radius greater than that of the horizon. This prevention of the formation of a horizon thereby precludes problems like the black hole information paradox.

There are a variety of proposals including the Mazur–Mottola “gravastar” (**gravitational vacuum star**) [37]. Mazur and Mottola’s gravastar scenario is a solution of Einstein’s equations which has a Schwarzschild exterior, a de–Sitter interior, and a rigid spherical shell of matter whose thickness is of the order of the Planck length, suspended approximately a couple of Planck lengths outside of the Schwarzschild radius. Due to their extreme compactness, it seems difficult to observationally distinguish gravastars from black holes. It has been argued that any star, with a surface, will emit much more radiation during accretion than black holes (which have no surface) (see [158] for a review), but it has also been shown that gravastars may be just as ‘black’ as black holes [159].

Although the gravastar model forwarded by Mazur and Mottola has not gained much attention by the majority of general relativists, it has led others to construct similar models. Bilić *et al.* consider a gravastar with a Born-Infeld-phantom interior geometry [160], while Cattoen *et al.* generate a method for creating generalised gravastars with anisotropic continuous pressures [161]. Another scenario envisages the horizon as an emergent property of a quantum phase transition analogous to liquid-vapor critical point of a Bose superfluid [36].

Visser and Wiltshire [38] sought to determine whether the Mazur–Mottola gravastar is dynamically stable against radial perturbations. To do so, rather than considering the original Mazur–Mottola gravastar, they considered a simplified model with three layers:

- An external Schwarzschild vacuum, $\rho = 0 = P$
- A single thin shell [162], with surface density σ and surface tension θ ; with radius

$$a \geq 2M.$$

- A de Sitter (dS) interior, $P = -\rho$.

Using this model they found a condition for stability for the thin shell against radial perturbations in terms of an ‘effective energy equation’ for a non-relativistic particle with ‘energy’ E in a ‘potential’ $V(a)$,

$$\frac{1}{2}\dot{a}^2 + V(a) = E. \quad (3.1)$$

See section 4 from [38] for a precise definition of $V(a)$ and the quantities therein. The thin shell will be stable against radial perturbations if and only if there exists some a_0 such that $V(a)$ satisfies

$$V(a_0) = 0; \quad V'(a_0) = 0; \quad V''(a_0) \geq 0. \quad (3.2)$$

Using Visser and Wiltshire’s method one is able to prescribe the interior matter, $m_-(a)$, exterior matter, $m_+(a)$, and the potential $V(a)$ of the gravastar to parametrically find the equation of state for the thin shell. Indeed, as we note below, the mass of the thin shell, $m_s(a) \equiv 4\pi\sigma(a) a^2$, can be calculated as an explicit function of $m_+(a)$, $m_-(a)$ and $V(a)$.

Visser and Wiltshire demonstrated that there exist large classes of potentials, and consequently, equations of state, for which gravastars are stable against spherically symmetric gravitational perturbations as well as large classes of potentials which are unstable. Consequently, particular choices of potentials and mass functions need to be studied on a case by case basis, since more general criteria for stability are not presently known.

The layout of this chapter is as follows. We begin Section two by briefly reviewing the Schwarzschild–gravastar formalism set up by Visser and Wiltshire [38], and generalising it to include a cosmological constant in the exterior geometry. We then introduce the dominant energy condition criteria for the thin shell and find parameters for the internal and external geometries which allow the shell to be stable to radial perturbations. We also present some examples of allowable equations of state for the thin shell. In Section three we repeat the analysis of section two, but instead of a cosmological constant the exterior geometry now has electric and/or magnetic charge.

3.2 Schwarzschild–(A)dS Gravastar

3.2.1 Definitions

Following directly on from the work of Visser and Wiltshire [38], we start with the general equations, (47) and (49), from their paper. These relate the surface density, $\sigma(a)$, and surface tension, $\theta(a)$, of the thin shell which makes up the surface of the gravastar, to the potential and mass functions via

$$\sigma(a) = -\frac{1}{4\pi a} \left[\left[\sqrt{1 - 2V(a) - \frac{2m(a)}{a}} \right] \right], \quad (3.3)$$

$$\theta(a) = -\frac{1}{8\pi a} \left[\left[\frac{1 - 2V(a) - m(a)/a - aV'(a) - m'(a)}{\sqrt{1 - 2V(a) - 2m(a)/a}} \right] \right]. \quad (3.4)$$

where $m_-(a)$ is the interior mass profile, $m_+(a)$ is the exterior mass profile, $V(a)$ is the effective energy potential, and

$$[[X]] \equiv X_+ - X_-. \quad (3.5)$$

See [163] for more details on this notation. See [38] for more discussion on the above expressions and definitions. We now specialise the exterior geometry to Schwarzschild–(A)dS, the interior to (A)dS, and the potential to zero. We therefore write

$$m_+(a) = M - \Lambda a^3/6, \quad (3.6)$$

$$m_-(a) = ka^3, \quad (3.7)$$

$$V(a) = 0, \quad (3.8)$$

where Λ is the asymptotic constant spatial curvature of the exterior geometry and k is the curvature of the interior geometry due to a vacuum energy. We note that in this analysis, for $E = 0$ in Eq.(3.1), the choice of $V(a) = 0$ provides a stable equilibrium for the gravastar thin shell, as $\dot{a} = 0$, and hence the radius, a , cannot change to some other value. Simultaneously, $V(a) = V'(a) = V''(a) = 0$ for all values of a . This specialization to $V(a) = 0$ closely follows the calculation of [38]. We now convert all variables to dimensionless parameters, parameterised by M ;

$$A = \frac{a}{M}, \quad L = \Lambda M^2, \quad K = kM^2, \quad \rho = \sigma M, \quad P = \theta M. \quad (3.9)$$

This leads to

$$\rho(A) = \frac{1}{4\pi A} \left[\sqrt{1 - 2KA^2} - \sqrt{1 - \frac{2}{A} + \frac{LA^2}{3}} \right], \quad (3.10)$$

$$P(A) = \frac{1}{8\pi A} \left[\frac{1 - 4KA^2}{\sqrt{1 - 2KA^2}} - \frac{1 - \frac{1}{A} + \frac{2LA^2}{3}}{\sqrt{1 - \frac{2}{A} + \frac{LA^2}{3}}} \right]. \quad (3.11)$$

Reality of the reparameterised surface density, ρ , and surface tension, P , requires

$$\begin{aligned} K &< \frac{1}{2A^2}, \\ L &> \frac{6}{A^3} - \frac{3}{A^2}. \end{aligned} \quad (3.12)$$

3.2.2 Solutions

We first present a detailed analysis of the dominant energy condition, as it provides the most restrictive conditions on the matter of the thin shell of the gravastar. Given that the matter is presumed to form through a quantum phase transition, we cannot specifically state the type of matter that forms the thin shell, but we shall assume the dominant energy condition continues to hold. For brevity we define the region satisfying the dominant energy condition by \mathcal{M} , and the boundary of \mathcal{M} by $\partial\mathcal{M}$. The left and right sides of $\partial\mathcal{M}$ are defined by the equations

$$\rho + P = 0, \quad \rho - P = 0, \quad (3.13)$$

respectively, satisfying the condition that $\rho \geq 0$. Solutions to the above equations give the points where the equation of state, $\rho(P)$, enters or exits \mathcal{M} . After some manipulation Eqs.(3.13) become,

$$\left(3 - \frac{5}{A} + \frac{4LA^2}{3}\right) \sqrt{1 - 2KA^2} = (3 - 8KA^2) \sqrt{1 - \frac{2}{A} + \frac{LA^2}{3}}, \quad (3.14)$$

and

$$(A - 3) \sqrt{1 - 2KA^2} = A \sqrt{1 - \frac{2}{A} + \frac{LA^2}{3}}, \quad (3.15)$$

respectively. Squaring these two expressions can lead to an inclusion of a relative minus sign between the different sides of the equations, which we account for by placing extra restrictions on K and L . For K and L satisfying (3.12) we can see that the *l.h.s.* of

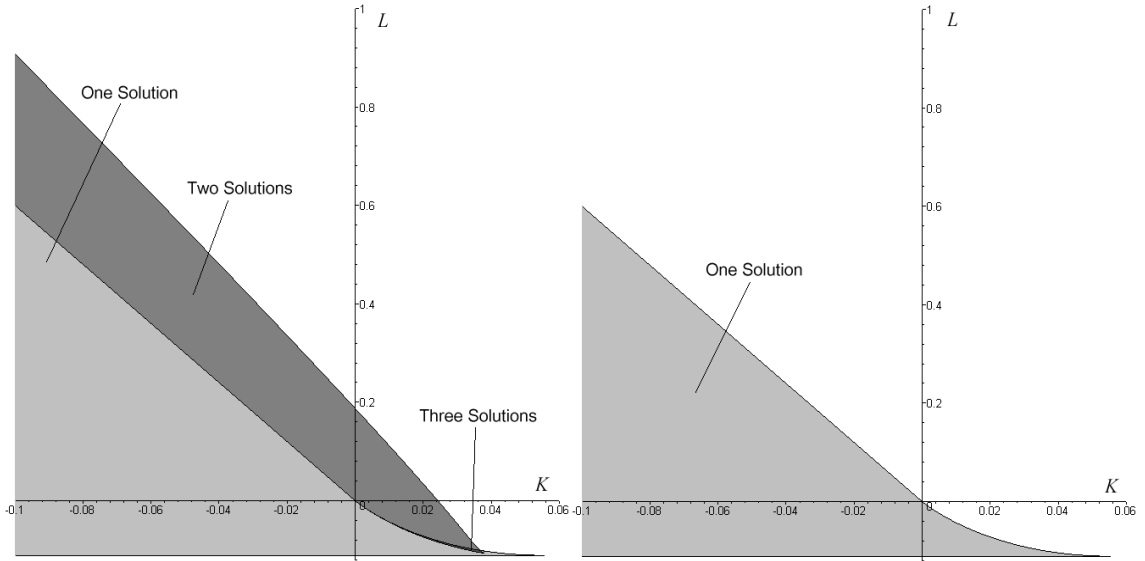


Figure 3.1: The solution space for stable gravastars with (A)dS interior and Schwarzschild–(A)dS exterior satisfying $\rho + P = 0$ in the left panel, or $\rho - P = 0$ in the right panel. The number of solutions in each graph indicates how many times the equation of state intersects the part of $\partial\mathcal{M}$ that the equation defining the graph represents. The unshaded parts have no solutions, and correspondingly have no interval of $\rho(P)$ which lies in \mathcal{M} .

(3.14) is positive. Therefore the *r.h.s.* is also positive, thereby providing the bound $K < \frac{3}{8A^2}$ which applies to Eq.(3.16) below. Similarly the *r.h.s.* of (3.15) is positive, which implies the *l.h.s.* is positive and hence $A > 3$ for Eq.(3.17) below. After some further manipulation we find the multivariate polynomials,

$$\begin{aligned} 0 = & (-32KL^2 - 192LK^2) A^8 + (16L^2 - 576K^2) A^6 \\ & + (240KL + 1152K^2) A^5 + (45L + 270K) A^4 \\ & + (-324K - 120L) A^3 - 450KA^2 - 108A + 225, \end{aligned} \quad (3.16)$$

and,

$$0 = -12A + 27 - 6KA^4 + 36KA^3 - 54KA^2 - LA^4. \quad (3.17)$$

The octic equation in A , (3.16), is not analytically solvable in general. We therefore solve this, and the quartic in A , (3.17), numerically and create a contour plot representing the number of solutions for A in the phase space parameterised by K and L . Such solutions will have a number of restrictions placed on them. Specifically, they must satisfy the inequality (3.12), $\rho > 0$, and any other conditions required for the

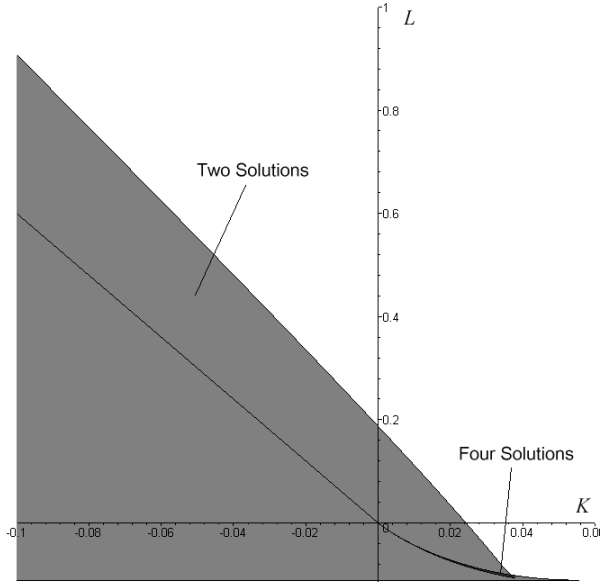


Figure 3.2: The solution space for stable Gravastars with (A)dS interior and (A)dS Schwarzschild exterior satisfying $\rho + P = 0$ or $\rho - P = 0$. The unshaded region has no solutions where $\rho(P)$ intersects $\partial\mathcal{M}$, and due to continuity of the equation of state, no interval of $\rho(P)$ lies in \mathcal{M} . The shaded regions with two solutions have one interval of $\rho(P)$ which lies in \mathcal{M} , while the region with four solutions has two intervals of $\rho(P)$ satisfying the dominant energy condition.

consistency of (3.14) and (3.15). Figure 3.1 displays the number of times the equation of state, $\rho(P)$, crosses the boundaries of \mathcal{M} , $\rho + P = 0$ and $\rho - P = 0$, separately. Figure 3.2 shows the combined results of the two panels in Fig. 3.1. Figure 3.1 is useful for determining the qualitative behavior of the equation of state, while Fig. 3.2 is useful for determining the existence of gravastar solutions which have a thin-shell satisfying the dominant energy condition.

One can see from Fig. 3.2 that there are many different regions of K and L that have real and finite solutions to the equations that define $\partial\mathcal{M}$. This means that for those values of K and L there is always an interval of the equation of state, $\rho(P)$, which satisfies the dominant energy condition. This means there can always be gravastars with thin shells of matter which satisfy the dominant energy condition and are stable to radial perturbations. Visser and Wiltshire's gravastar with an exterior Schwarzschild solution is reproduced as a special case in this diagram when $L = 0$. The unshaded

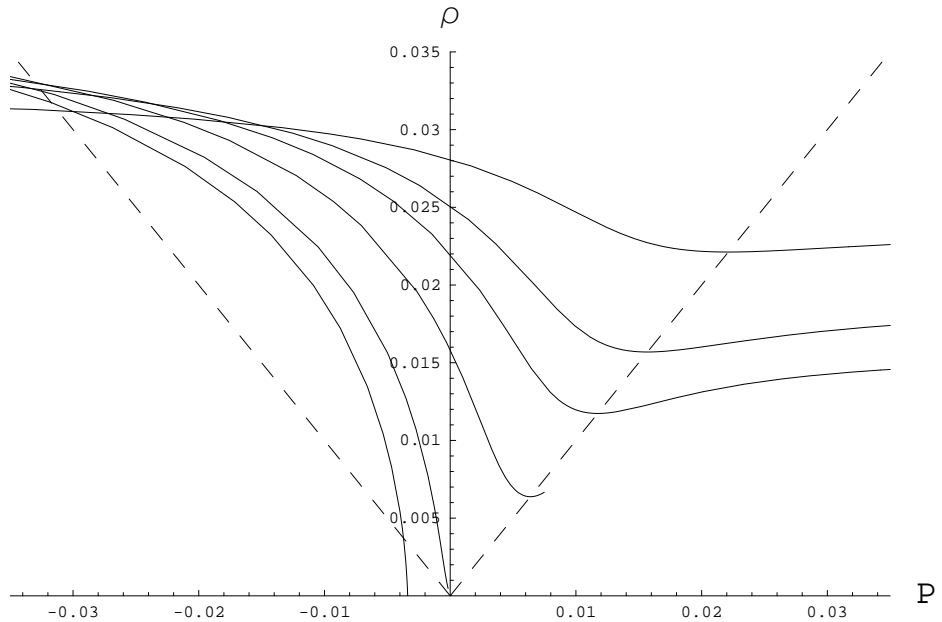


Figure 3.3: The behavior of $\rho(P)$ for the thin shell of a gravastar with $K = -0.01$ and a range of values of L . From left to right, $L = \{0.1, 0.06, 0, -0.0435, -0.7, -0.1\}$.

region has no solutions, implying that the equation of state does not enter or exit \mathcal{M} . One can check that for those parameter ranges $\rho(P)$ does not lie in \mathcal{M} . This means that for those values of the parameters K and L , it is not possible to form a gravastar which has a static thin-shell satisfying the dominant energy condition which is stable under radial perturbations.

One can find the five ‘bounding curves’, which are depicted by $L(K)$ in Fig. 3.2, by studying the factorised discriminants of Eqs. (3.16)-(3.17), where (3.16)-(3.17) are viewed as polynomials in A , and the restrictions on the parameters given by (3.12) that ensure ρ and P are real. The ‘bounding curves’ are the relevant parametric curves which bound the regions of the number of intersections of $\rho(P)$ with $\partial\mathcal{M}$. They are given by,

$$\begin{aligned}
 L &= -1/9, \\
 L &= -6K, \\
 L &= 2K \left(\frac{\sqrt{600K}}{3} - 3 \right), \\
 L &= 2K(\sqrt{72K} - 3),
 \end{aligned} \tag{3.18}$$

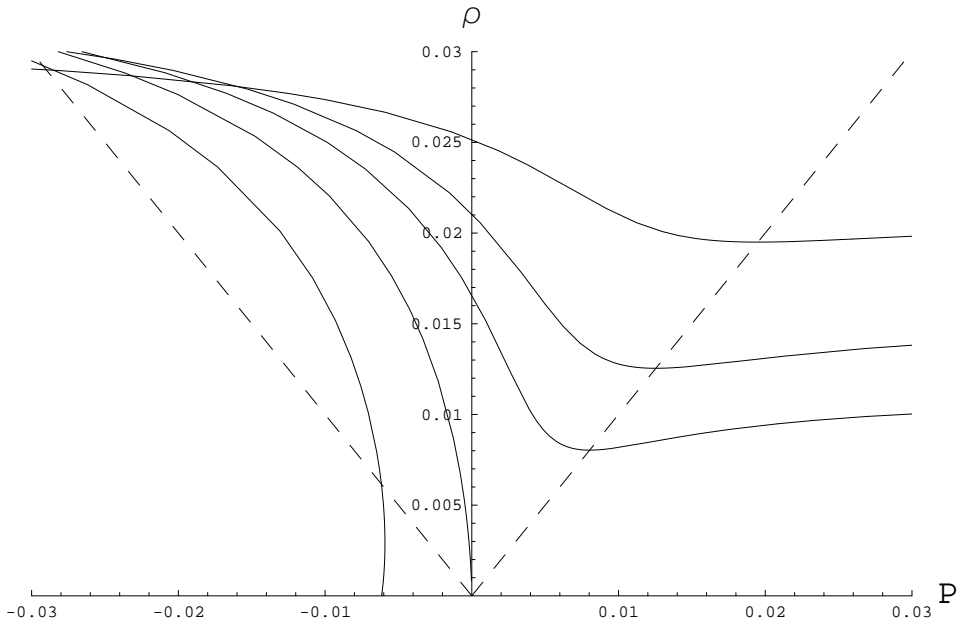


Figure 3.4: The behavior of $\rho(P)$ for the thin shell of a gravastar with $K = 0$ and a range of values of L . From left to right, $L = \{0.07, 0, -0.0435, -0.07, -0.1\}$.

and the ninth order polynomial in L , namely $L_9(K)$, which is found by factorising the discriminant of (3.16). (The actual expression is too large to fit here.)

There is a small region of the parameter space for K and L , with stable gravastar solutions when the interior is a de Sitter space, while there exists an infinitely large region of the parameter space for K and L when the interior is anti-de Sitter space. The region with a Schwarzschild-de Sitter exterior is much larger than the region with a Schwarzschild-anti-de Sitter exterior. The most important bounds on K and L , governing the existence of gravastar solutions, are given by $-1/9 < L < L_9(K)$.

There are different qualitative behaviors that $\rho(P)$ can take depending on the value of the parameters K and L , which we present in Figs. (3.3)–(3.5). The various graphs show the quantitative behavior of $\rho(P)$ for specific values of K and L , but each graph is indicative of the qualitative behavior of $\rho(P)$ for a particular range of values of K and L . The equation of state exhibits a smooth transition from one type of qualitative behavior to another as the values of K and L pass over the ‘bounding curves’.

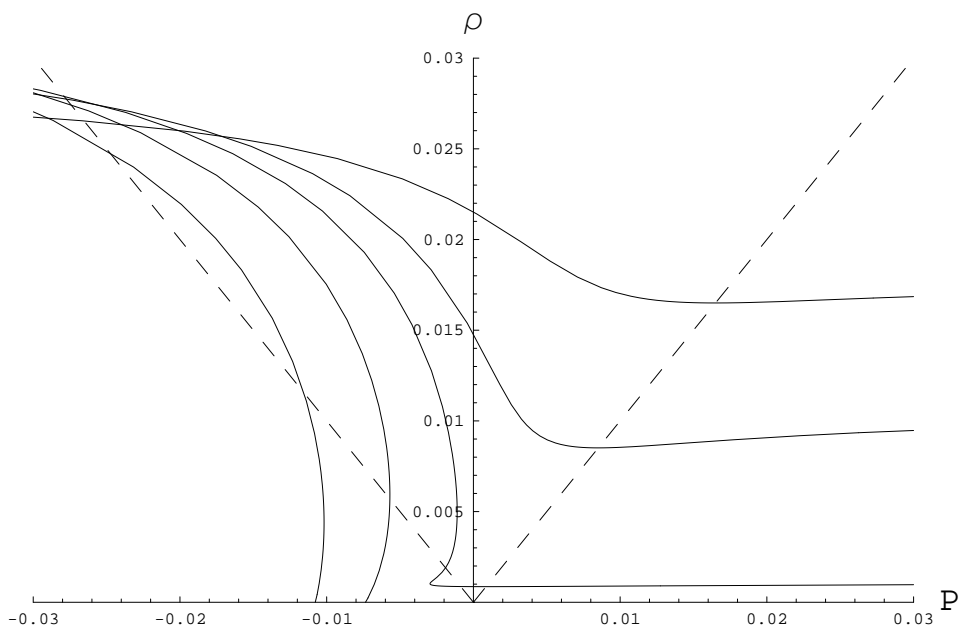


Figure 3.5: The behavior of $\rho(P)$ for the thin shell of a gravastar with $K = 0.01$ and a range of values of L . From left to right, $L = \{0.07, 0, -0.0435, -0.07, -0.1\}$.

3.3 Reissner–Nordström gravastar

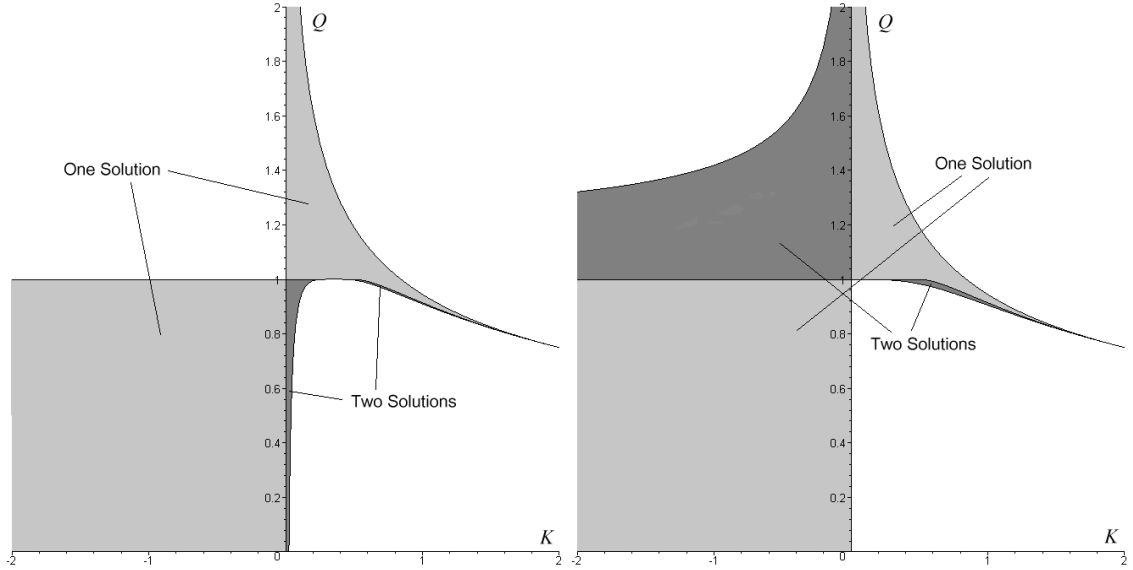


Figure 3.6: The solution space for stable Gravastars with (A)dS interior and Reissner–Nordström exterior, satisfying $\rho + P = 0$ in the left panel, or $\rho - P = 0$ in the right panel. The number of solutions describes how many times $\rho(P)$ passes through the left or right side of $\partial\mathcal{M}$ in the left or right panel respectively. If there are no solutions, then $\rho(P)$ does not cross $\partial\mathcal{M}$, and no interval of $\rho(P)$ satisfies the dominant energy condition.

We now consider a gravastar with charge q such that the radial electric field is given by $E_r = \frac{q}{r^2}$. In this case,

$$\begin{aligned} m_+ &= M - \frac{q^2}{2A}, \\ m_- &= kA^3. \end{aligned} \quad (3.19)$$

Following the same procedure as used for the Schwarzschild (A)dS case we find the dimensionless equations that define the endpoints of the interval of $\rho(P)$ in \mathcal{M} , located on the left ($\rho + P = 0$) and right ($\rho - P = 0$) sides of $\partial\mathcal{M}$, given respectively by,

$$\left(3 - \frac{5}{A} + \frac{2Q}{A^2}\right) \sqrt{1 - 2KA^2} = (3 - 8KA^2) \sqrt{1 - \frac{2}{A} + \frac{Q}{A^2}}, \quad (3.20)$$

and

$$\left(1 - \frac{3}{A} + \frac{2Q}{A^2}\right) \sqrt{1 - 2KA^2} = \sqrt{1 - \frac{2}{A} + \frac{Q}{A^2}}, \quad (3.21)$$

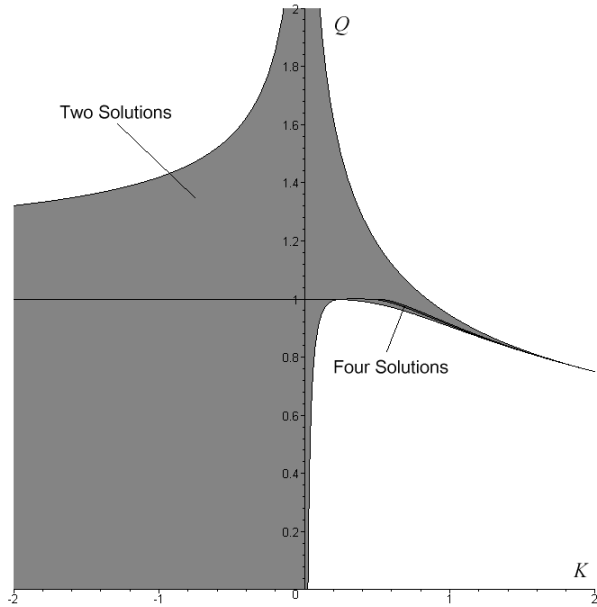


Figure 3.7: The solution space for stable Gravastars with (A)dS interior and Reissner–Nordström exterior, where $\rho(P)$ for the thin shell satisfies either $\rho + P = 0$ or $\rho - P = 0$. The regions with solutions have at least one interval of $\rho(P)$ which lies in \mathcal{M} . Therefore, for these regions, there exist stable gravastar solutions. Conversely, the regions without solutions do not allow stable gravastar solutions where the thin shell satisfies the dominant energy condition.

where $Q = \frac{q^2}{M^2} \geq 0$. The other dimensionless quantities are as shown in (3.9). These can be manipulated to give

$$\begin{aligned} 0 = & -64K^2A^8 + 128K^2A^7 + (30K - 64QK^2)A^6 - 36KA^5 - 20QA + 4Q^2 \\ & + (24KQ - 50K)A^4 + (40KQ - 12)A^3 + (3Q + 25 - 8KQ^2)A^2, \end{aligned} \quad (3.22)$$

and,

$$\begin{aligned} 0 = & -2KA^6 + 12KA^5 + (-8KQ - 18K)A^4 + (24KQ - 4)A^3 \\ & + (3Q + 9 - 8KQ^2)A^2 - 12QA + 4Q^2, \end{aligned} \quad (3.23)$$

respectively. Once again we demand that ρ and P be real which leads to

$$\begin{aligned} K &< \frac{1}{2A^2} \\ Q &> 2A - A^2. \end{aligned} \quad (3.24)$$

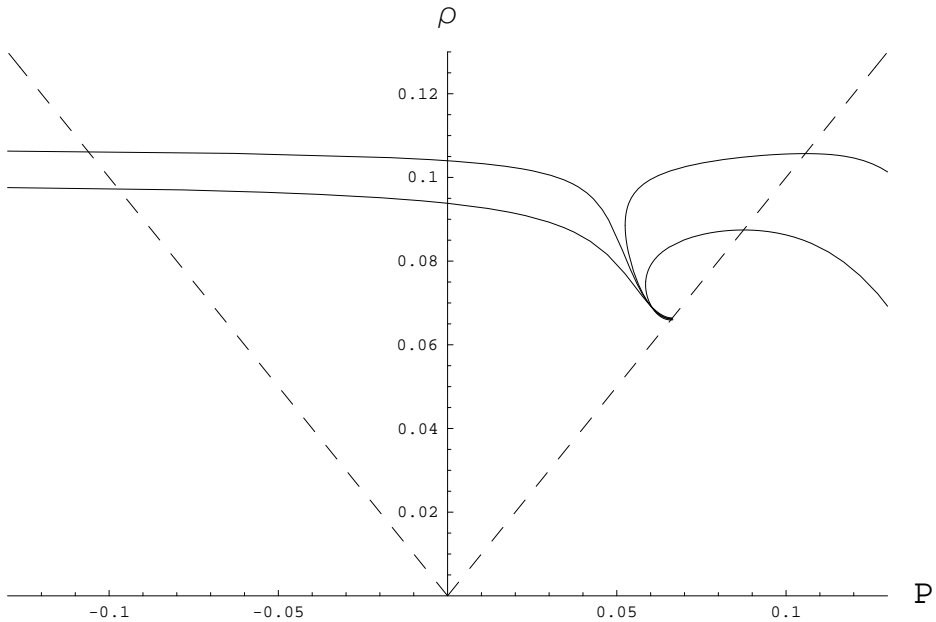


Figure 3.8: The behavior of $\rho(P)$ for the thin shell of a gravastar with $K = -0.5$ and a range of values of Q . From left to right, $Q = \{0.9, 0.99, 1.01, 1.1\}$. The behavior for $Q < 1$ is qualitatively different to that of $Q > 1$.

As before, squaring (3.20) and (3.21) can lead to an inclusion of a relative minus sign in (3.22) and (3.23) respectively, which we account for by placing extra restrictions on K and Q so that (3.22) and (3.23) are consistent with (3.20) and (3.21). We present our findings for the left and right sides of $\partial\mathcal{M}$, $\rho + P = 0$ and $\rho - P = 0$, separately in the left and right panels of Fig. 3.6, while we combine the panels in Fig. 3.7.

Once again the parametric bounds are given by some of the factors of the discriminants of (3.22) and (3.23) when they are viewed as polynomials in A , the condition that $\rho \geq 0$, and the inequalities in (3.24). The case studied by Visser and Wiltshire [38] is recovered here with $Q = 0$. There are five bounding curves. Three of them are given by,

$$Q = 1, \quad (3.25)$$

$$Q = \frac{3(2K^2)^{1/3}}{4K}, \quad (3.26)$$

$$Q = \frac{-1 + 2\sqrt{2K}}{2K}. \quad (3.27)$$

The fourth one is given by polynomial which is twelfth order in Q , found by factorising

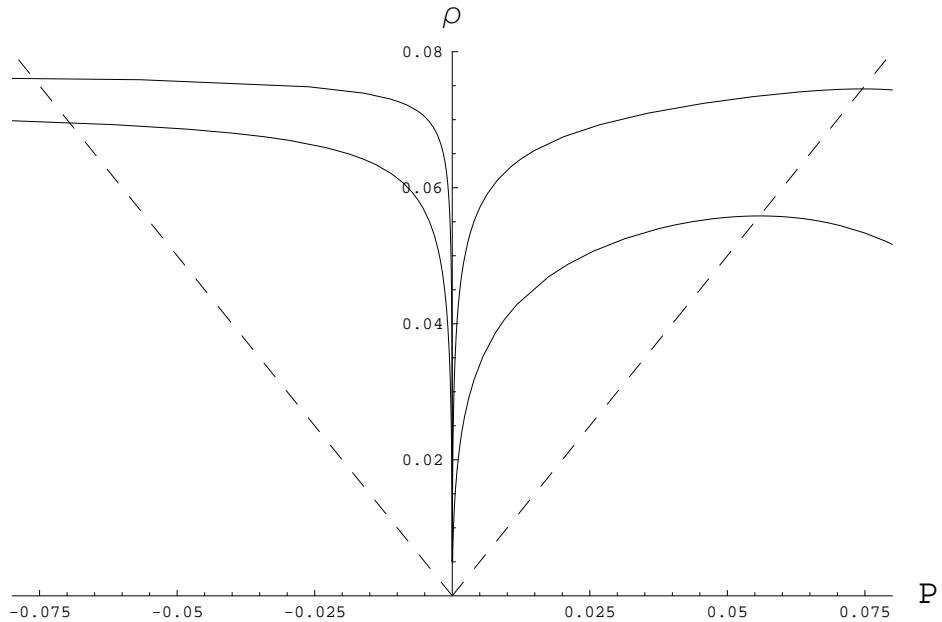


Figure 3.9: The behavior of $\rho(P)$ for the thin shell of a gravastar with $K = 0$ and a range of values of Q . From left to right, $Q = \{0.99, 0.999, 1.01, 1.1\}$. The behavior for $Q < 1$ is qualitatively different to that of $Q > 1$.

the discriminant of (3.20). The fifth bound is given by the octic in Q found by factorising the discriminant of (3.21). The qualitative behaviors of the equation of state depend on the choice of the parameters $\{K, Q\}$, as seen in Figs. 3.8–3.11.

Extending this section to include a magnetic charge is straight forward, via the substitution $q^2 \rightarrow q^2 + p^2$ where p is the total magnetic charge of the system. It does not change the results in terms of Q , instead it amounts to a redefinition of what we attribute Q to. We note that including a non-zero charge to the exterior of the gravastar greatly increases the range of parameter K of the (A)dS interior for which solutions exist. Gravastars with a charge approximately equal to their mass are ‘most favored’ for a de Sitter interior in the sense that for such values of Q the least amount of ‘fine-tuning’ of K is required. However, when $Q = 1$, $\rho(P)$ appears to be discontinuous for $K < 0.423798525400$ (13s.f.).

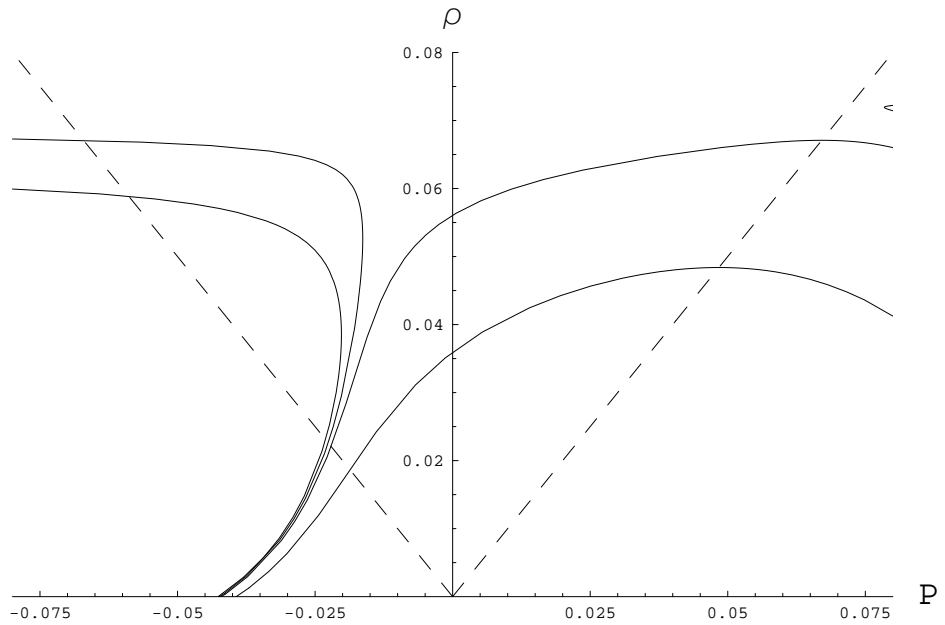


Figure 3.10: The behavior of $\rho(P)$ for the thin shell of a gravastar with $K = 0.1$ and a range of values of Q . From left to right, $Q = \{0.9, 0.99, 1.01, 1.1\}$. The behavior for $Q < 1$ is qualitatively different to that of $Q > 1$.

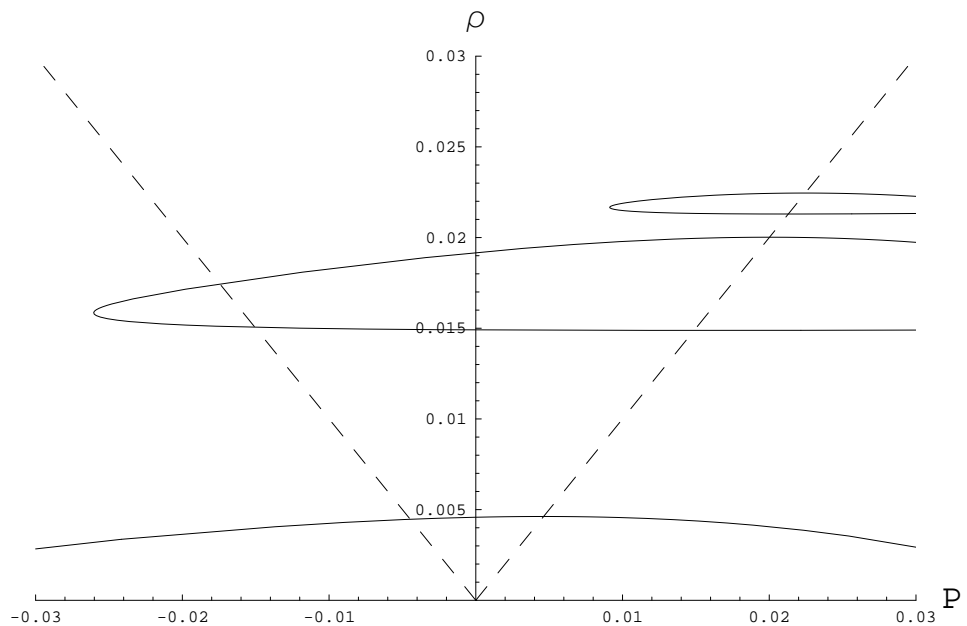


Figure 3.11: This figure shows the behavior of $\rho(P)$ for the thin shell of a gravastar with $K = 0.8$ and a range of values of Q . From top to bottom, $Q = \{0.945, 0.951, 1\}$. The qualitative behavior of the equation of state is continuous as $Q \rightarrow 1$.

3.4 Conclusion

In this chapter it has been demonstrated that the method presented by Visser and Wiltshire [38] can be used to generate stable gravastars with a non-trivial exterior involving either a vacuum energy or an electromagnetic charge. The Schwarzschild case they studied is retrieved here as a special case. The case with a Schwarzschild-(A)dS exterior, (see Fig. 3.2), puts bounds on both the interior and exterior values of a vacuum energy allowable for stable gravastar solutions to exist. The most important bound in this case is that the exterior vacuum energy satisfies $-\frac{1}{9}M^{-2} < \Lambda < L_9(K)M^{-2}$.

The Reissner–Nordström solution (Fig. 3.7) is very interesting as it is physically reasonable to allow massive stellar objects to have a (small) non-zero electric charge. We find that for a de Sitter interior, the range of the allowable vacuum energy smoothly increases as one adds charge, until the charge is close to the limit $q^2 = M^2$. At this point the range of the parameter governing the interior vacuum energy becomes greatly enlarged by comparison with the $q = 0$ (Schwarzschild) case. These results are important as they demonstrate that there exists a wide range of allowable gravastars with thin shells satisfying the dominant energy condition which are stable to radial perturbations.

For future research it would be interesting to study the model in [38] with $V(a) \neq 0$ or $\dot{a} \neq 0$ as these represent a wider class of configurations of potential gravastars. Another avenue for furthering this research would be to consider a gravastar with external Kerr–geometry, although the method provided by [38] would have to be generalised first to include off–diagonal terms in the metric, and that is likely to be highly non–trivial.

One source of a realistic gravastar interior might be a fundamental scalar field resulting from Kaluza–Klein compactification of extra dimensions [164] (see [165] or [166] for a review). Therefore it would be interesting to see what effect a scalar field has on the stability of the external geometry. Finally, investigating the implications of transitions in the equation of state from one type of qualitative behavior to another is of interest (see Figs. 3.8–3.10); we leave this work for a future paper.

Chapter 4

Hybrid Brane Worlds in the Salam-Sezgin Model

4.1 Hybrid Brane Worlds

The idea that our universe might be a surface (either a thin or thick “brane”) embedded in a higher-dimensional spacetime with large bulk dimensions [75]–[168] continues to be the focus of much interest. While 5-dimensional models based on the Randall–Sundrum scenarios [167, 168] have attracted the most attention, recently there has been growing interest in 6-dimensional models [169]–[185].

One reason for investigating 6-dimensional models is to determine whether or not some of the more interesting features of brane world models in five dimensions are peculiar to five dimensions. Another reason is that six dimensions allow one greater freedom in building models with positive tension branes only [94]. Possibly the strongest motivation for investigating six dimensional models is the possibility of solving the cosmological constant problem in a natural manner [176, 180]. While codimension two branes do pose technical problems for the cosmological constant issue [182], which might be more easily resolved in the model considered here, we will not address the solution of the cosmological constant problem directly in this chapter; it remains an interesting possibility for future work.

A common feature of many of the 6-dimensional models currently being investigated

is that, in order to localize gravity on a 3-brane, a 4-brane is incorporated into the model at a finite proper distance from the 3-brane. (See, for example, the work of refs. [94, 173, 177], which are based on extensions of the AdS soliton [186].) However, due to the form of the bulk geometry, Einstein's equations often preclude the insertion of simple 4-branes of pure tension into these models. Several mechanisms have been proposed to deal with this, including the addition of a particular configuration of matter fields to the brane [169] and “delocalization” of a 3-brane around the 4-brane [94]. In this chapter, we will by contrast discuss a 6-dimensional brane world model with localized gravity and a single 4-brane with tension coupled to a scalar field, generalizing an earlier construction by Louko and Wiltshire [172]. The construction is fundamentally different to those which consider our observed universe to be a codimension two defect; in particular the physical universe is a codimension one brane in six dimensions with an additional Kaluza–Klein direction.

The construction of ref. [172] was based on the bulk geometry of fluxbranes in 6-dimensional Einstein–Maxwell theory with a bulk cosmological constant [78], a model which continues to attract attention in its own right [187]. However, if one is interested in 6-dimensional models then a more natural choice might be a supersymmetric model, such as the chiral, $N = 2$ gauged supergravity model of Salam and Sezgin [188, 189]. Generally higher-dimensional models of gravity are introduced in the context of supergravity models, which are themselves low-energy limits of string– or M-theory.

Supersymmetry has of course played a central role in the recently studied codimension two brane world constructions, and the Salam–Sezgin model has featured in the supersymmetric large extra dimensions scenario [175, 176, 179, 183, 185]. One motivation for providing an alternative construction based on codimension one branes is that discontinuities associated with codimension one surfaces in general relativity are very well understood and easier to treat mathematically than codimension two or higher defects [190, 191]. While codimension two defects can be regularised a host of technical issues are introduced when additional matter fields are added to the brane [182, 192]. The construction of ref. [172] avoids these problems. Similarly, whereas the anti-de Sitter horizon in the bulk of the Randall–Sundrum II model [168] can become singular upon additional of matter fields, the construction of [172] involves

a geometry which closes in a completely regular fashion in the bulk. Full non-linear gravitational wave solutions were exhibited in the background of ref. [172], without additional singularities.

The biggest phenomenological problem faced by the model of [172] was that the parameter freedom available in 6-dimensional Einstein–Maxwell theory with a cosmological constant did not seem to allow the proper volume of the compact dimensions to be made arbitrarily large as compared to the proper circumference of the Kaluza–Klein circle, as would be required for a solution of the hierarchy problem. It is our aim in this chapter to demonstrate that a supersymmetric background can solve this problem, and that an interesting hybrid compactification without singularities arises.

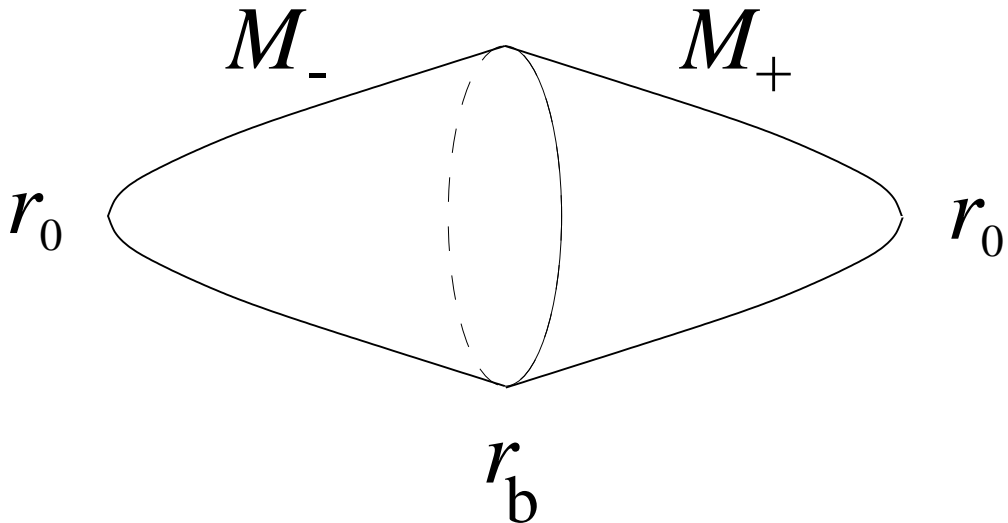


Figure 4.1: *An embedding of the bulk (r, θ) dimensions of \mathcal{M} into \mathbb{R}^3 .*

The model considered in this article can therefore be viewed as a five dimensional Kaluza–Klein universe that forms a co-dimension one surface within a six-dimensional bulk where the codimension has a \mathbb{Z}_2 symmetry across the brane which smoothly terminates in a totally geodesic submanifold, a “bolt”, which does not suffer a conical defect. An embedding diagram of the bulk is shown in Fig.4.1 where the bolts are at r_0 , the brane at r_b , and the bulk geometry has been mirrored across the brane. The topology of the bulk solution is thus $\mathbb{R}^4 \times S^2$. We consider the case where there is both a magnetic flux in the bulk (the fluxbrane) and a bulk scalar field, the potential of which is dictated by the form of the Salam-Sezgin action. While the model can in

principle support any Einstein space, we limit most of our analysis to the case where the 4-dimensional cosmological constant is zero (i.e. the observed universe is Minkowski) in order to solve the field equations exactly. Both the bulk magnetic field and the bulk scalar field will impact the behaviour of gravity on the brane and we show how one can explicitly calculate the essential features of the gravitational potential between two test masses on the brane. Since it is assumed that the brane will correspond to our universe (modulo the Kaluza-Klein dimension) this will indicate how the effects of the extra dimensions and their fields will modify four dimensional gravity.

The chapter is organized as follows. In Section 2 we introduce the Salam-Sezgin fluxbrane solution and discuss the structure of the bulk geometry. In Section 3 we go on to discuss junction conditions arising from the brane and show how the position of this brane is fixed by the bulk geometry alone. In section 4 we show how this construction gives rise to a Newton-like gravitational law in the brane, together with the exponential corrections expected of a model with compact extra dimensions. While the analysis is made by analogy to the case of a scalar propagator, the calculation contains the essential features important to the more involved calculation for gravitational perturbations. This is justified by the presentation of nonlinear gravitational wave solutions in Section 4.4.4. The hierarchy problem is addressed in Section 4.5. In section 4.6 general arguments are presented about the extension to the case of physical universes with the geometry of general Einstein spaces, which include the phenomenologically interesting case of de Sitter space.

4.2 Salam-Sezgin fluxbranes

The bosonic sector of $N = 2$ chiral Einstein-Maxwell supergravity in six dimensions – the Salam-Sezgin model [188, 189] – may be truncated to the degrees of freedom described by the action:

$$S = \int_M d^6x \sqrt{-g} \left(\frac{\mathcal{R}}{4\kappa^2} - \frac{1}{4} \partial_a \phi \partial^a \phi - \frac{1}{12} e^{-2\kappa\phi} G_{abc} G^{abc} - \frac{1}{4} e^{\kappa\phi} F_{ab} F^{ab} - \frac{\Lambda}{2\kappa^2} e^{-\kappa\phi} \right) \quad (4.1)$$

where F_{ab} is the field strength of a $U(1)$ gauge field, G_{abc} is the 3-form field strength of the Kalb-Ramond field, \mathcal{B}_{ab} , ϕ is the dilaton, $\kappa^2 = 4\pi G_6$ and $\Lambda = g_1^{-2}/(\kappa^2) > 0$, where

g_1 is the $U(1)$ gauge constant. Generically, the bosonic action (4.1) is supplemented by the contribution of additional scalars, Φ^A , belonging to hypermultiplets. However, these may be consistently set to zero.

We will also make the additional simplification of setting the Kalb-Ramond field, \mathcal{B}_{ab} , to zero, as we wish to consider just the simplest non-trivial fluxbrane solutions in the Salam-Sezgin model. This leaves us with the field equations:

$$G_{ab} = 2\kappa^2 e^{\kappa\phi} (F_{ac}F_b{}^c - \tfrac{1}{4}g_{ab}F^{cd}F_{cd}) + \kappa^2 (\partial_a\phi\partial_b\phi - \tfrac{1}{2}\partial^c\phi\partial_c\phi) - g_{ab}\Lambda e^{-\kappa\phi} \quad (4.2)$$

$$\partial_a (\sqrt{-g}e^{\kappa\phi}F^{ab}) = 0, \quad (4.3)$$

$$\square\kappa\phi - \tfrac{1}{2}\kappa^2 e^{\kappa\phi}F_{ab}F^{ab} + \Lambda e^{-\kappa\phi} = 0. \quad (4.4)$$

Static fluxbrane solutions may be found by assuming a metric ansatz of the form

$$ds_6^2 = r^2 \bar{g}_{\mu\nu} dx^\mu dx^\nu + \frac{f(r)^2 dr^2}{\Delta(r)} + \Delta(r) d\theta^2, \quad (4.5)$$

where θ is the Kaluza-Klein direction, r is the radion and $\bar{g}_{\mu\nu}(x)$ is the metric on a 4-dimensional Einstein spacetime of signature $(- +++)$, such that

$$\bar{\mathcal{R}}_{\mu\nu} = 3\bar{\lambda} \bar{g}_{\mu\nu}. \quad (4.6)$$

Additionally, we assume that $\phi = \phi(r)$, and that the $U(1)$ gauge field consists purely of magnetic flux in the bulk

$$\mathbf{F} = \frac{\sqrt{8}Bf e^{-\kappa\phi}}{\kappa r^4} dr \wedge d\theta, \quad (4.7)$$

Rather than solving the field equations directly, fluxbrane solutions are often conveniently obtained by double analytic continuation of black hole solutions with a central electric charge. This double analytic continuation technique was in fact first introduced when fluxbranes were first constructed [78], in D -dimensional Einstein-Maxwell theory with a cosmological constant. In the present model, the dual 6-dimensional black hole spacetime is obtained by the continuation

$$\bar{x}_0 \rightarrow i\tilde{x}_1; \quad \bar{x}_i \rightarrow \tilde{x}_{i+1} \quad (i = 1, 2, 3); \quad \theta \rightarrow it; \quad B \rightarrow -iQ; \quad (4.8)$$

where it is assumed that $\partial/\partial x_0$ is a Killing vector and that the Einstein space metric is written in coordinates with $\bar{g}_{00} < 0$ and $\bar{g}_{0i} = 0$.

Black hole type solutions are not well-studied in the case of the field equations (4.2)–(4.4), however, on account of the fact that no conventional black holes exist for the Einstein-Maxwell scalar with a Liouville potential. There are no solutions with a regular horizon which are asymptotically flat, asymptotically de Sitter or asymptotically anti-de Sitter [194]. There do exist black hole type solutions with regular horizons which possess “unusual asymptotics” at spatial infinity [194, 195]. From the point of view of the double analytically dual fluxbranes, the asymptotic structure of the black hole spacetimes is irrelevant, and we are simply interested in the most general solution to the field equations (4.2)–(4.4) with the ansatz (4.5)–(4.7).

To the best of our knowledge the full solutions of the field equations (4.2)–(4.4) with arbitrary $\bar{\lambda}$ and Λ have not been written down, either for the fluxbranes or the double analytically dual static black hole type geometries. The $\bar{\lambda} = 0$ case has been given previously [179]. The general case with non-zero $\bar{\lambda}$ does not appear to readily yield a closed form analytic solution. Its properties are discussed in section 4.6.

The fluxbrane solution for $\bar{\lambda} = 0$ takes the form

$$f(r) = r, \tag{4.9}$$

$$\phi(r) = \frac{2}{\kappa} \ln(r), \tag{4.10}$$

$$\Delta(r) = \frac{A}{r^2} - \frac{B^2}{r^6} - \frac{\Lambda}{8}r^2, \tag{4.11}$$

where we require that $A > 0$ so that $\Delta(r)$ has at least one root.

The finite limits of the range of the bulk coordinate r are the points at which $\Delta(r) = 0$, since $\Delta(r) > 0$ is required to preserve the metric signature. There are at most two positive zeroes of $\Delta(r)$, located at

$$r_{\pm}^4 = \frac{4A}{\Lambda} \left(1 \pm \sqrt{1 - \frac{B^2\Lambda}{2A^2}} \right). \tag{4.12}$$

For $\Lambda > 0$, reality of r implies the condition $B^2\Lambda \leq 2A^2$. For $\Lambda < 0$ there is a single positive zero of Δ at r_- . Our primary interest is of course for $\Lambda > 0$, which is the case in the Salam-Sezgin model.

We wish the geometry to be regular at points where $\Delta(r) = 0$ and we therefore

impose the condition that θ be periodic with period

$$\frac{4\pi}{\partial_r \Delta(r)} \Big|_{r_0}, \quad (4.13)$$

where r_0 is any positive zero of $\Delta(r)$ such that $\partial_r \Delta(r)|_{r_0} \neq 0$. In these circumstances the $r = r_0$ submanifold is totally geodesic, namely a ‘‘bolt’’ in the terminology of [105]. In the case that two zeroes of $\Delta(r)$ exist we can fix the bolt to be at either r_- or r_+ but not both simultaneously as the fixing of the period of θ allows the geometry to be regular at only one of the zeroes of $\Delta(r)$.

4.3 Adding a thin brane

We now follow the construction of [172] and add a thin brane – namely a timelike hypersurface of codimension one – at a point r_b such that $r_- \leq r_b \leq r_+$ and $\Delta(r_b) > 0$. To do this we add the term

$$S_{\text{brane}} = - \int d^6x \delta(r - r_b) \frac{T}{\kappa^2} e^{-\lambda\kappa\phi} \sqrt{-h}, \quad (4.14)$$

to the action (4.1) where h_{ij} is the induced metric on the brane, $h = \det(h_{ij})$, Latin indices i, j, \dots run over the five dimensions on the brane (θ, x^μ) , T is a nonvanishing constant proportional to the brane tension, and λ is a dimensionless coupling constant. The tension of the thin brane is coupled to the scalar field in order to make the scalar field equation consistent at the junction between the two spacetimes: given that the derivative of the scalar must be discontinuous there the boundary term which was assumed to vanish in deriving (4.4) will no longer be zero.

In a Gaussian normal coordinate system for the region near the thin brane, with normal coordinate $d\eta = \Delta^{-1/2} r dr$, the induced metric takes the form

$$h_{ij} = g_{ij} - n_i n_j = \begin{pmatrix} \Delta(r) & \mathbf{0} \\ \mathbf{0} & r^2 \bar{g}_{\mu\nu} \end{pmatrix}, \quad (4.15)$$

where

$$n_i = \partial_i \eta = \frac{r}{\sqrt{\Delta}} \delta_i^r. \quad (4.16)$$

We then impose \mathbb{Z}_2 symmetry about r_b by pasting a second copy of the bulk geometry on the other side of the thin brane. We label the bulk geometry to the left of the brane

\mathcal{M}_- , and the geometry to the right \mathcal{M}_+ . A pictorial embedding diagram of the bulk dimensions is shown in Fig. 4.1.

The field equations (4.2)–(4.4) are modified by terms arising from the variation of the action (4.14), but can still be satisfied by appropriate junction conditions, according to the standard thin-shell formalism. In particular, the modification to the Einstein equation (4.2) is satisfied provided the discontinuity in the extrinsic curvature, $K_{ij} = h_i^k h_j^\ell \nabla_k n_\ell$ is related to the 4-brane energy-momentum, S_{ij} , according to

$$[[K_{ij}]] = -2\kappa^2 \left(S_{ij} - \frac{1}{4}S h_{ij} \right). \quad (4.17)$$

Here $[[X]]$ denotes the discontinuity in X across the brane. The modified scalar equation is satisfied provided that the boundary term arising from the discontinuity in the derivative of ϕ cancels the variation of (4.14) w.r.t. ϕ , leading to

$$\left[-\frac{1}{2}\sqrt{-g} n^\mu \partial_\mu \phi + \frac{\lambda T}{\kappa} \sqrt{-h} e^{-\lambda \kappa \phi} \right]_{r_b} = 0. \quad (4.18)$$

The $U(1)$ gauge field strength, F_{ab} , can be chosen to be continuous at the junction, so that the Maxwell-type equation (4.3) is automatically satisfied. As observed in [172] it should be also possible to choose a gluing which would change the sign of F_{ab} across the junction at the expense of adding a further “cosmological current” action term to the brane in addition to (4.14). Such a term would now involve a coupling to the scalar field, and would therefore modify the analysis that follows. We will not pursue that option here.

On account of (4.10) the solution to (4.18) is

$$T = \lambda^{-1} r_b^{2\lambda-1}. \quad (4.19)$$

This reduces the three unknown parameters, T, λ, r_b , to two independent ones. Further restrictions result from (4.17). For a static brane in Gaussian normal coordinates, $K_{ij} = \frac{1}{2} \frac{\partial h_{ij}}{\partial \eta}$. Furthermore, while η does not change sign across the brane, the direction of r changes sign across the brane as r points from r_- to r_b , or r_b to r_+ , depending on whether the bolt is at r_- or r_+ . Thus

$$\epsilon \left(\frac{dr}{d\eta} \right)^{(-)} = -\epsilon \left(\frac{dr}{d\eta} \right)^{(+)} = \frac{\sqrt{\Delta}}{r} \quad (4.20)$$

where $\epsilon = \text{sign}(r_b - r_0)$, and the superscripts (\pm) refer to the two sides of the 4-brane and are not to be confused with r_\pm . Hence the jump in the extrinsic curvature is

$$[[K_{ij}]] = -\epsilon \frac{\sqrt{\Delta}}{r} \frac{\partial h_{ij}}{\partial r} \Big|_{r=r_b} = \frac{-T}{2} e^{-\lambda\kappa\phi} h_{ij}, \quad (4.21)$$

where we have also used $S_{ij} = -\frac{T}{\kappa^2} e^{-\lambda\kappa\phi} h_{ij}$. Using (4.15) to substitute for the induced metric, eq. (4.21) reduces to the pair of equations

$$\partial_r \Delta(r_b) = \frac{\epsilon T}{2} r_b \sqrt{\Delta(r_b)} e^{-\lambda\kappa\phi(r_b)} \quad (4.22)$$

$$\sqrt{\Delta(r_b)} = \frac{\epsilon T}{4} r_b^2 e^{-\lambda\kappa\phi(r_b)} \quad (4.23)$$

or equivalently

$$\frac{\partial}{\partial r} \left(\frac{\Delta}{r^2} \right) \Big|_{r_b} = 0. \quad (4.24)$$

Solving (4.24) we find

$$r_b^4 = \frac{2B^2}{A} = \frac{2r_+^4 r_-^4}{r_+^4 + r_-^4}. \quad (4.25)$$

We note that the brane position does not depend on the value of the scalar potential Λ . Combining (4.10), (4.19) and (4.23) we find

$$\lambda = \frac{\epsilon}{4} \frac{r_b}{\sqrt{\Delta(r_b)}}, \quad (4.26)$$

and

$$T = 4\epsilon \sqrt{\Delta(r_b)} r_b^{\frac{\epsilon r_b}{2\sqrt{\Delta(r_b)}} - 2}, \quad (4.27)$$

where r_b is given by (4.25) and $\Delta(r_b)$ by

$$\Delta(r_b) = \left(\frac{A}{2} \right)^{3/2} \frac{1}{B} \left(1 - \frac{B^2 \Lambda}{2A} \right), \quad (4.28)$$

in terms of A , B and Λ . The tension is positive if we choose the bolt to be at $r_0 = r_-$ so that $\epsilon = 1$. We will avoid any potential problems associated with negative tension branes by henceforth choosing the bolt to be at r_- .

4.3.1 Consistency conditions when adding a thin-brane

It is possible to consider models without the restrictions which we have chosen to place on our parameters so that we could solve the bulk field equations. If we remove

the restrictions we placed on $f, \bar{\lambda}, \phi$ then we may consider what would be required of the parameters in the bulk to leave the field equations consistent upon addition of a thin brane at a finite distance from the fluxbrane, without explicitly solving Einstein's equations for the bulk or junction conditions. Even solving the Einstein equations is difficult in the general case, although we present arguments in section 4.6 that a class of solutions does exist in phenomenologically interesting cases, such as a positive cosmological constant, $\bar{\lambda} > 0$, on the brane.

Consistency conditions of the form given in [94] can be used to further restrict the parameters of the model. Putting $D = 6$, $p = 3$ and $q = 4$ in equation (2.17) of [94] and integrating over the boundary of the internal space we get

$$0 = \oint dr d\theta r^{\alpha+2} \left(\alpha \bar{\mathcal{R}} r^{-2} + (3 - \alpha) \tilde{\mathcal{R}} - (\alpha + 3) \Lambda_{\text{Bulk}} \right. \\ \left. - \kappa^2 \left[(9 - \alpha) \frac{T}{\kappa^2} e^{-\lambda\kappa\phi} \delta(r - r_b) - (3 - \alpha) \mathcal{T}_\mu^\mu - 3(\alpha - 1) \mathcal{T}_m^m \right] \right). \quad (4.29)$$

Equations (4.5) and (4.6) give

$$\bar{\mathcal{R}} = 12\bar{\lambda}, \quad (4.30)$$

$$\tilde{\mathcal{R}} = \frac{\partial_r f \partial_r \Delta - f \partial_r \partial_r \Delta}{f^3}, \quad (4.31)$$

and from (4.7)

$$\mathcal{T}_\mu^\mu = \frac{8B^2}{\kappa^2 r^{10} f^2} e^{\kappa\phi} - \frac{(\partial_r \phi)^2 \Delta}{f^2} - \frac{2}{\kappa^2} \Lambda e^{\kappa\phi}, \quad (4.32)$$

$$\mathcal{T}_m^m = e^{\kappa\phi} \frac{4B^2}{\kappa^2 r^{10} f^2} - e^{\kappa\phi} \frac{\Lambda}{\kappa^2}. \quad (4.33)$$

Putting $\alpha = 3$ and $\Lambda_{\text{Bulk}} = 0$ in (4.29) this becomes

$$0 = \oint dr d\theta r^5 \left(\frac{36\bar{\lambda}}{r^2} - 6T e^{-\lambda\kappa\phi} \delta(r - r_b) + \frac{24B^2 e^{\kappa\phi}}{r^{10} f^2} - 6\Lambda e^{\kappa\phi} \right) \quad (4.34)$$

By examining the signs of the various terms we can find the parameter restrictions given in Table 4.1.

Some further small restrictions on the value of B may result from the junction conditions once the function $\Delta(r)$ is specified for a particular geometry, as occurs in the analogous case of ref. [172]. However, as we are only able to specify an exact $\Delta(r)$ in the $\bar{\lambda} = 0$ case (4.11), and not in the general case $\bar{\lambda} \neq 0$ case, we have not considered these additional restrictions in Table 4.1.

	$\Lambda < 0$	$\Lambda = 0$	$\Lambda > 0$
$\bar{\lambda} < 0$	none	$B \neq 0$ or $T < 0$	$B \neq 0$ or $T < 0$
$\bar{\lambda} = 0$	$T > 0$	$T > 0$ and $B \neq 0$	$B \neq 0$ or $T < 0$
$\bar{\lambda} > 0$	$T > 0$	$T > 0$	none

Table 4.1: *Restrictions on B and the sign of T for given $\bar{\lambda}$ and Λ .*

4.4 Static potential of the massless scalar field

The phenomenologically important derivation of the Newtonian limit and corrections should ideally be conducted in the context of a full tensorial perturbation analysis about the background solution. However, as was observed by Giddings, Katz and Randall [196] in the case of the Randall Sundrum model, if one is just interested in the static potential the relevant scalar gravitational mode shares the essential features with the static potential of a massless scalar field on the background. This approach was adopted in [172]. In this section we will perform a similar analysis for the background geometry described by eqs. (4.5)-(4.11) in the case that $\bar{g}_{\mu\nu} = \eta_{\mu\nu}$.

4.4.1 Scalar propagator

Our calculation will closely follow that of section 5 of ref. [172]. We will add a massless minimally coupled scalar field, Φ , to the model, with action

$$S_\Phi = -\frac{1}{2} \int_{\mathcal{M}_-} d^6x \sqrt{-g} (\nabla_a \Phi)(\nabla^a \Phi). \quad (4.35)$$

on \mathcal{M}_- . This additional field Φ should not be confused with the scalar field, ϕ , of the Salam-Sezgin model (4.1). We will calculate the static potential of a scalar field, Φ , between two points on the thin brane with fixed θ .

Rather than continuing with the coordinate basis of (4.5) it is convenient to introduce a new radial coordinate ρ by

$$\rho = \frac{r^4 - r_-^4}{r_+^4 - r^4}, \quad (4.36)$$

which maps the interval $r_- < r < r_b$ to the interval $0 < \rho < \rho_b$, where

$$\rho_b = \left(\frac{r_-}{r_+} \right)^4, \quad (4.37)$$

is the position of the brane. In terms of the new radial coordinate ρ the metric (4.5) becomes,

$$ds_6^2 = r^2 \bar{g}_{\mu\nu} dx^\mu dx^\nu + \frac{r^2 \rho^{-1} d\rho^2 + \gamma^2 r^{-6} \rho d\theta^2}{2\Lambda (1+\rho)^2}, \quad (4.38)$$

where by inverting (4.36)

$$r^2 = \sqrt{\frac{r_-^4 + r_+^4 \rho}{1 + \rho}}, \quad (4.39)$$

and the constant γ is defined by

$$\gamma = \frac{\Lambda}{2} (r_+^4 - r_-^4) = 4A \sqrt{1 - \frac{\Lambda B^2}{2A^2}}. \quad (4.40)$$

We shall only be interested in the case of a flat lower-dimensional metric, $\bar{g}_{\mu\nu} = \eta_{\mu\nu}$, in what follows.

The scalar Green's function, G_Φ , is determined by the solution of the massless Klein-Gordon equation,

$$\nabla_a \nabla^a G_\Phi = \frac{1}{\sqrt{-g}} \partial_a (\sqrt{-g} g^{ab} \partial_b G_\Phi) = \frac{\delta(\rho - \rho') \delta(\theta - \theta') \delta^4(x - x')}{\sqrt{-g}}. \quad (4.41)$$

To simplify this problem we make the Fourier decomposition

$$G_\Phi(x, \rho, \phi; x', \rho', \phi') = \int \frac{d^4 k}{(2\pi)^5} e^{ik_\mu(x^\mu - x'^\mu)} \sum_{n=-\infty}^{\infty} e^{in(\theta - \theta')} G_{k,n}(\rho, \rho') \quad (4.42)$$

where the indices of k_μ are raised and lowered by $\eta_{\mu\nu}$. We substitute (4.42) in (4.41) to obtain

$$\left\{ \partial_\rho (\rho \partial_\rho) + \frac{q^2}{2\Lambda (1+\rho)^2} - \frac{n^2}{\rho} \left(\beta + \frac{2\rho}{\Lambda(1+\rho)} \right)^2 \right\} G_{k,n}(\rho, \rho') = \frac{\delta(\rho - \rho')}{\gamma}. \quad (4.43)$$

where $q^2 = -k_\mu k^\mu = k_0^2 - \mathbf{k}^2$, and the constant β is defined by

$$\beta = \frac{r_-^4}{\gamma} = \frac{2\rho_b}{\Lambda(1-\rho_b)}. \quad (4.44)$$

When $\rho \neq \rho'$ (4.43) is a Sturm-Liouville equation, with the general solution

$$G_{k,n} = C_n X_n(\rho) + D_n Y_n(\rho), \quad (4.45)$$

where C_n and D_n are constants and for $n = 0$,

$$X_0 = \sqrt{\frac{2}{\gamma}} \mathcal{P}_{\nu-1} \left(\frac{1-\rho}{1+\rho} \right), \quad Y_0 = \sqrt{\frac{2}{\gamma}} \mathcal{Q}_{\nu-1} \left(\frac{1-\rho}{1+\rho} \right), \quad (4.46)$$

\mathcal{P} and \mathcal{Q} being Legendre functions of the first and second kind respectively, while for $n \neq 0$,

$$\begin{aligned} X_n &= \frac{\rho^{n\beta} (1+\rho)^{1-\nu}}{\sqrt{2n\beta\gamma}} {}_2F_1 \left(\left[1 - \nu + \frac{2n}{\Lambda} + 2n\beta, 1 - \nu - \frac{2n}{\Lambda} \right]; 1 + 2n\beta; -\rho \right), \\ &= \frac{\rho^{n\beta} (1+\rho)^{2n/\Lambda}}{\sqrt{2n\beta\gamma}} {}_2F_1 \left(\left[\nu - \frac{2n}{\Lambda}, 1 - \nu - \frac{2n}{\Lambda} \right]; 1 + 2n\beta; \frac{\rho}{1+\rho} \right), \end{aligned} \quad (4.47)$$

and

$$\begin{aligned} Y_n &= \frac{(1+\rho)^{1-\nu}}{\sqrt{2n\beta\gamma} \rho^{n\beta}} {}_2F_1 \left(\left[1 - \nu + \frac{2n}{\Lambda}, 1 - \nu - \frac{2n}{\Lambda} - 2n\beta \right]; 1 - 2n\beta; -\rho \right), \\ &= \frac{(1+\rho)^{2n(\beta+1/\Lambda)}}{\sqrt{2n\beta\gamma} \rho^{n\beta}} {}_2F_1 \left(\left[\nu - \frac{2n}{\Lambda} - 2n\beta, 1 - \nu - \frac{2n}{\Lambda} - 2n\beta \right]; 1 - 2n\beta; \frac{\rho}{1+\rho} \right), \end{aligned} \quad (4.48)$$

where ${}_2F_1$ is a standard hypergeometric function [198], and for all values of n , including $n = 0$,

$$\nu \equiv \frac{1}{2} \left(1 + \sqrt{1 + \frac{2q^2}{\Lambda} + \frac{16n^2}{\Lambda^2}} \right). \quad (4.49)$$

For $n \neq 0$, as $\rho \rightarrow 0$, the leading two terms in the series expansions for $X_n(\rho)$ and $Y_n(\rho)$ match those of Bessel functions, $J_{\pm 2n\beta}$, or modified Bessel functions, $I_{\pm 2n\beta}$ in the argument $\left| \frac{2}{\Lambda} (8n^2\beta - q^2) \rho \right|^{1/2}$ up to an overall constant of proportionality:

$$\begin{aligned} X_n(\rho) &= \frac{\rho^{n\beta}}{\sqrt{2n\beta}} \left[1 + \frac{8n^2\beta - q^2}{2\Lambda(1+2n\beta)} \rho + O(\rho^2) \right] \\ &\propto \begin{cases} J_{2n\beta} \left(\sqrt{\frac{2}{\Lambda} (q^2 - 8n^2\beta)} \rho \right) + O(\rho^{2+n\beta}), & n^2 < q^2/(8\beta) \\ I_{2n\beta} \left(\sqrt{\frac{2}{\Lambda} (8n^2\beta - q^2)} \rho \right) + O(\rho^{2+n\beta}), & n^2 > q^2/(8\beta) \end{cases}, \end{aligned} \quad (4.50)$$

and

$$\begin{aligned} Y_n(\rho) &= \frac{\rho^{-n\beta}}{\sqrt{2n\beta}} \left[1 + \frac{8n^2\beta - q^2}{2\Lambda(1-2n\beta)} \rho + O(\rho^2) \right] \\ &\propto \begin{cases} J_{-2n\beta} \left(\sqrt{\frac{2}{\Lambda} (q^2 - 8n^2\beta)} \rho \right) + O(\rho^{2-n\beta}), & n^2 < q^2/(8\beta) \\ I_{-2n\beta} \left(\sqrt{\frac{2}{\Lambda} (8n^2\beta - q^2)} \rho \right) + O(\rho^{2-n\beta}), & n^2 > q^2/(8\beta) \end{cases}. \end{aligned} \quad (4.51)$$

Using (4.46), (4.50) and (4.51) the Wronskian of the linearly independent solutions satisfies

$$\mathcal{W}[X_n(\rho), Y_n(\rho)] \equiv X_n \partial_\rho Y_n - Y_n \partial_\rho X_n = \frac{-1}{\gamma\rho}. \quad (4.52)$$

The overall coefficients in (4.46), (4.47) and (4.48) were chosen to make the r.h.s. of (4.52) independent of n .

4.4.2 Boundary and matching conditions

We now wish to solve the inhomogeneous version of (4.43). Without loss of generality, we pick the brane to be to a distance $\xi = \rho_b - \rho' > 0$ to the right of the discontinuity. We will later let $\xi \rightarrow 0$ so that the brane explicitly becomes the source of the discontinuity. We have general solutions to the left and right of the discontinuity at $\rho = \rho'$, labelled

$$G_{k,n} = \begin{cases} G_<(\rho, \rho') = A_1(\rho')X_n(\rho) + A_2(\rho')Y_n(\rho), & \rho < \rho', \\ G_>(\rho, \rho') = B_1(\rho')X_n(\rho) + B_2(\rho')Y_n(\rho), & \rho > \rho', \end{cases} \quad (4.53)$$

We will assume that $G_{k,n}(\rho, \rho')$ is finite at $\rho = 0$, and adopt a Neumann boundary condition at the brane $\rho = \rho_b$,

$$\partial_\rho G_{k,n}|_{\rho=\rho_b} = 0, \quad (4.54)$$

as this is the appropriate boundary condition at the brane for a non-linear gravitational wave when viewed as a scalar field on this background. We will prove this claim in the following section. Imposition of regularity of the solution as $\rho \rightarrow 0$ excludes Y_n as a solution, leading to the choice $A_2(\rho') = 0$. Furthermore, (4.54) applied to $G_>(\rho, \rho')$ implies

$$\frac{B_2(\rho')}{B_1(\rho')} = -\frac{X_{n,b}}{Y_{n,b}}. \quad (4.55)$$

where

$$X_{n,b} \equiv \partial_\rho X_n|_{\rho=\rho_b}, \quad Y_{n,b} \equiv \partial_\rho Y_n|_{\rho=\rho_b}. \quad (4.56)$$

The matching conditions at $\rho = \rho'$ are

$$(G_< - G_>)|_{\rho=\rho'} = 0, \quad (4.57)$$

$$\partial_\rho (G_> - G_<)|_{\rho=\rho'} = \frac{1}{\gamma\rho'}. \quad (4.58)$$

Combining the boundary conditions, the matching conditions and (4.52) we find the solution of the boundary value problem,

$$G_{k,n}(\rho, \rho') = \begin{cases} G_<(\rho, \rho') = \frac{X_n(\rho)}{X_{n,b}} (X_n(\rho')Y_{n,b} - Y_n(\rho')X_{n,b}), & \rho < \rho', \\ G_>(\rho, \rho') = \frac{X_n(\rho')}{X_{n,b}} (X_n(\rho)Y_{n,b} - Y_n(\rho)X_{n,b}), & \rho > \rho'. \end{cases} \quad (4.59)$$

The scalar Green's function, G_Φ , is now determined by substituting (4.59) into (4.42) and prescribing the integration as desired at the poles, which in this case correspond to the zeroes of $X_{n,b}$.

4.4.3 Static potential on the brane

Given the brane is the source of the discontinuity for the Green's function, we set $\rho' = \rho_b$ by letting $\xi \rightarrow 0$. With $\rho = \rho_b$, and using (4.52), the Green's function (4.59) reduces to

$$G_{k,n}(\rho_b) = -\frac{X_n(\rho_b)}{\gamma \rho_b X_{n,b}}. \quad (4.60)$$

To obtain the static potential, we explicitly integrate the retarded Green's function (4.42), (4.60) over the time difference, $t - t'$. We note that G_Φ is non-zero only for $t - t' > 0$, so multiplying it by $\theta(t - t')$ leaves it unchanged. We can then perform the integration over t to find

$$V_\Phi(\mathbf{x}, \phi; \mathbf{x}', \phi') = -\sum_{n=-\infty}^{\infty} e^{in(\theta-\theta')} \int \frac{d^3\mathbf{k}}{(2\pi)^5} e^{i\mathbf{k}\cdot(\mathbf{x}-\mathbf{x}')} \int_{-\infty}^{\infty} \frac{dk^0}{i(k^0 - i\epsilon)} \frac{X_n(\rho_b)}{\gamma \rho_b X_{n,b}}, \quad (4.61)$$

We are interested in the retarded Green's function, which requires that we perform the k^0 integral by a contour integration with $q^2 \rightarrow (k^0 + i\epsilon)^2 - \mathbf{k}^2$, $\epsilon \rightarrow 0_+$. We close the contour in the upper half plane, to avoid the poles which correspond to the zeroes of $X_{n,b}$ on the real line, and which are moved below the real line by the ϵ -procedure. The only residue is then due to the simple pole at $k^0 = 0$, and the integration yields

$$\begin{aligned} V_\Phi(\mathbf{x}, \phi; \mathbf{x}', \phi') &= -\sum_{n=-\infty}^{\infty} e^{in(\theta-\theta')} \int \frac{d^3\mathbf{k}}{(2\pi)^4} e^{i\mathbf{k}\cdot(\mathbf{x}-\mathbf{x}')} \mathcal{G}_n(-k^2), \\ &= -\sum_{n=-\infty}^{\infty} e^{in(\theta-\theta')} \int_0^\infty \frac{dk}{4\pi^3} \frac{k \sin(k|\mathbf{x} - \mathbf{x}'|)}{|\mathbf{x} - \mathbf{x}'|} \mathcal{G}_n(-k^2), \\ &= -\sum_{n=-\infty}^{\infty} e^{in(\theta-\theta')} \text{Im} \left(\int_{-\infty}^{\infty} \frac{dk}{8\pi^3} \frac{k e^{ik|\mathbf{x}-\mathbf{x}'|}}{|\mathbf{x} - \mathbf{x}'|} \mathcal{G}_n(-k^2) \right), \end{aligned} \quad (4.62)$$

where $k = |\mathbf{k}|$, and $\mathcal{G}_n(-k^2) \equiv G_{k,n}(\rho_b)|_{q^2=-\mathbf{k}^2}$.

The final integral in (4.62) can be performed by a careful choice of contour, subject to convergence of the integrand, which we have checked numerically. It is found that for $n = 0$, $\mathcal{G}_0(-k^2)$ has a second order pole at $k = 0$, together with first order poles at $k = \pm iq_{0,j}$, where $q_{0,j} > 0$, $j = 1, \dots, \infty$. For $n \neq 0$, all poles occur at $k = \pm iq_{n,j}$, where $q_{n,j} > 0$, $j = 1, \dots, \infty$. We close the contour in the upper half plane, but perform a cut on the $\text{Im}(k)$ axis on the interval $k \in (\frac{1}{2}i\bar{q}, \infty)$, where $\bar{q} = \inf \{q_{n,j} | j = 1, \dots, \infty\}$. Integrating back and forth around the cut, first from $k = \epsilon + i\infty$ to $k = \epsilon + \frac{1}{2}i\bar{q}$ in the

$\text{Re}(k) > 0$ quadrant and then back from $k = -\epsilon + \frac{1}{2}i\bar{q}$ to $k = -\epsilon + i\infty$ in the $\text{Re}(k) < 0$ quadrant before taking the limit $\epsilon \rightarrow 0$, has the net effect of circumscribing each of the poles on the positive imaginary axis once in a clockwise fashion.

We will not analytically determine each coefficient in the sum of terms in (4.62) which result from the enclosed poles at $k = iq_{n,j}$, but simply note that the Laurent expansion of $\mathcal{G}_n(-k^2)$ at each of these poles takes the form

$$\mathcal{G}_n(-k^2) = \frac{C_{n,j}(\rho_b)}{k^2 + q_{n,j}^2} + \mathcal{O}(1), \quad (4.63)$$

in terms of coefficients $C_{n,j}(\rho_b)$, and the residue gives a Yukawa correction in each case.

The pole at $k = 0$ is not enclosed by the contour, but since it lies on the contour, taking the principal part gives a net contribution to the static potential, which is readily determined analytically by applying identities which hold for the Legendre function solutions (4.46) for $n = 0$. In particular,

$$\begin{aligned} \text{Res} \left(k e^{ik|\mathbf{x}-\mathbf{x}'|} \mathcal{G}_0(-k^2) \right)_{k=0} &= \text{Res} \left(\frac{-k e^{ik|\mathbf{x}-\mathbf{x}'|} \mathcal{P}_{\nu-1}(y)}{\frac{1}{2}\gamma(1-y^2)\partial_y \mathcal{P}_{\nu-1}(y)} \right)_{k=0, \rho=\rho_b} \\ &= \text{Res} \left(\frac{-2k e^{ik|\mathbf{x}-\mathbf{x}'|} \mathcal{P}_{\nu-1}(y)}{\gamma\nu [y\mathcal{P}_{\nu-1}(y) - P_{\nu}(y)]} \right)_{k=0, \rho=\rho_b} \\ &= \lim_{\nu \rightarrow 1} \frac{4\Lambda \mathcal{P}_{\nu-1}(y)}{\gamma [y\partial_{\nu} \mathcal{P}_{\nu-1}(y) - \partial_{\nu} P_{\nu}(y)]} \Big|_{\rho=\rho_b} \\ &= \frac{2\Lambda(1+\rho_b)}{\gamma\rho_b}, \end{aligned} \quad (4.64)$$

where in the intermediate steps y is defined implicitly by $y = (1-\rho)/(1+\rho)$, and we have used the fact that as $k \rightarrow 0$, $\nu \simeq 1 - k^2/(2\Lambda)$, $\mathcal{P}_0(y) = 1$, and the identities $\lim_{\nu \rightarrow 1} \partial_{\nu} \mathcal{P}_{\nu-1}(y) = \ln[\frac{1}{2}(1+y)]$, and $\lim_{\nu \rightarrow 1} \partial_{\nu} \mathcal{P}_{\nu}(y) = y \ln[\frac{1}{2}(1+y)] + y - 1$.

The final expression for the static potential then becomes¹

$$V_{\Phi}(\mathbf{x}, \phi; \mathbf{x}', \phi') = \frac{-(1+\rho_b)\Lambda}{4\pi^2\gamma\rho_b|\mathbf{x}-\mathbf{x}'|} - \sum_{n=-\infty}^{\infty} \sum_{j=1}^{\infty} \frac{C_{n,j}(\rho_b) e^{-q_{n,j}|\mathbf{x}-\mathbf{x}'|}}{8\pi^2|\mathbf{x}-\mathbf{x}'|}. \quad (4.65)$$

which as expected is a Newtonian-type potential supplemented by Yukawa-type corrections. The constant γ may be re-expressed in terms of r_- and ρ_b on account of (4.44).

¹Eq. (4.65) corrects a small numerical factor in the Newton-like term given in ref. [199].

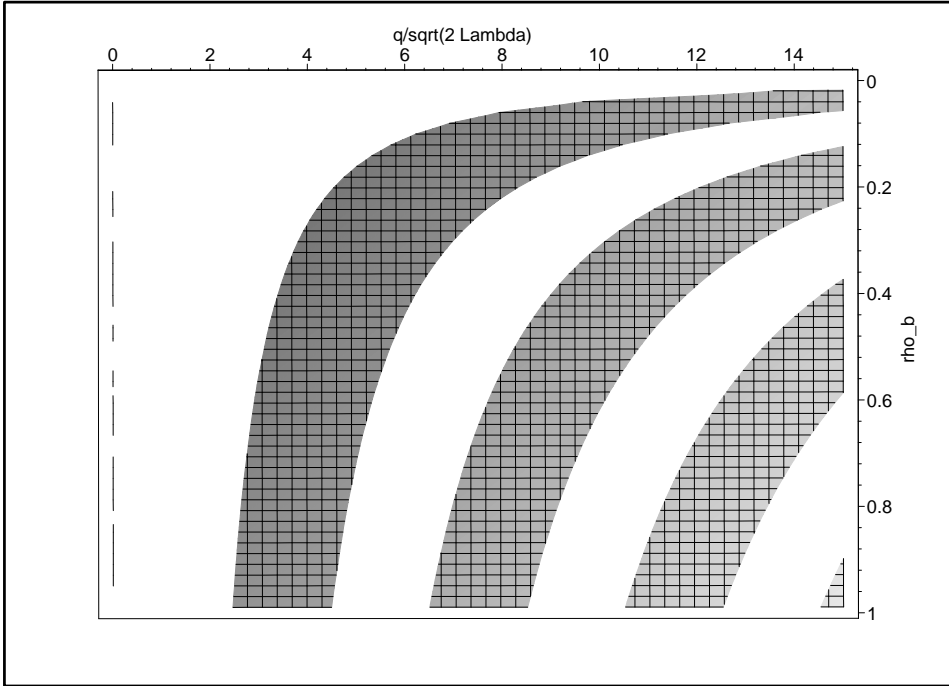


Figure 4.2: A plot of the denominator of $\mathcal{G}_{0/\Lambda}(q^2/2\Lambda)$. The denominator is positive in the hashed regions, negative in the white regions and zero at the boundaries. The transition between bands indicates where the poles of $\mathcal{G}_0(q^2/2\Lambda)$ lie. Note that $\mathcal{G}_0(0) = 0$.

The locations of the poles, $q_{n,j}$, and the coefficients, $C_{n,j}$, for the functions, $\mathcal{G}_n(-k^2)$, have been numerically determined. Fig. 4.2 demonstrates the behaviour of the denominator of $\mathcal{G}_0(q^2/2\Lambda)$. For a given value of ρ_p , one can see that the zeroes of the denominator are discrete, which implies that the poles of $\mathcal{G}_0(q^2/2\Lambda)$ are also discrete. Similar behaviour can be seen for the denominators of $\mathcal{G}_{2/\Lambda}(q^2/2\Lambda)$ and $\mathcal{G}_{3/\Lambda}(q^2/2\Lambda)$ in Figs 4.3 and 4.4 respectively. However, one crucial difference between the $n = 0$ and $n \neq 0$ cases is that the denominator of $\mathcal{G}_0(0)$ is zero for all ρ_b , while the denominator of $\mathcal{G}_{n/\Lambda}(0)$ is non-zero for all ρ_b . This means that only $\mathcal{G}_0(q^2/2\Lambda)$ contributes to the $1/|\mathbf{x} - \mathbf{x}'|$ part of the static potential, while every other term contributes Yukawa type exponential corrections. This behaviour can be seen most clearly in Fig. 4.5. It should also be noted that for increasing n , the position of the occurrence of the first pole of $\mathcal{G}_{n/\Lambda}(q^2/2\Lambda)$, $q_{n,1}$, is increasing, meaning that the exponential corrections to the static potential, $e^{-q_{n,1}|\mathbf{x} - \mathbf{x}'|}/|\mathbf{x} - \mathbf{x}'|$, coming from higher n are significantly weaker and drop off significantly faster than those that come from lower n . This can also be seen most easily in Fig. 4.5.

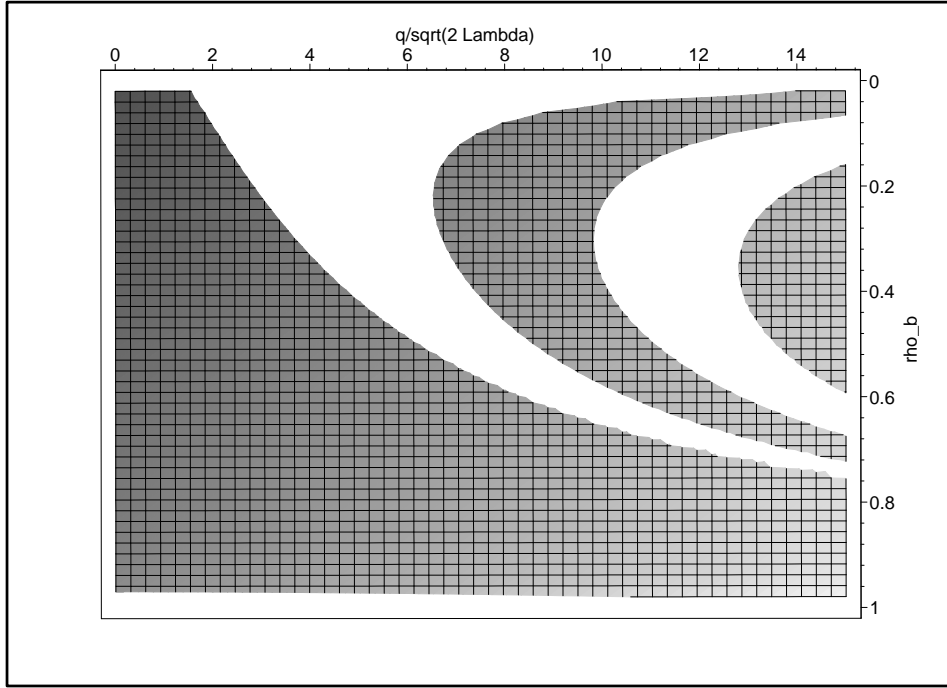


Figure 4.3: A plot of the denominator of $\mathcal{G}_{1/\Lambda}(q^2/2\Lambda)$. The denominator is positive in the hashed regions, negative in the white regions and zero at the boundaries. The transition between bands indicates where the poles of $\mathcal{G}_{1/\Lambda}(q^2/2\Lambda)$ lie.

While the coefficient associated with the Newtonian term has been determined analytically, the other coefficients have only been determined numerically. We present plots of the behaviour of the coefficients for $\rho_b = 0.5$ in Fig. 4.6, and for $n = 1$ in plot Fig. 4.7. It should be noted that while the plots are drawn with continuous lines, the poles and hence coefficients exist only at discrete places. The figures have been plotted with continuous lines in order to aid comprehension of the underlying behaviour of the coefficients.

Fig. 4.6 shows that as n increases the value of the coefficients increase. It also shows that for each $n \neq 0$ as j increases that coefficient $C_{n,j}$ decreases, while to the numerical accuracy presented here, $C_{0,j} = C_{0,j+1}$ for all $j \in \mathbb{Z}^+$. Fig. 4.7 illustrates that for the $n = 1$ case, which is similar in behaviour to all $n \neq 0$ cases, the effects of modifying the brane position, ρ_b , on the coefficients in the static potential. As ρ_b increases, the coefficients generically decrease. They also decrease with q as noted above. Picking successively higher values of n results in similar graphs, but shifts them in accordance with the results in Fig. 4.6.

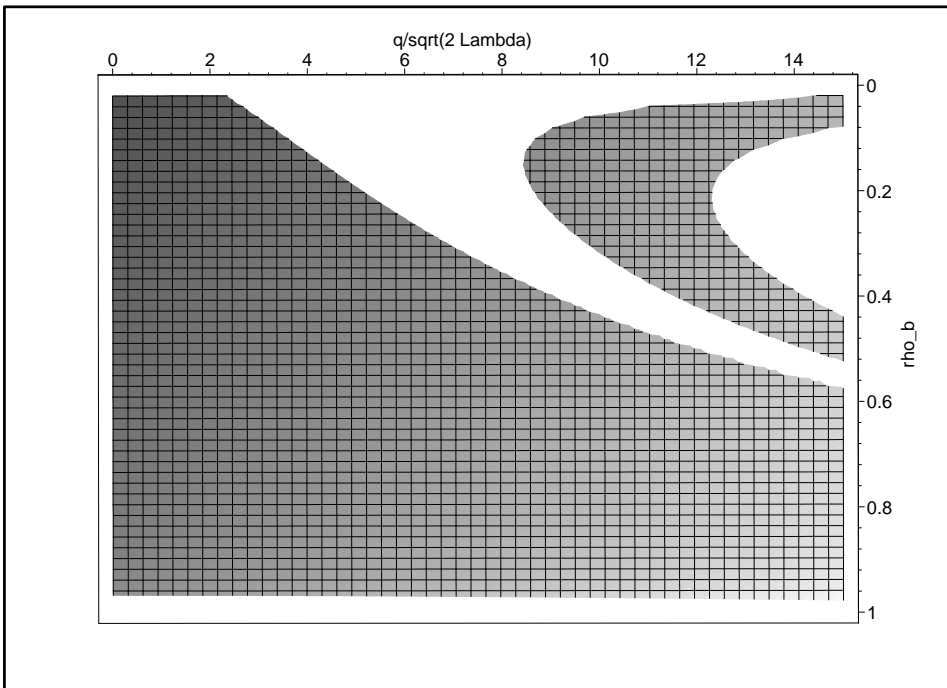


Figure 4.4: A plot of the denominator of $\mathcal{G}_{2/\Lambda}(q^2/2\Lambda)$. The denominator is positive in the hashed regions, negative in the white regions and zero at the boundaries. The transition between bands indicates where the poles of $\mathcal{G}_{2/\Lambda}(q^2/2\Lambda)$ lie.

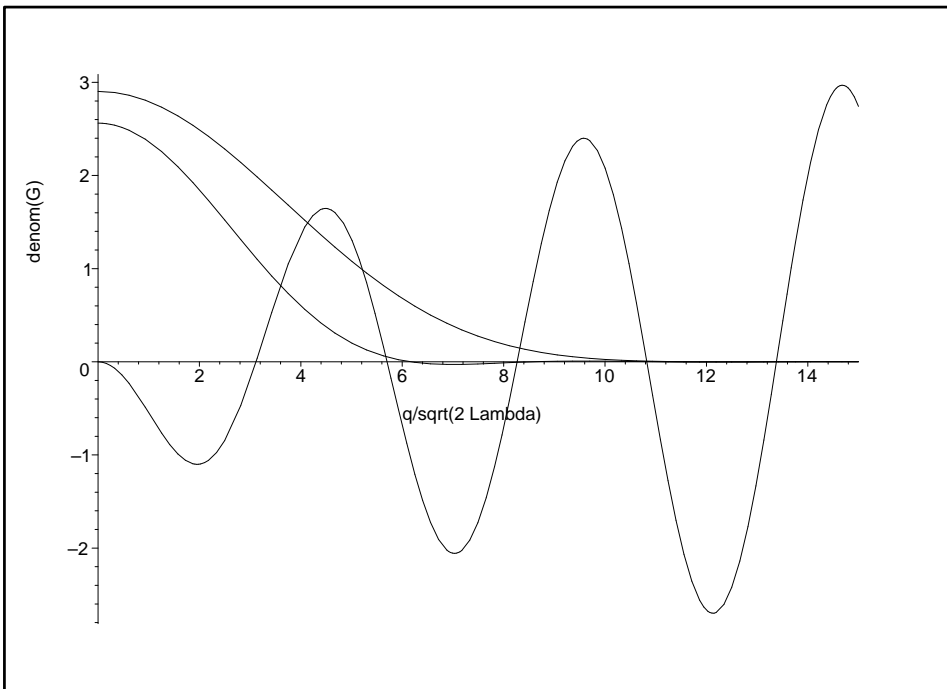


Figure 4.5: A plot of the denominator of $\mathcal{G}_{n/\Lambda}(q^2/2\Lambda)$ for $n = 0, 1, 2$ and $\rho_b = 0.5$. Note that $\text{denom}(\mathcal{G}_{n/\Lambda}(0) = 0)$ only when $n = 0$. The value of the position of the first pole increases with n .

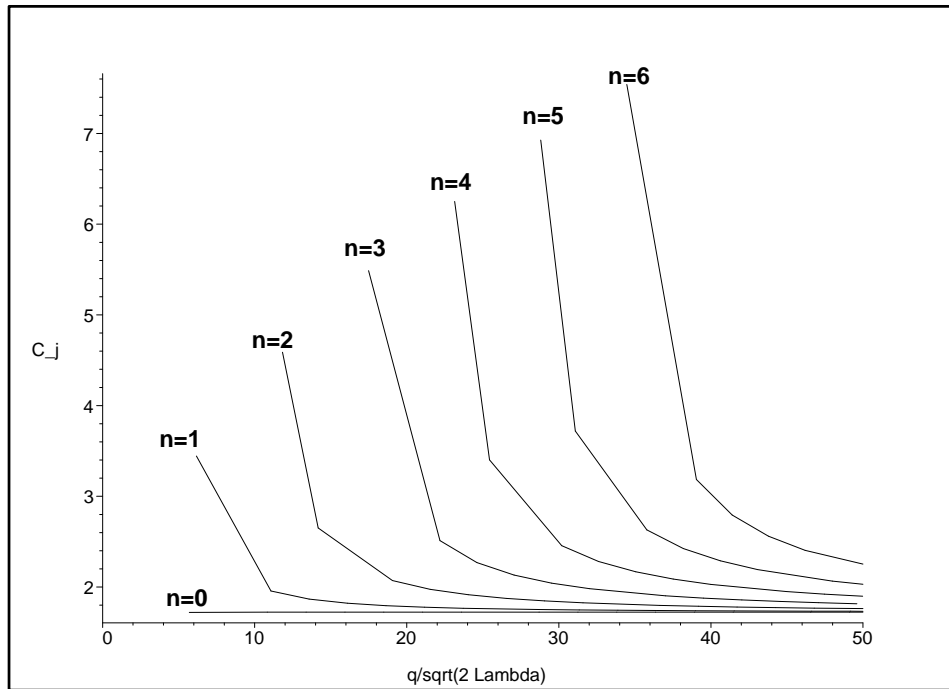


Figure 4.6: A plot of the $C_{n/\Lambda,j}$'s for $n = 0$ to 6 and $\rho_b = 0.5$. The values of the coefficients decrease with increasing q and increase with increasing n .

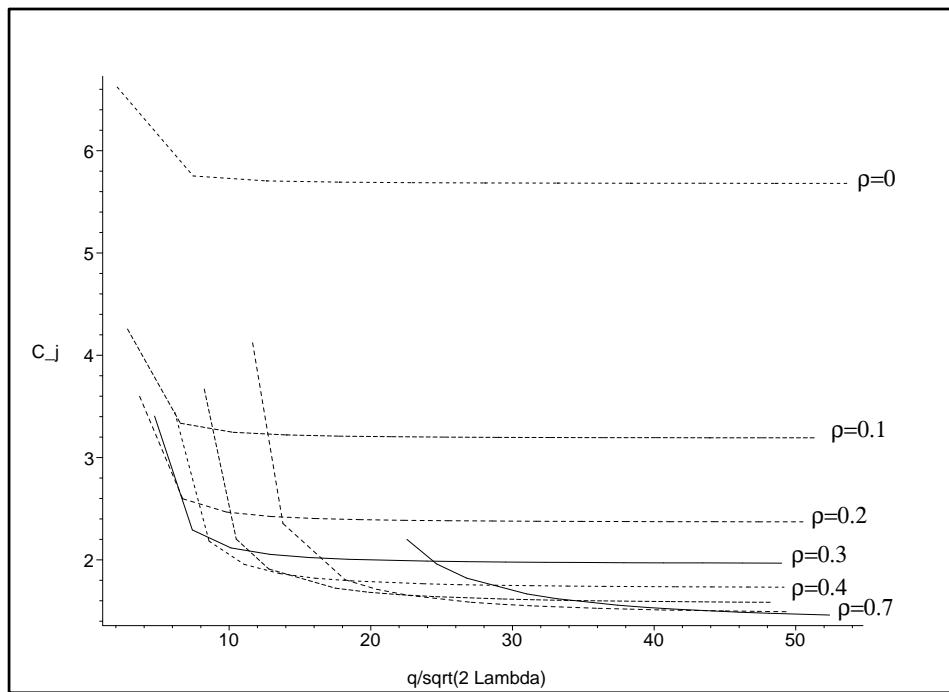


Figure 4.7: A plot of the $C_{n/\Lambda,j}$'s for $n = 1$ and $\rho_b = 0$ to 0.7 . The values of the coefficients decrease with increasing ρ_b or q .

4.4.4 Nonlinear gravitational waves on the brane

We will now further justify the claim that the calculation of the static potential for a minimally coupled massless scalar field given above reproduces all the essential features of the corresponding calculation for the graviton. We observe that the construction of nonlinear gravitational waves which was developed in ref. [172] by a generalization of the technique of Garfinkle and Vachaspati [197], is unchanged when applied to the background (4.5). In particular, nonlinear gravitational waves can be constructed on the background in the case that the geometry, \mathcal{M}_{low} , generated by the 4-dimensional metric $\bar{g}_{\mu\nu}$ admits a hypersurface-orthogonal null Killing vector, k^μ . If \bar{z} is a locally defined scalar such that $\partial_{[\mu}k_{\nu]} = k_{[\nu}\partial_{\mu]}\bar{z}$ and $k^\mu\partial_\mu z = 0$, where Greek indices are lowered and raised with $\bar{g}_{\mu\nu}$ and its inverse, then the nonlinear wave spacetime is given by adding to (4.5) the term

$$r^2 H e^{-z} k_\mu k_\nu dx^\mu dx^\nu, \quad (4.66)$$

where z is the pullback of \bar{z} to (4.5), and H is a scalar function on the bulk spacetime (4.5), which satisfies $\nabla^a \nabla_a H = 0$, and $\ell^a \partial_a H = 0$. Here ∇_a is the covariant derivative in the metric (4.5) and $\ell^a = (k^\mu, 0, 0)$ is the extension of k^μ to (4.5), with indices raised and lowered by the full spacetime metric (4.5). The vector, ℓ^a , is also null and hypersurface orthogonal, and satisfies $\partial_{[a} \ell_{b]} = \ell_{[b} \partial_{a]}(z + 2 \ln r)$ and $\ell^a \partial_a(z + 2 \ln r) = 0$.

In addition to the junction conditions (4.18), (4.22)–(4.24), we now have the additional relation

$$\frac{\sqrt{\Delta(r_b)}}{r_b} \partial_r(r^2 H)|_{r_b} = \frac{\epsilon T}{2} e^{-\lambda \kappa \phi(r_b)} r_b^2 H(r_b) \quad (4.67)$$

Using (4.23) we see that (4.67) is equivalent to the Neumann condition

$$\partial_r H|_{r_b} = 0, \quad (4.68)$$

at the brane, if H is viewed as a massless scalar field on the spacetime without the term (4.66). In the case that $\bar{g}_{\mu\nu} = \eta_{\mu\nu}$ the field H therefore satisfies the same wave equation and boundary conditions as were given above for massless scalar field, Φ .

To make the correspondence explicit, we take $\bar{g}_{\mu\nu} = \eta_{\mu\nu}$, and adopt double null coordinates, $(u, v, x_\perp^1, x_\perp^2)$, on the Minkowski space, \mathcal{M}_{low} . If we choose $k^\mu = (\partial_v)^\mu$,

the solution with the gravitational wave term (4.66) reads

$$ds^2 = r^2 \left[-du dv + H(u, x_\perp^k, r, \phi) du^2 + \delta_{AB} dx_\perp^A dx_\perp^B \right] + \frac{r^2 dr^2}{\Delta} + \Delta d\phi^2, \quad (4.69)$$

where Δ is given by (4.11). Note that H does not depend on v but its dependence on u is arbitrary. The scalar wave equation for H explicitly reads

$$H_{,rr} + \left(\frac{3}{r} + \frac{\Delta_{,r}}{\Delta} \right) H_{,r} + \frac{r^2 H_{,\phi\phi}}{\Delta^2} + \frac{\delta^{AB} H_{,AB}}{\Delta} = 0. \quad (4.70)$$

The general linearized limit of the nonlinear gravitational solution can be discussed as in [100]. We note that $H = h_{AB}(u) x_\perp^A x_\perp^B$, where $h_{22}(u) = -h_{11}(u)$, is clearly a solution: it satisfies $\delta^{AB} H_{,AB} = 0$, and its linearized limit is analogous to the famous normalizable massless mode in the Randall–Sundrum II model [168]. If we transform the radial parameter to ρ by (4.36) and make a Fourier decomposition as in (4.42), then (4.70) becomes equivalent to the homogeneous part of (4.43). Our analysis above for the massless scalar field therefore applies equally to the graviton mode.

The nonlinear gravitational wave construction also applies firstly to any other Ricci–flat geometry on \mathcal{M}_{low} which admits a hypersurface orthogonal null Killing vector, and secondly with suitable modifications to other Einstein space geometries for \mathcal{M}_{low} , provided appropriate solutions can be found.

4.5 The hierarchy problem

One of the principal motivations for studying brane world models is the attempt to provide a natural solution to the hierarchy problem between the Planck and electroweak scales. The construction of ref. [172] potentially offers a concrete realization of the phenomenological solution to the hierarchy problem proposed by Antoniadis [79], Arkani-Hamed, Dimopoulos and Dvali [80, 81]. In particular, if the non-gravitational forces can be introduced in such a way as to be confined to the brane, then provided that the distance between the thin brane and the bolt can be made large enough, higher–dimensional gravitational corrections could become manifest close to the TeV scale.

Since the construction is a hybrid one, there is an ordinary Kaluza–Klein direction within the 4–brane in addition to the direction transverse to the brane. A phenom-

enologically realistic solution to the hierarchy problem can therefore only be obtained if the distance between the brane and the bolt can be made many orders of magnitude larger than the circumference of the Kaluza–Klein circle. In the original construction of ref. [172], based on Einstein–Maxwell gravity with a higher-dimensional cosmological constant, a natural solution to the hierarchy problem proved to be impossible as the brane–bolt distance was at most comparable to the circumference of the Kaluza–Klein circle. The present model has more degrees of freedom, however, and so it is possible that this problem can be overcome.

In order to make the volume of the internal space, \mathcal{V} , sufficiently large to accommodate TeV scale gravity, we must be able to find a set of parameters (A, B, Λ) which allows the ratio, $R = \mathcal{V}/\mathcal{C}$, to be arbitrarily large. The idea is that a particular value of \mathcal{V} fixes gravity to be TeV scale. However, if the related set of parameters (A, B, Λ) imply that \mathcal{C} is large enough that the associated standard model Kaluza Klein excitations are noticeable, for example in particle colliders/cosmic ray showers, then that set of parameters would be unphysical. If we find a set (or sets) of parameters (A, B, Λ) which allow the ratio $R = \mathcal{V}/\mathcal{C}$, to be arbitrarily large then we can confidently say that we can pick \mathcal{V} to solve the hierarchy problem while hiding the effects of the Kaluza–Klein dimension.

The proper circumference of the Kaluza–Klein direction is

$$\mathcal{C} = \frac{4\pi\sqrt{\Delta(r_b)}}{\Delta'(r_-)} = \frac{2^{3/4}\pi\rho_b^{1/2}}{\sqrt{\Lambda}\sqrt[4]{1+\rho_b}}. \quad (4.71)$$

The volume of the internal space, $\mathcal{V} = 2 \int_{r_-}^{r_b} \int_0^{4\pi/\Delta'(r_-)} d\ell_\theta d\ell_r$ is

$$\mathcal{V} = (r_b^2 - r_-^2) \frac{4\pi}{\Delta'(r_-)} \quad (4.72)$$

The ratio, $R = \mathcal{V}/\mathcal{C}$ is then simply

$$R = \frac{(r_b^2 - r_-^2)}{\sqrt{\Delta(r_b)}} = \sqrt{\frac{2}{\Lambda}} r_- F(\rho_b) \quad (4.73)$$

where r_- is given by (4.12),

$$F(\rho_b) = \frac{4\rho_b^{1/2}}{1-\rho_b} \left(\sqrt{\frac{2}{1+\rho_b}} - 1 \right) \sqrt[4]{\frac{1+\rho_b}{2}}, \quad (4.74)$$

and on account of (4.12) and (4.37),

$$\rho_b = \frac{A - \sqrt{A - \frac{1}{2}B^2\Lambda}}{A + \sqrt{A - \frac{1}{2}B^2\Lambda}}. \quad (4.75)$$

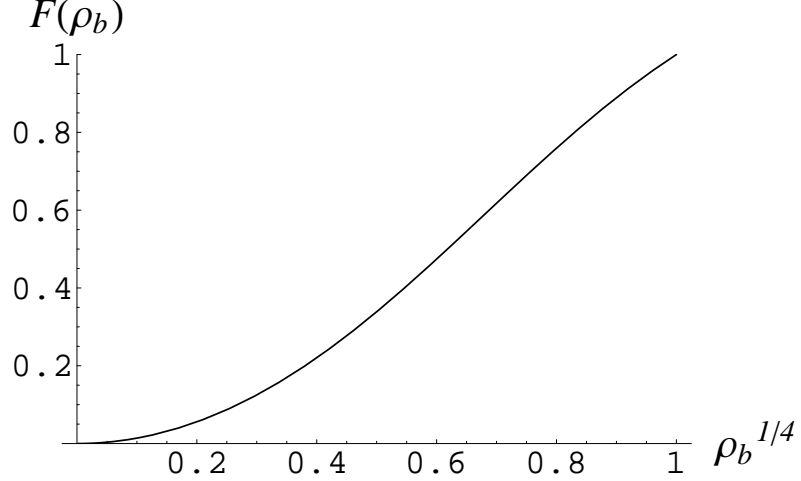


Figure 4.8: The ratio of volume of the internal space to its circumference is a multiple of $F(\rho_b)$, as given by (4.73), (4.74). It is plotted here versus $\rho_b^{1/4}$.

The quantity $F(\rho_b)$ defined by (4.74) is depicted in Fig. 4.8. It is a monotonic function which increases from $F = 0$ to $F = 1$ on the interval $\rho_b \in [0, 1]$. The limit $\rho_b \rightarrow 1$ occurs when $\frac{B^2\Lambda}{2A^2} \rightarrow 1$, i.e., when $r_- \approx r_+ \approx r_b \approx \frac{4A}{\Lambda}$. In this case $\mathcal{C} \approx \sqrt{2}\pi\Lambda^{-1/2}$, and $R = \mathcal{V}/\mathcal{C} \approx 2^{5/2}A\Lambda^{-3/2}$. The requirement that \mathcal{C} must be small enough to be interpreted as a conventional Kaluza–Klein direction means that Λ must be suitably large. Since the parameter A is still free, however, we can still make R arbitrarily large to overcome its dependence on the $\Lambda^{-3/2}$ factor. Thus it appears that a solution to the hierarchy problem may be feasible.

For smaller values of ρ_b similar arguments apply. In particular, consider the extreme limit $\rho_b \rightarrow 0$ which corresponds to $0 < \frac{B^2\Lambda}{2A^2} \ll 1$. Then $r_-^4 \approx B^2/A$, $r_+^4 \approx 8A/\Lambda$ and $F(\rho_b) \approx 4(\sqrt{2} - 1)\rho_b^{1/2}$. Hence $R \approx 2(\sqrt{2} - 1)B^{3/2}A^{-5/4}$ and $\mathcal{C} \approx 2^{-3/4}\pi BA^{-1}$, which are both independent of Λ . Since the constants A and B are not constrained except by the requirement $\frac{B}{A} \ll \sqrt{\frac{2}{\Lambda}}$, we can again make R arbitrarily large while keeping \mathcal{C} small. If we denote R_0 and \mathcal{C}_0 to be phenomenologically desirable values of R and \mathcal{C} ,

we can conversely fix both A and B . We find $A_0 = \pi^6 R_0^4 2^{-17/2} (\sqrt{2} - 1)^{-4} \mathcal{C}_0^{-6}$ and $B_0 = \pi^5 R_0^4 2^{-31/4} (\sqrt{2} - 1)^{-4} \mathcal{C}_0^{-5}$, while for consistency of the limit $0 < \Lambda_0 \ll \frac{\pi^2}{\sqrt{2} \mathcal{C}_0^2}$.

We have demonstrated here that a solution of the hierarchy problem is possible regardless of the value of ρ_b . We note, however, that once the Newton potential for the tensor modes, equivalent to the first term of (4.65), is determined then two of the parameters, r_- , Λ and ρ_b would be fixed phenomenologically via equations similar to (4.65) and (4.71), in terms of the Newton constant and the energy scale for the ordinary Kaluza–Klein circle direction. From (4.73) we see that just enough parameter freedom remains to choose the remaining independent parameter to solve the hierarchy problem as desired.

4.6 General fluxbrane and dual static black hole-like solutions

The global properties of certain static solutions of electrically charged dilaton spacetimes with a dilaton potential of Liouville form were classified in ref. [194] without explicitly writing down the general solution. The solutions considered in ref. [194] include spherically symmetric spacetimes, but in the most general case include geometries for which the spatial sections at spatial infinity consist of an arbitrary Einstein space, rather than simply a $(D - 2)$ -sphere in the case of D spacetime dimensions. Electrically charged solutions with these symmetries are of interest, since in cases in which a regular horizon exists fluxbranes may be obtained from them by the double analytic continuation technique that was first introduced in [78]. The field equations considered in ref. [194] include our equations (4.2)–(4.2) as a special case.

At a first glance, it would appear that the Salam-Sezgin model is a special case of the class of models analysed in ref. [194]. Unfortunately, however, the particular coupling constants which appear in the exponential coupling of the scalar to the $U(1)$ gauge field, and the Liouville potential, are in fact a degenerate case of the analysis of ref. [194].

In this section we will therefore repeat the analysis of [194] in the case of the Salam-

Sezgin model, but in a slightly more general framework which incorporates fluxbranes at the outset, in addition to their dual solutions. Rather than simply restricting our attention to the Salam-Sezgin model in six dimensions, we will investigate relevant solutions for the whole degenerate case omitted in [194]. The relevant field equations are those which follow from variation of the D -dimensional action

$$S = \int d^D x \sqrt{-g} \left\{ \frac{\mathcal{R}}{4\kappa^2} - \frac{1}{D-2} g^{ab} \partial_a \phi \partial_b \phi - \frac{1}{4} \exp \left(\frac{4\kappa\phi}{D-2} \right) F_{ab} F^{ab} - \frac{\Lambda}{2\kappa^2} \exp \left(\frac{-4\kappa\phi}{D-2} \right) \right\}, \quad (4.76)$$

The field content of (4.76) is the same as that of action (4.1) in the absence of the Kalb-Ramond field, and the field equations obtained by variation of this action reduce to (4.2)–(4.2) (4.1) when $D = 6$. The model of ref. [194] was more general than (4.76) in allowing for two additional arbitrary coupling constants: one in the dilaton / $U(1)$ coupling, and one in the Liouville potential. In the notation of ref. [194] our conventions are the same, but we have chosen $g_0 = -1$ and $g_1 = 1$: in this case the results of [194] are degenerate.

The field equations obtained by varying (4.76) are most easily integrated explicitly for static geometries by using the radial coordinate of Gibbons and Maeda [201], for which the metric is given by

$$ds^2 = \varepsilon e^{2u} \left[-\epsilon_Q dt^2 + R^{2(D-2)} d\xi^2 \right] + R^2 \bar{g}_{ij} d\tilde{x}^i d\tilde{x}^j, \quad (4.77)$$

where $u = u(\xi)$, $R = R(\xi)$, and \bar{g}_{ij} is the metric of a $(D-2)$ -dimensional Einstein space,

$$\bar{\mathcal{R}}_{ab} = (D-3)\bar{\lambda} \bar{g}_{ab}, \quad a, b = 1, \dots, D-2, \quad (4.78)$$

$\epsilon_Q = \pm 1$ and $\varepsilon = \pm 1$. If $\epsilon_Q = +1$ and $\varepsilon = +1$ one obtains the geometry relevant to the domain of outer communications of a black hole, or of a naked singularity. The case $\epsilon_Q = +1$ and $\varepsilon = -1$ would correspond to the interior of a black hole in the case that regular horizons exist. If we take $\epsilon_Q = -1$ and $\varepsilon = +1$ we have the case of a fluxbrane, assuming t to be an angular coordinate.

We choose \mathbf{F} to be the field of an isolated electric charge,

$$\mathbf{F} = \exp \left(2u - \frac{4\kappa\phi}{D-2} \right) \frac{Q}{\kappa} dt \wedge d\xi, \quad (4.79)$$

in the case that $\epsilon_Q = +1$, and a magnetic field in the case that $\epsilon_Q = -1$. In the later case the ansatz (4.79) is the same, except that t is now an angular coordinate and Q is the magnetic charge.

With the ansatz (4.77), (4.79) and assuming $\phi = \phi(\xi)$, the field equations can be written [194] as the system

$$\ddot{\eta} = 2\varepsilon\epsilon_Q Q^2 e^{2\eta} \quad (4.80)$$

$$\ddot{\zeta} = (D-3)^2\varepsilon\bar{\lambda}e^{2\zeta} - 2\varepsilon\Lambda e^{2\chi}, \quad (4.81)$$

$$\ddot{\chi} = (D-2)(D-3)\varepsilon\bar{\lambda}e^{2\zeta} - 2\varepsilon\Lambda e^{2\chi}, \quad (4.82)$$

with the constraint

$$(D-2) \left[\dot{\zeta}^2 - 2\dot{\zeta}\dot{\chi} \right] + (D-3)\dot{\chi}^2 + \dot{\eta}^2 + (D-2)(D-3)\varepsilon\bar{\lambda}e^{2\zeta} - 2\varepsilon\Lambda e^{2\chi} - 2\varepsilon\epsilon_Q Q^2 e^{2\eta} = 0, \quad (4.83)$$

where the overdot denotes $d/d\xi$. Eq. (4.80) is readily integrated if we multiply it by $\dot{\eta}$, yielding

$$\dot{\eta}^2 = 2\epsilon_Q Q^2 e^{2\eta} + \epsilon_2(D-2)k_2^2, \quad (4.84)$$

where k_2 is an arbitrary constant and $\epsilon_2 = +1, 0, -1$. If $\epsilon_Q = +1$ (“black hole” case) then a further integration yields three possible solutions, distinguished by the parameter ϵ_2 :

$$\frac{2Q^2}{D-2}e^{2\eta} = \begin{cases} \frac{k_2^2}{\sinh^2[\sqrt{D-2}k_2(\xi-\xi_2)]}, & \epsilon_2 = +1, \\ \frac{1}{(D-2)(\xi-\xi_2)^2}, & \epsilon_2 = 0, \\ \frac{k_2^2}{\sin^2[\sqrt{D-2}k_2(\xi-\xi_2)]}, & \epsilon_2 = -1, \end{cases} \quad (4.85)$$

where ξ_2 is an arbitrary constant. If $\epsilon_Q = -1$ (“fluxbrane” case) then we must have $\epsilon_2 = +1$ and the only solution is

$$\frac{2Q^2}{D-2}e^{2\eta} = \frac{k_2^2}{\cosh^2[\sqrt{D-2}k_2(\xi-\xi_2)]}. \quad (4.86)$$

Linear combinations of (4.81) and (4.82) yield

$$\ddot{\chi} - \ddot{\zeta} = (D-3)\varepsilon\bar{\lambda}e^{2\zeta}, \quad (4.87)$$

$$(D-3)\ddot{\chi} - (D-2)\ddot{\zeta} = 2\varepsilon\Lambda e^{2\chi}, \quad (4.88)$$

while the constraint (4.83) becomes

$$\dot{\zeta}^2 - 2\dot{\zeta}\dot{\chi} + \left(\frac{D-3}{D-2}\right)\dot{\chi}^2 + (D-3)\varepsilon\bar{\lambda}e^{2\zeta} - \frac{2\varepsilon\Lambda e^{2\chi}}{D-2} + \epsilon_2 k_2^2 = 0. \quad (4.89)$$

In the special cases that $\Lambda = 0$, or $\bar{\lambda} = 0$, eqs. (4.88)–(4.89), can be further integrated, as follows:

(i) Special $\Lambda = 0$ solution (as previously given in [194]):

$$\varepsilon\bar{\lambda}e^{2\zeta} = \begin{cases} \frac{k_1^2}{\sinh^2[(D-3)k_1(\xi-\xi_1)]}, & \epsilon_1 = +1, \varepsilon\bar{\lambda} > 0, \\ \frac{1}{(D-3)^2(\xi-\xi_1)^2}, & \epsilon_1 = 0, \varepsilon\bar{\lambda} > 0, \\ \frac{k_1^2}{\sin^2[(D-3)k_1(\xi-\xi_1)]}, & \epsilon_1 = -1, \varepsilon\bar{\lambda} > 0, \\ \frac{-k_1^2}{\cosh^2[(D-3)k_1(\xi-\xi_1)]}, & \epsilon_1 = +1, \varepsilon\bar{\lambda} < 0, \end{cases} \quad (4.90)$$

where ξ_1 is an arbitrary constant and

$$(D-3)\epsilon_1 k_1^2 = \epsilon_2(D-2)k_2^2 + \left(\frac{D-3}{D-2}\right)c_1^2, \quad (4.91)$$

with k_1, c_1 constants constrained only by the requirement that (4.91) have real solutions.

(ii) Special $\bar{\lambda} = 0$ solution:

$$2\varepsilon\Lambda e^{2\chi} = \begin{cases} \frac{-k_3^2}{\sinh^2[k_3(\xi-\xi_3)]}, & \epsilon_3 = +1, \varepsilon\Lambda < 0, \\ \frac{-1}{(\xi-\xi_3)^2}, & \epsilon_3 = 0, \varepsilon\Lambda < 0, \\ \frac{-k_3^2}{\sin^2[k_3(\xi-\xi_3)]}, & \epsilon_3 = -1, \varepsilon\Lambda < 0, \\ \frac{k_3^2}{\cosh^2[k_3(\xi-\xi_3)]}, & \epsilon_3 = +1, \varepsilon\Lambda > 0, \end{cases} \quad (4.92)$$

where ξ_3 is an arbitrary constant and

$$\frac{\epsilon_3 k_3^2}{D-2} = \epsilon_2 k_2^2 + c_3^2, \quad (4.93)$$

with k_3, c_3 constants constrained only by the requirement that (4.93) have real solutions. The solution for the $\bar{\lambda} = 0$ Salam–Sezgin fluxbrane ($D = 6, \epsilon_Q = -1, \epsilon_2 = +1, \varepsilon > 0, \Lambda > 0$) has been given previously in terms of these variables by Gibbons, Güven and Pope [200], and is readily seen to agree with the above upon making the replacements $\eta \rightarrow x, \chi \rightarrow y, 2(\zeta - \chi) \rightarrow z, k_2 \rightarrow \frac{1}{2}\lambda_1, k_3 \rightarrow \lambda_2, c_2 \rightarrow \frac{1}{2}\lambda_3$, to make contact with their notation.

The general solution other than in the special cases (4.90)–(4.93) does not appear to have an obvious simple analytic form. However, general properties of the solutions can be gleaned following the method of [194]. The constraint (4.89) may be used to eliminate $\varepsilon\bar{\lambda}e^{2\zeta}$ from (4.87), to yield a 3–dimensional autonomous system of first–order ODEs. If we define $X \equiv \dot{\zeta}$, $V \equiv \dot{\chi}$ and $W \equiv \sqrt{2}e^{\chi}/\sqrt{D-2}$, this system is given by

$$\dot{X} = -(D-3)P - \varepsilon\Lambda W^2 \quad (4.94)$$

$$\dot{V} = -(D-2)P \quad (4.95)$$

$$\dot{W} = VW \quad (4.96)$$

where

$$P \equiv X^2 - 2XV + \left(\frac{D-3}{D-2}\right)V^2 + \epsilon_2 k_2^2. \quad (4.97)$$

The fact we have a 3–dimensional system means that the analysis is considerably simpler than in the 5–dimensional examples of ref. [194], and is closer to the phase space of a simple spherically symmetric uncharged black hole with a Liouville potential [202].

Trajectories with $W = 0$ remain confined to the plane. Consequently, in the full 3–dimensional phase space we can take $W \geq 0$ without loss of generality.

As is the case in refs. [194, 202] the only critical points at a finite distance from the origin are given by the 1–parameter locus of points with $W = 0$ and $P = 0$. From (4.97) it follows that the critical points are: (i) hyperbolae in the first and third quadrants of the $W = 0$ plane if $\epsilon_2 > 0$; (ii) straight lines $V = \sqrt{D-2} [\sqrt{D-2} \pm 1] X/(D-3)$ if $\epsilon_2 = 0$; and (iii) hyperbolae which cross all quadrants if $\epsilon_2 < 0$. The $W = 0$, $P = 0$ curve is described by the locus (X_0, V_0) , where

$$V_0 = \frac{\sqrt{D-2}}{D-3} \left[\sqrt{D-2} X_0 \pm \sqrt{X_0^2 - (D-3) \epsilon_2 k_2^2} \right]. \quad (4.98)$$

These critical points are found to correspond to asymptotic regions $R \rightarrow \infty$, or singularities with $R \rightarrow 0$, except in the special case that $X_0 = V_0 = \sqrt{D-2} k_2$. For the special case $R \rightarrow \text{const}$, which represents a horizon in the black hole case, or a bolt in the fluxbrane case.

The integral curves which lie in the plane $W = 0$ are the lines

$$V = \left(\frac{D-2}{D-3}\right) X + \text{const}, \quad (4.99)$$

and these of course correspond to the special solutions (4.90), (4.91). Such lines cross the $W = 0$, $P = 0$ curve once in the first quadrant and once in the third quadrant if $\epsilon_2 = 0, +1$.

An analysis of small perturbations about the critical points (4.98) shows that the eigenvalues are $\{0, 2X_0, V_0\}$. Thus points in the first quadrant repel a 2-dimensional bunch of trajectories out of the $W = 0$ plane, while points in the third quadrant attract a 2-dimensional bunch of trajectories out of the $W = 0$ plane for all values of ϵ_2 . For $\epsilon_2 = -1$ the points in the second and fourth quadrants are saddle points with respect to directions out of the $W = 0$ plane. Points in the second quadrant each attract one of the lines (4.99) in $W = 0$ plane, while points in the fourth quadrants similarly each eject one of the lines (4.99).

We will henceforth restrict our attention to the case $\varepsilon = +1$, so that we are dealing with the domain of outer communications in the case of a black hole or naked singularity ($\epsilon_Q = +1$); or with a fluxbrane ($\epsilon_Q = -1$).

The following critical points are found at the phase space infinity, and coincide with a subset of the critical points of the more general system of ref. [194]. We will label them identically to the notation of ref. [194]. The points are:

- L_{5-8} located at $X = \pm\infty$, $V = [D-2 \pm \sqrt{D-2}]X/(D-3)$, $W = 0$. These points are the endpoints of the 1-parameter family of critical points with $P = 0$ at finite values of X and V in the $W = 0$ plane. The eigenvalues for small perturbations are again $\{0, 2X_0, V_0\}$.
- $M_{1,2}$ located at $X = \pm\infty$, $V = (\frac{D-2}{D-3})X$, $W = 0$. These points correspond to asymptotically flat solutions, and have $P = -X^2/(D-3)$ and $\bar{\lambda} > 0$. The eigenvalues for small perturbations are $\{-1, -1, 1/(D-3)\}$. The two dimensional set of solutions attracted are simply the integral curves (4.99) which represent solutions for the system with no scalar potential, i.e., $\Lambda = 0$.
- $P_{1,2}$ located at $X = \pm\infty$, $V = X$, $W = |X|/\sqrt{-(D-2)\Lambda}$. These points only exist if $\Lambda < 0$, and have $P = -X^2/(D-2)$ and $\bar{\lambda} = 0$. They are thus are endpoints for integral curves with all possible signs of $\bar{\lambda}$. The eigenvalues for small perturbations are $\{-1, -1, 0\}$. It is quite possible that higher order terms

would lift the degeneracy of the zero eigenvalue. However, we will not investigate this further, as the solutions with $\Lambda < 0$ are not our prime concern in this chapter. The points $P_{1,2}$ represent the $r \rightarrow \infty$ asymptotic region for solutions which are not asymptotically flat, but which have the unusual asymptotics listed in Table II of ref. [194] with $g_1 = -1$.

Although the present model is a degenerate case of the more general analysis of ref. [194], all of the possible asymptotic properties of the solutions outlined above are special cases of the analysis of [194], and thus the general conclusions obtained there also hold here. In particular, there are no regular black hole solutions with $\bar{\lambda} > 0$ apart from a class with unusual asymptotics which exist if $\Lambda < 0$. In the case of the Salam–Sezgin model, $\Lambda > 0$, and so no regular uncompactified black holes exist in that case.

For the purposes of the construction of [172], which we generalize in this chapter, the particulars of the asymptotic solutions are not important, however, since part of the spacetime is excluded once the thin brane is inserted in the fluxbrane background. Whether or not dual black holes with standard (or even unusual) asymptotic properties exist is therefore not of primary importance. What is important is that the spacetime from the bolt to the thin brane should be regular. Provided a regular horizon exists in the black hole case, which is dual to a bolt in the fluxbrane, then the construction of ref. [172] should lead to regular hybrid compactifications. The analysis above shows that such solutions can be obtained only in the special case that $X_0 = V_0 = \sqrt{D-2} k_2$, as there then exists a 2-dimensional bunch of trajectories with any sign of $\bar{\lambda}$, including the $\bar{\lambda} > 0$ case relevant to a positive cosmological term on the brane.

We therefore believe that the construction used in this chapter can be extended to a small class of solutions with $\bar{\lambda} > 0$ in the case of the Salam–Sezgin model. Since it appears that such solutions could only be constructed numerically [185], we have not investigated them in further detail. We have no reason to suspect that the qualitative properties of the hybrid compactifications on such backgrounds should differ from those of the $\bar{\lambda} = 0$ solutions.

4.7 Conclusion

We have extended the construction of ref. [172] to produce a new hybrid brane world compactification in six dimensions with a number of desirable features. As is the case with the earlier model, the observable universe corresponds to a codimension one brane which has one extra Kaluza–Klein direction and which closes regularly in the bulk at bolts, namely geodesically complete submanifolds where a rotational Killing vector $\partial/\partial\theta$ vanishes. The regularity of the geometry ensures that construction avoids potential problems that often arise when extra matter is added to models with additional horizons or singularities in the bulk. The construction of nonlinear gravitational waves in §4.4 is an explicit demonstration of this. Furthermore, we have demonstrated that such gravitational wave equations include a mode which may be considered as a massless minimally coupled scalar field on the unperturbed bulk geometry, with Neumann boundary conditions at the brane, and that such a mode has a static potential with a long range Newtonian potential plus Yukawa corrections.

The most significant improvement that the present model has over the earlier construction of ref. [172], is that the supersymmetric Salam–Sezgin action allows a hybrid brane world construction in which there appears to be just enough parameter freedom to make a solution to the hierarchy problem feasible. For those parameter ranges which achieve this, giving a “deep bulk” direction as compared to the radius of the Kaluza–Klein circle, it is quite possible that the spacing of the Yukawa levels would become so close that their sum would approximate inverse powers of $|\mathbf{x} - \mathbf{x}'|$ rather than a single Yukawa–like term. Such corrections would then be similar to those of the Randall–Sundrum II model [168].

In comparison to brane world models in six dimensions which view the physical universe as a codimension two topological defect, we note that the position of the four-brane in the bulk is uniquely determined by the bulk geometry and does therefore not require the addition of other branes in the bulk, or of special matter field configurations on them. The degree of naturalness by which the cosmological constant problem might be solved in this model is an interesting open problem which we have not pursued.

In order to solve the field equations analytically it was necessary to assume that

the 4–dimensional cosmological constant was zero. However, our construction does not seem to preclude the possibility of the model having a non-zero cosmological constant in four dimensions, similar to the explicit solutions found for the model of [172]. The analysis of section 4.6 suggests that such solutions exist but are unlikely to have a simple analytic form. Even though they would be non–singular in the bulk, the existence of such solutions is not precluded by the recent uniqueness theorem of Gibbons, Güven and Pope [200], since the presence of the codimension one brane provides a loophole to its proof. If analytic solutions with non–zero 4–dimensional cosmological constant could be found, then the nonlinear gravitational wave construction of §4.4.4 should generalise directly. Examples of the bulk solutions in question have recently been given numerically by Tolley *et al.* [185]. It would also be interesting to consider the influence that matter sources on the brane would have on such solutions, a question that has recently been considered at the linearised level in other 6–dimensional models [192].

Even in the absence of a cosmological constant, the solutions (4.6), (4.7), (4.9)–(4.11), together with the hybrid construction offer the possibility of generating brane world black hole solutions as well as the gravitational wave solutions already presented. Since the solutions given apply to arbitrary Ricci–flat geometries in the physical 4–dimensions, they include the Schwarzschild and Kerr geometries as particular examples. The most important open problem is an analysis of gravitational perturbations on such backgrounds analogous to the case of the 4–dimensional flat background studied in §4.4. Such an analysis would resolve the important question of the stability of such black holes in the 6–dimensional setting, and also give some idea of potential signatures of higher dimensions on black hole physics. Given that the construction of brane world black holes is generally far from trivial, the hybrid compactifications offer a promising arena for studying concrete realisations of such solutions.

In conclusion, we believe that the construction of ref. [172] combines some of the best features of both the Randall–Sundrum and Kaluza–Klein scenarios, and leads naturally to a class of hybrid compactifications which should be further studied. The present chapter shows that the extension to bulk geometries of the supersymmetric Salam–Sezgin background provides further phenomenological reasons for doing so.

Appendix A

Physical Units

We use rationalised units in which the constants c , k , \hbar and μ_0 do not appear, or equivalently may be considered to have numerical value unity. The constant G appears explicitly, however. It generally refers to the D -dimensional gravitational constant, $\kappa^2 = 4\pi G$, $[G] = L^{d-2}$. One may transform between our natural units and rationalised practical (SI) units by making the following transformations for the five SI base dimensions:

$$\text{Length: } x = x_{\text{SI}}$$

$$\text{Time: } t = ct_{\text{SI}}$$

$$\text{Mass: } m = \frac{c}{\hbar} m_{\text{SI}}$$

$$\text{Temperature: } T = \frac{k}{\hbar c} T_{\text{SI}}$$

$$\text{Current: } i = \left(\frac{\mu_0}{\hbar c}\right)^{1/2} i_{\text{SI}}.$$

Appendix B

Series solutions for a static scalar potential in a Salam-Sezgin Supergravitational hybrid braneworld

Benedict M.N. Carter and Alex B. Nielsen

gr-qc/0512024

Gen. Rel. Grav. **37** (2005) 1629

B.1 Abstract

The static potential for a massless scalar field shares the essential features of the scalar gravitational mode in a tensorial perturbation analysis about the background solution. Using the fluxbrane construction of [203] we calculate the lowest order of the static potential of a massless scalar field on a thin brane using series solutions to the scalar field's Klein Gordon equation and we find that it has the same form as Newton's Law of Gravity. We claim our method will in general provide a quick and useful check that one may use to see if their model will recover Newton's Law to lowest order on the brane.

B.2 Introduction

It has long been a dream to derive the properties of our four-dimensional world from the symmetries of some higher dimensional spacetime. Randall-Sundrum models use warped metrics in five dimensions to obtain a low-energy effective Newtonian potential for four-dimensional gravity. Two models have been proposed: Randall-Sundrum I [167] and Randall Sundrum II [168]. Randall-Sundrum I contains two branes in a compact spacetime and Randall-Sundrum II contains only one brane embedded in a five-dimensional non-compact Anti de-Sitter spacetime. However, while the model met with a lot of interest, for example it may provide an explanation for the large energy difference between the weak-unification scale and the Planck scale, it has also led to some problems. It can be shown for example that under general assumptions the compact Randall-Sundrum I model must contain a negative tension brane [94]. It has been pointed out that such negative tension branes violate all the standard energy conditions [92]. Embedding black holes in Randall-Sundrum II-type models has also led to some problems, although the tension of the single brane can now be strictly positive. The Einstein equations evaluated across the brane forbid simple black holes in our universe (on the brane) and black strings extending off the brane develop Gregory-Laflamme instabilities at the AdS horizon and are unstable far from the brane [97].

In six (and higher) dimensions however, it is possible to have solutions that contain only positive tension branes. It may even be possible to have stable black hole solutions in six-dimensions [104]. Here we present an example of a six-dimensional model based on a supersymmetric fluxbrane solution of [104] and [78] and give a general argument to show that its low energy limit is four-dimensional Newtonian gravity. The model contains a single brane embedded in a six-dimensional spacetime. Scalar and electromagnetic fields propagate in the bulk, and we impose regular closure of the geometry off the brane.

The basic idea is to investigate the behavior of gravity by approximating the full tensorial analysis with a scalar field argument. To do this we solve the Klein-Gordon equation on the background spacetime solution. The background solution must obey

certain boundary conditions, in particular the Einstein equations across the brane must hold. Solving this equation allows us to derive a static potential for the Newtonian limit which should qualitatively resemble that of the observed universe.

Further details appear in [203] (also chapter 4).

B.3 The Model

We start with the metric (which equates to the bosonic sector of the model considered in [189]),

$$S = \int_M d^6x \sqrt{-g} \left(\frac{\mathcal{R}}{4\kappa^2} - \frac{1}{4} \partial_\mu \phi \partial^\mu \phi - \frac{1}{4} e^{-\kappa\phi} F_{ab} F^{ab} - \frac{\Lambda}{2\kappa^2} e^{\kappa\phi} \right). \quad (\text{B.1})$$

The metric assumption we use is

$$ds^2 = \Delta(r) d\theta^2 + \frac{r^2}{\Delta(r)} dr^2 + r^2 \bar{g}_{ij} dx^i dx^j, \quad (\text{B.2})$$

where \bar{g}_{ij} will, for simplicity, be taken to be the Minkowski metric. We consequently find solutions of the form [179]

$$\Delta(r) = \frac{A}{r^2} - \frac{B^2}{r^6} - \frac{1}{8} \Lambda r^2. \quad (\text{B.3})$$

For later use we define r_\pm to be the two zeroes of Δ (there are only two solutions for $r > 0$). To this background fluxbrane geometry we add a single brane and interpret our four-dimensional universe to be restricted to the brane in the usual manner. Note that in general both the scalar field ϕ and the Maxwell field will exist off the brane. Further details of the construction appear in [203].

In order to consistently reproduce our four-dimensional universe on the brane, the gravitational interactions on the brane must reduce, at low energies, to the observed Newtonian potential. The basic idea here is to use a massless scalar field to model the behavior of gravity. Therefore we look for solutions to the massless Klein-Gordon equation

$$\nabla^2 G_\Phi = \frac{1}{\sqrt{-g}} \partial_\mu (\sqrt{-g} g^{\mu\nu} \partial_\nu G_\Phi) = \frac{\delta(r - r') \delta(\theta - \theta') \delta(\mathbf{x} - \mathbf{x}')}{\sqrt{-g}}, \quad (\text{B.4})$$

with boundary conditions

$$G_\Phi|_{r \rightarrow r_-} < \infty, \quad (\text{B.5})$$

$$\partial_r G_\Phi|_{r=r_*} = 0. \quad (\text{B.6})$$

B.4 The Solution

To simplify the analysis of (B.4) we perform a change of variables to put the differential equation into Sturm-Liouville form with the variable ρ .

$$\rho = e^{\int (r^4 \Delta(r))^{-1} dr} \quad (\text{B.7})$$

which becomes

$$\rho = \frac{r^4 - r_-^4}{r_+^4 - r_-^4} \geq 0, \quad (\text{B.8})$$

where r_+ and r_- are the two roots of $\Delta(r)$. We also perform the Fourier decomposition of the Green's function

$$G_\Phi = \int \frac{d^4 k}{(2\pi)^5} e^{ik_\mu (x^\mu - x'^\mu)} \sum_{n=-\infty}^{\infty} e^{in(\phi - \phi')} y_{q,n}(\rho, \rho'). \quad (\text{B.9})$$

This gives a differential equation of the form

$$\partial_\rho (\rho \partial_\rho y_{q,n}) - \frac{\bar{n}^2}{\rho} \left(\frac{\rho + \frac{r_-^4}{r_+^4}}{\rho + 1} \right)^2 y_{q,n} + \frac{\bar{q}^2}{(\rho + 1)^2} y_{q,n} = \delta(\rho - \rho'), \quad (\text{B.10})$$

where

$$q^2 = -k_\mu k^\mu, \quad (\text{B.11})$$

$$\bar{q}^2 = q^2 \frac{\Lambda}{8} (r_+^4 - r_-^4)^2, \quad (\text{B.12})$$

$$\bar{n}^2 = n^2 r_+^8. \quad (\text{B.13})$$

An obvious way to investigate the behavior of solutions to this differential equation is to use the method of Frobenius and expand the solution out as a power series. Provided the r coordinate is close to r_- the value of ρ will be small. The two linearly independent solutions are

$$y_1 = \sum_{k=0}^{\infty} a_k \rho^{k+c_1} \quad (\text{B.14})$$

$$y_2 = \begin{cases} \sum_{k=0}^{\infty} b_k \rho^{k+c_2} & n \neq 0 \\ \log(|\rho|) y_1 + \sum_{k=0}^{\infty} b_k \rho^k & n = 0. \end{cases} \quad (\text{B.15})$$

where c_1 and c_2 are the solutions of the indicial equation for (B.10),

$$c^2 - (nr_-^4)^2 = 0. \quad (\text{B.16})$$

If we impose the requirement that the solution be regular as $\rho \rightarrow 0$, then we must set the coefficient of the second independent solution to 0 and we are just left with the first solution. The Einstein equations at the brane also require a Neumann-type boundary condition for the function G_Φ at the brane. This, along with the usual braneworld matching conditions that the metric should be continuous at the brane and its first derivative should just be a step function (the stress-energy tensor contains a delta function source due to the brane), result in the on-brane solution at $\rho = \rho_* = r_-/r_+ < 1$,

$$y_{q,n} = \frac{y_1(\rho_*)}{\rho_* \partial_\rho y_1(\rho_*)} \quad (\text{B.17})$$

The $n = 0$ mode represents the lowest order of the potential. For $n = 0$ we find

$$y_1(\rho_*) = \sum_{k=0}^{\infty} \left((-1)^k \sum_{j=0}^k e_{j,k} q^{2j} \right) \rho_*^k, \quad (\text{B.18})$$

where $e_{0,0} = 1$, $e_{0,k} = 0$ for all $k > 0$ and $e_{j,k} \geq 0$ for all $j > 0$ and $k > 0$. In the case where this double summation converges absolutely then all rearrangements converge to the same limit and we can write

$$y_1(\rho_*) = \sum_{j=0}^{\infty} \left(\sum_{k=j}^{\infty} (-1)^k e_{j,k} \rho_*^k \right) q^{2j}. \quad (\text{B.19})$$

Similarly

$$\rho_* \partial_\rho y_1(\rho_*) = \sum_{j=0}^{\infty} \left(\sum_{k=j}^{\infty} (-1)^k k e_{j,k} \rho_*^k \right) q^{2j}. \quad (\text{B.20})$$

We can then write out (B.17) as

$$y_{q,0}(\rho_*) = \sum_{k=-1}^{\infty} Q_{k,0} q^{2k} \quad (\text{B.21})$$

and calculate $Q_{i,0}$ ($Q_{i,n}$ is the general term) order by order in q^2 using the relationship

$$y_1(\rho_*) = [y_{q,0}(\rho_*)][\rho_* \partial_\rho y_1(\rho_*)]. \quad (\text{B.22})$$

For example,

$$Q_{-1,0} = -\frac{(1 + \rho_*)2\Lambda}{\rho_*}. \quad (\text{B.23})$$

Substituting the series back into the expression for the potential we find

$$V_\Phi = \int \frac{d^3\mathbf{k}}{(2\pi)^5} e^{-i\mathbf{k} \cdot (\mathbf{x} - \mathbf{x}')} \int_{-\infty}^{\infty} \frac{dk^0}{i(k^0 - i\epsilon)} \left(\frac{Q_{-1,0}}{q^2} + \sum_{j=0}^{\infty} Q_{j,0} q^{2j} \right). \quad (\text{B.24})$$

The term proportional to q^{-2} just gives a contribution of

$$V_\Phi = \frac{Q_{-1,0}}{2\pi} \int \frac{d^3\mathbf{k}}{(2\pi)^3} \frac{e^{-i\mathbf{k} \cdot (\mathbf{x} - \mathbf{x}')}}{\mathbf{k}^2} \quad (\text{B.25})$$

and thus the potential to lowest order becomes

$$V_\Phi = -\frac{(1 + \rho_*)\Lambda}{4\pi^2 \rho_*} \frac{1}{|\mathbf{x} - \mathbf{x}'|}, \quad (\text{B.26})$$

which has the desired $1/\mathbf{x}$ dependence of the familiar Newtonian gravitational potential.

B.5 Conclusion

The basic model outlined here is capable of reproducing Newton's law of gravity at low energies, and our method demonstrated here provides a method for quickly checking this. Our method does not in general allow one to easily calculate the correction to the lowest order of the static gravitational potential on the brane. Reproduction of Newton's law of gravity to lowest order seems to be a generic property of (6D) models constructed in this manner. Several other models have achieved the same result although often without the added feature of regularity in the bulk and with added restrictions on the brane [179]. It is the regular closure of the bulk geometry at the totally geodesic submanifolds (bolts) that gives hope to the idea that perturbations of black holes and gravitational waves will not grow without limit and thus further study should be carried out in this direction.

B.6 Acknowledgements

We thank Dr. David Wiltshire for introducing us to this problem and for his supervision. This research was supported in part by the Marsden Fund administered by the Royal Society of New Zealand.

References

- [1] C. Rovelli, “*Notes for a brief history of quantum gravity*”, in “*The Ninth Marcel Grossmann meeting : Proceedings*”, eds. V.G. Gurzadyan, R.T. Jantzen, R. Ruffini. (World Scientific, Singapore, 2002) pp. 742-768 [arXiv:gr-qc/0006061].
- [2] C. Rovelli, “*Quantum Gravity*” (Cambridge University Press, 2004)
- [3] K. V. Kuchar, “*Canonical quantum gravity*”, in “*General relativity and gravitation 1992 : proceedings*”, eds. R.J. Gleiser, C.N. Kozameh, O.M. Moreschi, (IOP, Philadelphia, Pa., 1993) pp. 119-150.
- [4] D. L. Wiltshire, “*An introduction to quantum cosmology*”, in “*Cosmology: The Physics of the Universe*”, eds. B. Robson, N. Visvanathan and W.S. Woolcock, (World Scientific, Singapore, 1996) pp. 473-531, [arXiv:gr-qc/0101003].
- [5] K. Schwarzschild, “*Über das Gravitationsfeld eines Massenpunktes nach der Einsteinschen Theorie*”, Sitzungsber. Preuss. Akad. Wiss., Phys. Math. Kl., **1** 1916.
- [6] S. Antoci and D. E. Liebscher, “*Reinstating Schwarzschild’s original manifold and its singularity*,” [arXiv:gr-qc/0406090].
- [7] http://www.theory.caltech.edu/people/preskill/new_naked_bet.html
- [8] R. P. Kerr, “*Gravitational Field Of A Spinning Mass As An Example Of Algebraically Special Metrics*”, Phys. Rev. Lett. **11** (1963) 237.
- [9] R. P. Kerr and A. Schild, “*Some algebraically degenerate solutions of Einstein’s gravitational field equations*”, Proc. Symp. Appl. Math. **17**, 199 (1965).

- [10] G. W. Gibbons, H. Lu, D. N. Page and C. N. Pope, “*The general Kerr-de Sitter metrics in all dimensions*”, J. Geom. Phys. **53** (2005) 49 [arXiv:hep-th/0404008].
- [11] W. de Sitter, Mon. Not. Roy. Astron. Soc. **78**, (1917), 3, Proc. Kon. Ned. Akad. Wet. **20**, (1921) , 1309.
- [12] F. Kottler, “*Über die physikalische Grundlagen der Einsteinischen Gravitations-theorie*” Ann. Phys. (Leipzig) **56**, 1918, 401-62,
- [13] B. Carter, *Hamilton-Jacobi and Schrödinger separable solutions of Einstein’s equations*, Commun. Math. Phys. **10**, 280 (1968).
- [14] B. Carter, “*Black hole equilibrium states*”, in *Black Holes (Les Houches Lectures)*, eds. B.S. DeWitt and C. DeWitt (Gordon and Breach, New York, 1972).
- [15] E. T. Newman, R. Couch, K. Chinnapared, A. Exton, A. Prakash, R. Torrence, “*Metric of a Rotating, Charged Mass*”, J. Math. Phys. **6**, 1965, 918-919.
- [16] R. M. Wald, “*Nernst theorem’ and black hole thermodynamics*”, Phys. Rev. D **56**, 1997, 6467-74.
- [17] J. D. Bekenstein, “*Generalized Second Law Of Thermodynamics In Black Hole Physics*”, Phys. Rev. D **9**, 3292 (1974).
- [18] J. M. Bardeen, B. Carter and S. W. Hawking, “*The Four Laws Of Black Hole Mechanics*”, Commun. Math. Phys. **31** (1973) 161.
- [19] S. W. Hawking, “*Particle Creation By Black Holes*”, Commun. Math. Phys. **43** (1975) 199 Erratum-ibid. **46** (1976) 206.
- [20] Robert M. Wald, “*The Thermodynamics of Black Holes*”, Living Rev. Relativity **4**, (2001), 6. URL (cited on 21/04/2006): <http://www.livingreviews.org/lrr-2001-6>
- [21] M. Visser, “*Essential and inessential features of Hawking radiation*”, Int. J. Mod. Phys. D **12** (2003) 649 [arXiv:hep-th/0106111].
- [22] S. M. Carroll, “*Spacetime and Geometry: An Introduction to general relativity*”, San Francisco: Benjamin Cummings, 2003.

[23] S. W. Hawking, “*Breakdown Of Predictability In Gravitational Collapse*”, Phys. Rev. D **14** (1976) 2460.

[24] S. W. Hawking, “*The Unpredictability Of Quantum Gravity*”, Commun. Math. Phys. **87** (1982) 395.

[25] S. W. Hawking, “*Nontrivial Topologies In Quantum Gravity*”, Nucl. Phys. B **244**, 135 (1984).

[26] S. W. Hawking, “*Information loss in black holes*”, Phys. Rev. D **72** (2005) 084013 [arXiv:hep-th/0507171].

[27] G. ’t Hooft, “*On The Quantum Structure Of A Black Hole*”, Nucl. Phys. B **256**, 727 (1985).

[28] G. ’t Hooft, “*The Black hole horizon as a quantum surface*”, Phys. Scripta **T36**, 247 (1991).

[29] C. R. Stephens, G. ’t Hooft and B. F. Whiting, “*Black hole evaporation without information loss*”, Class. Quant. Grav. **11**, 621 (1994) [arXiv:gr-qc/9310006].

[30] G. ’t Hooft, “*The scattering matrix approach for the quantum black hole: An overview*”, Int. J. Mod. Phys. A **11** (1996) 4623 [arXiv:gr-qc/9607022].

[31] J. Chadwick, “*Possible Existence Of A Neutron*”, Nature **129** (1932) 312.

[32] W. Baade, F. Zwicky, “*Supernovae and Cosmic rays*”, Phys. Rev. **45**, (1934) 130139

[33] M. Gell-Mann, “*Symmetries Of Baryons And Mesons*”, Phys. Rev. **125** (1962) 1067.

[34] B. Freedman and L. D. McLerran, “*Quark Star Phenomenology*”, Phys. Rev. D **17** (1978) 1109.

[35] M. H. Anderson, J. R. Ensher, M. R. Matthews, C. E. Wieman and E. A. Cornell, “*Observation of Bose-Einstein condensation in a dilute atomic vapor*”, Science **269**, 198 (1995).

[36] G. Chapline, E. Hohlfeld, R. B. Laughlin and D. I. Santiago, “*Quantum phase transitions and the breakdown of classical general relativity*”, Int. J. Mod. Phys. A **18**, 3587 (2003) [arXiv:gr-qc/0012094].

[37] P. O. Mazur and E. Mottola, “*Dark energy and condensate stars: Casimir energy in the large*”, [arXiv:gr-qc/0405111].
 P. O. Mazur and E. Mottola, “*Gravitational vacuum condensate stars*”, Proc. Nat. Acad. Sci. **111**, 9545 (2004) [arXiv:gr-qc/0407075].

[38] M. Visser and D. L. Wiltshire, “*Stable gravastars - an alternative to black holes?*”, Class. Quant. Grav. **21**, 1135 (2004) [arXiv:gr-qc/0310107].

[39] http://en.wikipedia.org/wiki/Neutron_star

[40] N. Chamel, “*Effective mass of free neutrons in neutron star crust*”, [arXiv:nucl-th/0512034].

[41] S. L. Shapiro and S. A. Teukolsky, “*Black Holes, White Dwarfs, And Neutron Stars: The Physics Of Compact Objects*”, (New York, USA: Wiley, 1983)

[42] C. Rovelli, “*Loop Quantum Gravity*”, Living Rev. Relativity 1, (1998), 1. URL (cited on 24/02/2006): <http://www.livingreviews.org/lrr-1998-1>

[43] M. Li, “*Introduction to M theory*”, [arXiv:hep-th/9811019].

[44] B. A. Ovrut, “*Lectures on heterotic M-theory*”, [arXiv:hep-th/0201032].

[45] P. Ehrenfest, Proc. K. Acad. Wetensch. Amsterdam **20** (1920) 200-209; Ann. Phys. Leipzig **61** 440-446

[46] F. R. Tangherlini, Nuovo Cimento **27** (1963) 636-651

[47] R. C. Myers and M. J. Perry, “*Black Holes In Higher Dimensional Space-Times*”, Annals Phys. **172** (1986) 304.

[48] M. Heusler, “*Stationary Black Holes: Uniqueness and Beyond*”, Living Rev. Relativity 1, (1998), 6. URL (cited on 09/02/2006): <http://www.livingreviews.org/lrr-1998-6>

[49] H. Luckock and I. Moss, “*Black Holes Have Skyrmion Hair*”, Phys. Lett. B **176** (1986) 341.

[50] P. Bizon and T. Chmaj, “*Gravitating skyrmions*”, Phys. Lett. B **297** (1992) 55.

[51] S. Droz, M. Heusler and N. Straumann, “*New black hole solutions with hair*”, Phys. Lett. B **268** (1991) 371.

[52] R. Emparan and H. S. Reall, “*A rotating black ring in five dimensions*”, Phys. Rev. Lett. **88**, 101101 (2002) [arXiv:hep-th/0110260].

[53] T. Kaluza, Sitzungsber. Preuss. Akad. Wiss. (1921) 966-972

[54] O. Klein, Z. Phys. (1926) **31** 895-906; Nature **118** (1926) 516

[55] A. Salam and J. A. Strathdee, “*On Kaluza-Klein Theory*”, Annals Phys. **141**, 316 (1982).

[56] E. W. Kolb and R. Slansky, “*Dimensional Reduction In The Early Universe: Where Have The Massive Particles Gone?*”, Phys. Lett. B **135**, 378 (1984).

[57] G. W. Gibbons and P. J. Ruback, “*Classical Gravitons And Their Stability In Higher Dimensions*”, Phys. Lett. B **171**, 390 (1986).

[58] B. S. DeWitt, in “*Relativity, Groups and Topology: Les Houches, 1963*”, eds. C. DeWitt and B.S. DeWitt, (Gordon and Breach, New York, 1964) p. 725

[59] R. Kerner, Ann. Inst. H. Poincaré **9** (1968) 143-152

[60] Y. M. Cho and P. G. O. Freund, “*Nonabelian Gauge Fields In Nambu-Goldstone Fields*”, Phys. Rev. D **12** (1975) 1711.

[61] Y. M. Cho, “*Higher - Dimensional Unifications Of Gravitation And Gauge Theories*”, J. Math. Phys. **16** (1975) 2029.

[62] Y. M. Cho and P. S. Jang, “*Unified Geometry Of Internal Space With Space-Time*”, Phys. Rev. D **12** (1975) 3789.

[63] E. Cremmer and B. Julia, “*The $N=8$ Supergravity Theory. 1. The Lagrangian*”, Phys. Lett. B **80**, 48 (1978).

[64] E. Cremmer and B. Julia, “*The $SO(8)$ Supergravity*”, Nucl. Phys. B **159**, 141 (1979).

[65] J. Scherk and J. H. Schwarz, “*Spontaneous Breaking Of Supersymmetry Through Dimensional Reduction*”, Phys. Lett. B **82**, 60 (1979).

[66] J. Scherk and J. H. Schwarz, “*How To Get Masses From Extra Dimensions*”, Nucl. Phys. B **153**, 61 (1979).

[67] M. J. Duff, B. E. W. Nilsson, C. N. Pope and N. P. Warner, “*On The Consistency Of The Kaluza-Klein Ansatz*”, Phys. Lett. B **149**, 90 (1984).

[68] M. J. Duff and C. N. Pope, “*Consistent Truncations In Kaluza-Klein Theories*”, Nucl. Phys. B **255**, 355 (1985).

[69] E. Witten, “*Instability Of The Kaluza-Klein Vacuum*”, Nucl. Phys. B **195**, 481 (1982).

[70] F. Mellor and I. Moss, “*Black Holes And Gravitational Instantons*,” Class. Quant. Grav. **6** (1989) 1379.

[71] S. W. Hawking, C. J. Hunter and M. M. Taylor-Robinson, “*Rotation and the AdS/CFT correspondence*”, Phys. Rev. D **59**, 064005 (1999) [arXiv:hep-th/9811056].

[72] M. M. Caldarelli, G. Cognola and D. Klemm, “*Thermodynamics of Kerr-Newman- AdS black holes and conformal field theories*”, Class. Quant. Grav. **17**, 399 (2000) [arXiv:hep-th/9908022].

[73] M. Giannatto and I. G. Moss, Class. Quant. Grav. **22** (2005) 1803 [arXiv:gr-qc/0502046].

[74] A. Achucarro, J. M. Evans, P. K. Townsend and D. L. Wiltshire, “*Super P -Branes*”, Phys. Lett. B **198** (1987) 441.

[75] K. Akama, “*Pregeometry*”, in K. Kikkawa, N. Nakanishi and H. Nariai (eds), “*Gauge Theory and Gravitation*”, Lect. Notes Phys. **176** (1982) 267 [arXiv:hep-th/0001113].

[76] V. A. Rubakov and M. E. Shaposhnikov, “*Do We Live Inside A Domain Wall?*”, Phys. Lett. B **125**, 136 (1983).

[77] M. Visser, “*An Exotic Class Of Kaluza-Klein Models*”, Phys. Lett. B **159**, 22 (1985) [arXiv:hep-th/9910093].

[78] G. W. Gibbons and D. L. Wiltshire, “*Space-Time As A Membrane In Higher Dimensions*”, Nucl. Phys. B **287**, 717 (1987) [arXiv:hep-th/0109093].

[79] I. Antoniadis, “*A Possible New Dimension At A Few Tev*”, Phys. Lett. B **246** (1990) 377.

[80] N. Arkani-Hamed, S. Dimopoulos and G. R. Dvali, “*The hierarchy problem and new dimensions at a millimeter*”, Phys. Lett. B **429** (1998) 263 [arXiv:hep-ph/9803315].

[81] I. Antoniadis, N. Arkani-Hamed, S. Dimopoulos and G. R. Dvali, “*New dimensions at a millimeter to a Fermi and superstrings at a TeV*”, Phys. Lett. B **436** (1998) 257 [arXiv:hep-ph/9804398].

[82] N. Arkani-Hamed, S. Dimopoulos and G. R. Dvali, “*Phenomenology, astrophysics and cosmology of theories with sub-millimeter dimensions and TeV scale quantum gravity*”, Phys. Rev. D **59** (1999) 086004 [arXiv:hep-ph/9807344].

[83] T. Flacke, D. Hooper and J. March-Russell, “*Improved bounds on universal extra dimensions and consequences for LKP dark matter*”, [arXiv:hep-ph/0509352].

[84] C. Csaki, “*TASI lectures on extra dimensions and branes*”, in “*Theoretical Advanced Study Institute In Elementary Particle Physics (TASI 2002) : Proceedings*” eds. H.E. Haber, A.E. Nelson, (World Scientific, River Edge, 2004) pp. 605-698 [arXiv:hep-ph/0404096].

[85] C. P. Bachas, “*Lectures on D-branes*”, in “*A Newton Institute Euroconference On Duality And Supersymmetric Theories : Proceedings*” eds. D.I. Olive, P.C. West, (Cambridge Univ. Pr., 1999) pp. 414-473 [arXiv:hep-th/9806199].

[86] M. Azreg-Ainou, G. Clement, C. P. Constantinidis and J. C. Fabris, “Electrostatic solutions in Kaluza-Klein theory: Geometry and stability,” *Grav. Cosmol.* **6** (2000) 207 [arXiv:gr-qc/9911107].

[87] L. Randall and R. Sundrum, “*A large mass hierarchy from a small extra dimension*”, *Phys. Rev. Lett.* **83** (1999) 3370 [arXiv:hep-ph/9905221].

[88] L. Randall and R. Sundrum, “*An alternative to compactification*”, *Phys. Rev. Lett.* **83** (1999) 4690 [arXiv:hep-th/9906064].

[89] R. Maartens, “*Brane-World Gravity*”, *Living Rev. Relativity* **7**, (2004), 7. URL (cited on 24/03/2006): <http://www.livingreviews.org/lrr-2004-7>

[90] P. Callin and C. P. Burgess, “*Deviations from Newton’s law in supersymmetric large extra dimensions*”, arXiv:hep-ph/0511216.

[91] D. Marolf and M. Trodden, “*Black holes and instabilities of negative tension branes*”, *Phys. Rev. D* **64**, 065019 (2001) [[arXiv:hep-th/0102135].

[92] C. Barceló and M. Visser, “*D-brane surgery: Energy conditions, traversable wormholes, and voids*”, *Nucl. Phys. B* **584** (2000) 415 [arXiv:hep-th/0004022].

[93] C. Barceló and M. Visser, “*Twilight for the energy conditions?*”, *Int. J. Mod. Phys. D* **11** (2002) 1553 [arXiv:gr-qc/0205066].

[94] F. Leblond, R. C. Myers and D. J. Winters, “*Consistency conditions for brane worlds in arbitrary dimensions*”, *JHEP* **0107**, 031 (2001) [arXiv:hep-th/0106140].

[95] T. Shiromizu, K. I. Maeda and M. Sasaki, “*The Einstein equations on the 3-brane world*”, *Phys. Rev. D* **62** (2000) 024012 [arXiv:gr-qc/9910076].

[96] S. B. Giddings, E. Katz and L. Randall, “*Linearized gravity in brane backgrounds*”, *JHEP* **0003** (2000) 023 [arXiv:hep-th/0002091].

[97] A. Chamblin, S. W. Hawking and H. S. Reall, “*Brane-world black holes*”, *Phys. Rev. D* **61**, 065007 (2000) [arXiv:hep-th/9909205].

[98] A. Chamblin, H. S. Reall, H. a. Shinkai and T. Shiromizu, “*Charged brane-world black holes*”, Phys. Rev. D **63**, 064015 (2001) [arXiv:hep-th/0008177].

[99] D. Brecher, A. Chamblin and H. S. Reall, “*AdS/CFT in the infinite momentum frame*”, Nucl. Phys. B **607**, 155 (2001) [arXiv:hep-th/0012076].

[100] A. Chamblin and G. W. Gibbons, “*Nonlinear supergravity on a brane without compactification*”, Phys. Rev. Lett. **84**, 1090 (2000) [arXiv:hep-th/9909130].

[101] T. Gherghetta and M. E. Shaposhnikov, “*Localizing gravity on a string-like defect in six dimensions*”, Phys. Rev. Lett. **85**, 240 (2000) [arXiv:hep-th/0004014].

[102] T. Gherghetta, E. Roessl and M. E. Shaposhnikov, “*Living inside a hedgehog: Higher-dimensional solutions that localize gravity*”, Phys. Lett. B **491**, 353 (2000) [arXiv:hep-th/0006251].

[103] E. Ponton and E. Poppitz, “*Gravity localization on string-like defects in codimension two and the AdS/CFT correspondence*”, JHEP **0102**, 042 (2001) [arXiv:hep-th/0012033].

[104] J. Louko and D. L. Wiltshire, “*Brane worlds with bolts*”, JHEP **0202** (2002) 007 [arXiv:hep-th/0109099].

[105] G. W. Gibbons and S. W. Hawking, “*Classification Of Gravitational Instanton Symmetries*”, Commun. Math. Phys. **66**, 291 (1979).

[106] J. M. Maldacena, “*The large N limit of superconformal field theories and supergravity*”, Adv. Theor. Math. Phys. **2**, 231 (1998) [Int. J. Theor. Phys. **38**, 1113 (1999)] [arXiv:hep-th/9711200]. S. S. Gubser, I. R. Klebanov and A. M. Polyakov, “*Gauge theory correlators from non-critical string theory*”, Phys. Lett. B **428**, 105 (1998) [arXiv:hep-th/9802109] ; E. Witten, “*Anti-de Sitter space and holography*”, Adv. Theor. Math. Phys. **2**, 253 (1998) [arXiv:hep-th/9802150] ;

[107] E. Witten, “*Anti-de Sitter space, thermal phase transition, and confinement in gauge theories*”, Adv. Theor. Math. Phys. **2**, 505 (1998) [arXiv:hep-th/9803131].

[108] S. W. Hawking and D. N. Page, “*Thermodynamics Of Black Holes In Anti-De Sitter Space*”, Commun. Math. Phys. **87**, 577 (1983).

[109] S. W. Hawking and H. S. Reall, “*Charged and rotating AdS black holes and their CFT duals*”, Phys. Rev. D **61**, 024014 (2000) [arXiv:hep-th/9908109].

[110] R. B. Mann, “*Entropy of rotating Misner string spacetimes*”, Phys. Rev. D **61**, 084013 (2000) [arXiv:hep-th/9904148];

[111] A. M. Awad and C. V. Johnson, “*Holographic stress tensors for Kerr-AdS black holes*”, Phys. Rev. D **61**, 084025 (2000) [arXiv:hep-th/9910040].

[112] K. Landsteiner and E. Lopez, “*The thermodynamic potentials of Kerr-AdS black holes and their CFT duals*”, JHEP **9912**, 020 (1999) [arXiv:hep-th/9911124].

[113] D. Birmingham, “*Topological black holes in anti-de Sitter space*”, Class. Quant. Grav. **16**, 1197 (1999) [arXiv:hep-th/9808032].

[114] R. G. Cai, “*The Cardy-Verlinde formula and AdS black holes*”, Phys. Rev. D **63**, 124018 (2001) [arXiv:hep-th/0102113].

[115] I. P. Neupane, “*Thermodynamic and gravitational instability on hyperbolic spaces*”, Phys. Rev. D **69**, 084011 (2004) [arXiv:hep-th/0302132].

[116] G. W. Gibbons, H. Lu, D. N. Page and C. N. Pope, “*The general Kerr-de Sitter metrics in all dimensions*”, J. Geom. Phys. **53**, 49 (2005) [arXiv:hep-th/0404008];

[117] G. W. Gibbons, H. Lu, D. N. Page and C. N. Pope, “*Rotating black holes in higher dimensions with a cosmological constant*”, Phys. Rev. Lett. **93**, 171102 (2004) [arXiv:hep-th/0409155].

[118] G. W. Gibbons, M. J. Perry and C. N. Pope, “*The first law of thermodynamics for Kerr - anti-de Sitter black holes*”, Class. Quant. Grav. **22**, 1503 (2005) [arXiv:hep-th/0408217].

[119] M. Cvetic, H. Lu and C. N. Pope, “*Charged Kerr-de Sitter black holes in five dimensions*”, Phys. Lett. B **598**, 273 (2004) [arXiv:hep-th/0406196]; “*Charged*

*rotating black holes in five dimensional $U(1)^{**3}$ gauged $N = 2$ supergravity”, Phys. Rev. D **70**, 081502 (2004) [arXiv:hep-th/0407058];*

M. Cvetic, G. W. Gibbons, H. Lu and C. N. Pope, “Rotating black holes in gauged supergravities: Thermodynamics, supersymmetric limits, topological solitons and time machines”, [arXiv:hep-th/0504080].

[120] O. Madden and S. F. Ross, “*On uniqueness of charged Kerr-AdS black holes in five dimensions*”, Class. Quant. Grav. **22**, 515 (2005) [arXiv:hep-th/0409188].

[121] M. Vasudevan, K. A. Stevens and D. N. Page, “*Separability of the Hamilton-Jacobi and Klein-Gordon equations in Kerr-de Sitter metrics*”, Class. Quant. Grav. **22**, 339 (2005) [arXiv:gr-qc/0405125].

[122] H. K. Kunduri and J. Lucietti, “*Integrability and the Kerr-(A)dS black hole in five dimensions*”, Phys. Rev. D **71**, 104021 (2005) [arXiv:hep-th/0502124].

[123] V. P. Frolov and D. Stojkovic, “*Quantum radiation from a 5-dimensional rotating black hole*”, Phys. Rev. D **67**, 084004 (2003) [arXiv:gr-qc/0211055]; “*Particle and light motion in a space-time of a five-dimensional rotating black hole*”, Phys. Rev. D **68**, 064011 (2003) [arXiv:gr-qc/0301016].

[124] I. Papadimitriou and K. Skenderis, “*Thermodynamics of asymptotically locally AdS spacetimes*”, JHEP **0508**, 004 (2005) [arXiv:hep-th/0505190].

[125] M. Cvetic, P. Gao and J. Simon, “*Supersymmetric Kerr-anti-de Sitter solutions*”, Phys. Rev. D **72**, 021701 (2005) [arXiv:hep-th/0504136].

[126] M. Henneaux and C. Teitelboim, “*Asymptotically Anti-De Sitter Spaces*”, Commun. Math. Phys. **98**, 391 (1985).

[127] A. Ashtekar and S. Das, “*Asymptotically anti-de Sitter space-times: Conserved quantities*”, Class. Quant. Grav. **17**, L17 (2000). [arXiv:hep-th/9911230].

[128] S. Das and R. B. Mann, “*Conserved quantities in Kerr-anti-de Sitter spacetimes in various dimensions*”, JHEP **0008**, 033 (2000). [arXiv:hep-th/0008028].

[129] N. Deruelle and J. Katz, “*On the mass of a Kerr-anti-de Sitter spacetime in D dimensions*”, *Class. Quant. Grav.* **22**, 421 (2005) [arXiv:gr-qc/0410135].

[130] S. Deser, I. Kanik and B. Tekin, “*Conserved charges of higher D Kerr-AdS spacetimes*”, *Class. Quant. Grav.* **22**, 3383 (2005) [arXiv:gr-qc/0506057].

[131] G. W. Gibbons, M. J. Perry and C. N. Pope, “*Bulk / boundary thermodynamic equivalence, and the Bekenstein and cosmic-censorship bounds for rotating charged AdS black holes*”, *Phys. Rev. D* **72**, 084028 (2005) [arXiv:hep-th/0506233].

[132] M. Visser, “*Dirty black holes: Thermodynamics and horizon structure*”, *Phys. Rev. D* **46**, 2445 (1992) [arXiv:hep-th/9203057].

[133] H. Nomura, S. Yoshida, M. Tanabe and K. i. Maeda, “*The fate of a five-dimensional rotating black hole via Hawking radiation*”, *Prog. Theor. Phys.* **114**, 707 (2005) [arXiv:hep-th/0502179].

[134] R. G. Cai, L. M. Cao and D. W. Pang, “*Thermodynamics of dual CFTs for Kerr-AdS black holes*”, *Phys. Rev. D* **72**, 044009 (2005) [arXiv:hep-th/0505133].

[135] C. V. Vishveshwara, “*Stability Of The Schwarzschild Metric*,” *Phys. Rev. D* **1** (1970) 2870.

[136] F. J. Zerilli, “*Effective Potential For Even Parity Regge-Wheeler Gravitational Perturbation Equations*,” *Phys. Rev. Lett.* **24** (1970) 737.

[137] F. J. Zerilli, “*Gravitational Field Of A Particle Falling In A Schwarzschild Geometry Analyzed In Tensor Harmonics*,” *Phys. Rev. D* **2** (1970) 2141.

[138] S. Chandrasekhar, S. Detweiler “*On the Equations Governing the Perturbations of the Schwarzschild Black Hole*,” *Proc. Roy. Soc. Lond. A* **343** (1975) 289.

[139] S. A. Teukolsky, “*Rotating Black Holes - Separable Wave Equations For Gravitational And Electromagnetic Perturbations*,” *Phys. Rev. Lett.* **29** (1972) 1114.

[140] S. A. Teukolsky, “*Perturbations Of A Rotating Black Hole. 1. Fundamental Equations For Gravitational Electromagnetic, And Neutrino Field Perturbations*,” *Astrophys. J.* **185** (1973) 635.

[141] W. H. Press and S. A. Teukolsky, “*Perturbations of a rotating black hole II. Dynamical stability of the Kerr metric*,” *Astrophys. J.* **185** (1973) 649.

[142] J. B. Hartle and D. C. Wilkins, “*Analytic properties of the Teukolsky equation*”, *Commun. Math. Phys.* **38** (1974) 47-63

[143] S. Chandrasekhar, S. Detweiler “*On the Equations Governing the Axisymmetric Perturbations of the Kerr Black Hole*,” *Proc. Roy. Soc. Lond. A* **345** (1975) 145.

[144] S. Chandrasekhar, “*The Gravitational Perturbations Of The Kerr Black Hole. I. Perturbations in the Quantities which Vanish in the Stationary State*,” *Proc. Roy. Soc. Lond. A* **358** (1978) 421.

[145] S. Chandrasekhar, “*The Gravitational Perturbations Of The Kerr Black Hole. II. Perturbations in the Quantities which are Finite in the Stationary State*,” *Proc. Roy. Soc. Lond. A* **358** (1978) 441.

[146] S. Chandrasekhar, “*The Gravitational Perturbations Of The Kerr Black Hole. III. Further Amplifications*,” *Proc. Roy. Soc. Lond. A* **365** (1979) 425.

[147] S. Chandrasekhar, “*The Gravitational Perturbations Of The Kerr Black Hole. IV. The Completion of the Solution*,” *Proc. Roy. Soc. Lond. A* **372** (1979) 425.

[148] B. F. Whiting, “*Mode Stability Of The Kerr Black Hole*,” *J. Math. Phys.* **30** (1989) 1301.

[149] T. Damour, N. Deruelle and R. Ruffini, “*On Quantum Resonances In Stationary Geometries*,” *Lett. Nuovo Cim.* **15** (1976) 257.

[150] T. J. M. Zouros and D. M. Eardley, “*Instabilities Of Massive Scalar Perturbations Of A Rotating Black Hole*,” *Annals Phys.* **118** (1979) 139.

[151] S. Detweiler, “*Klein-Gordon Equation And Rotating Black Holes*,” *Phys. Rev. D* **22**, 2323 (1980).

[152] A. Higuchi, “*Symmetric Tensor Spherical Harmonics On The N Sphere And Their Application To The De Sitter Group $SO(N,1)$* ”, *J. Math. Phys.* **28** (1987) 1553 Erratum-*ibid.* **43** (2002) 6385.

[153] A. Ishibashi and R. M. Wald, *Class. Quant. Grav.* **21** (2004) 2981 [arXiv:hep-th/0402184].

[154] G. Gibbons and S. A. Hartnoll, “*A gravitational instability in higher dimensions*”, *Phys. Rev. D* **66**, 064024 (2002) [arXiv:hep-th/0206202].

[155] I. P. Neupane, “*Effective Lagrangian from higher curvature terms: Absence of vDVZ discontinuity in AdS space*”, *Class. Quant. Grav.* **19**, 1167 (2002) [arXiv:hep-th/0108194].

[156] H. Kodama and A. Ishibashi, “*A master equation for gravitational perturbations of maximally symmetric black holes in higher dimensions*”, *Prog. Theor. Phys.* **110**, 701 (2003) [arXiv:hep-th/0305147].

[157] N. D. Birrell and P. C. W. Davies, “*Quantum fields in curved space*”, (Cambridge Univ. Press, 1982).

[158] C. Done, “*Accretion Flows in X-ray Binaries*”, *Phil. Trans. Roy. Soc. Lond. A* **360**, 1967 (2002) [arXiv:astro-ph/0203246].

[159] M. A. Abramowicz, W. Kluzniak and J. P. Lasota, “*No observational proof of the black-hole event-horizon*”, *Astron. Astrophys.* **396** (2002) L31 [arXiv:astro-ph/0207270].

[160] N. Bilic, G. B. Tupper and R. D. Viollier, “*Born-Infeld phantom gravastars*”, arXiv:astro-ph/0503427.

[161] C. Cattoen, T. Faber and M. Visser, “*Gravastars must have anisotropic pressures*”, *Class. Quant. Grav.* **22**, 4189 (2005) [arXiv:gr-qc/0505137].

[162] W. Israel, “*Singular hypersurfaces and thin shells in general relativity*”, *Nuovo Cim. B* **44S10** (1966) 1 Erratum-*ibid. B* **48** (1967) 463 ;
 K. Lanczos, “*Flächenhafte Verteilung der Materie in der Einsteinschen Gravitationstheorie*”, *Ann. Phys. (Leipzig)* **74** (1924) 518;
 N. Sen, “*Über die Grenzbedingungen des Schwerkraftfelds an unstetig Keilstäben*”, *Ann. Phys. (Leipzig)* **73** (1924) 365.

[163] M. Visser, “*Lorentzian Wormholes: From Einstein To Hawking*”, AIP Press (Springer-Verlag, New York, 1995).

[164] G. W. Gibbons and D. L. Wiltshire, “*Black Holes In Kaluza–Klein Theory*”, Annals Phys. **167**, 201 (1986) Erratum-ibid. **176**, 393 (1987).

[165] J. M. Overduin and P. S. Wesson, “*Kaluza–Klein gravity*”, Phys. Rept. **283**, 303 (1997) [arXiv:gr-qc/9805018].

[166] T. Applequist and A. Chodos, “*Modern Kaluza–Klein theories*”, (Addison–Wesley, Reading, 1987)

[167] L. Randall and R. Sundrum, “*A large mass hierarchy from a small extra dimension*”, Phys. Rev. Lett. **83**, 3370 (1999) [arXiv:hep-ph/9905221].

[168] L. Randall and R. Sundrum, “*An alternative to compactification*”, Phys. Rev. Lett. **83**, 4690 (1999) [arXiv:hep-th/9906064].

[169] Z. Chacko, P. J. Fox, A. E. Nelson and N. Weiner, “*Large extra dimensions from a small extra dimension*”, JHEP **0203**, 001 (2002) [arXiv:hep-ph/0106343].

[170] J. W. Chen, M. A. Luty and E. Ponton, “*A critical cosmological constant from millimeter extra dimensions*”, JHEP **0009**, 012 (2000) [arXiv:hep-th/0003067].

[171] P. Kanti, R. Madden and K. A. Olive, “*A 6-D brane world model*”, Phys. Rev. D **64**, 044021 (2001) [arXiv:hep-th/0104177].

[172] J. Louko and D. L. Wiltshire, “*Brane worlds with bolts*”, JHEP **0202**, 007 (2002) [arXiv:hep-th/0109099].

[173] C. P. Burgess, J. M. Cline, N. R. Constable and H. Firouzjahi, “*Dynamical stability of six-dimensional warped brane-worlds*”, JHEP **0201**, 014 (2002) [arXiv:hep-th/0112047].

[174] D. K. Park and H. s. Kim, “*Single 3-brane brane-world in six dimension*”, Nucl. Phys. B **650**, 114 (2003) [arXiv:hep-th/0206002].

[175] Y. Aghababaie, C. P. Burgess, S. L. Parameswaran and F. Quevedo, “*SUSY breaking and moduli stabilization from fluxes in gauged 6D supergravity*”, JHEP **0303**, 032 (2003) [arXiv:hep-th/0212091].

[176] Y. Aghababaie, C. P. Burgess, S. L. Parameswaran and F. Quevedo, “*Towards a naturally small cosmological constant from branes in 6D supergravity*”, Nucl. Phys. B **680**, 389 (2004) [arXiv:hep-th/0304256].

[177] J. M. Cline, J. Descheneau, M. Giovannini and J. Vinet, “*Cosmology of codimension-two braneworlds*”, JHEP **0306**, 048 (2003) [arXiv:hep-th/0304147].

[178] C. P. Burgess, C. Nunez, F. Quevedo, G. Tasinato and I. Zavala, “*General brane geometries from scalar potentials: Gauged supergravities and accelerating universes*”, JHEP **0308**, 056 (2003) [arXiv:hep-th/0305211].

[179] Y. Aghababaie *et al.*, “*Warped brane worlds in six dimensional supergravity*”, JHEP **0309**, 037 (2003) [arXiv:hep-th/0308064].

[180] C. P. Burgess, “*Towards a natural theory of dark energy: Supersymmetric large extra dimensions*”, AIP Conf. Proc. **743** (2005) 417 [arXiv:hep-th/0411140] ; “*Supersymmetric large extra dimensions and the cosmological constant problem*”, [arXiv:hep-th/0510123].

[181] I. Navarro and J. Santiago, I. Navarro and J. Santiago, “*Gravity on codimension 2 brane worlds*”, JHEP **0502**, 007 (2005) [arXiv:hep-th/0411250].

[182] J. Vinet and J. M. Cline, “*Codimension-two branes in six-dimensional supergravity and the cosmological constant problem*”, Phys. Rev. D **71**, 064011 (2005) [arXiv:hep-th/0501098].

[183] H. M. Lee and C. Ludeling, “*The general warped solution with conical branes in six-dimensional supergravity*”, JHEP **0601** (2006) 062 [arXiv:hep-th/0510026].

[184] P. Callin and C. P. Burgess, “*Deviations from Newton’s law in supersymmetric large extra dimensions*”, arXiv:hep-ph/0511216.

[185] A. J. Tolley, C. P. Burgess, D. Hoover and Y. Aghababaie, “*Bulk singularities and the effective cosmological constant for higher co-dimension branes*”, [arXiv:hep-th/0512218].

[186] G. T. Horowitz and R. C. Myers, “*The AdS/CFT correspondence and a new positive energy conjecture for general relativity*”, Phys. Rev. D **59**, 026005 (1999) [arXiv:hep-th/9808079].

[187] S. Mukohyama, Y. Sendouda, H. Yoshiguchi and S. Kinoshita, “*Warped flux compactification and brane gravity*”, JCAP **0507**, 013 (2005) [arXiv:hep-th/0506050]; “*Dynamical stability of six-dimensional warped flux compactification*”, [arXiv:hep-th/0512212].

[188] H. Nishino and E. Sezgin, “*Matter And Gauge Couplings Of $N=2$ Supergravity In Six-Dimensions*”, Phys. Lett. B **144**, 187 (1984).

[189] A. Salam and E. Sezgin, “*Chiral Compactification On Minkowski $X S^{*2}$ Of $N=2$ Einstein-Maxwell Supergravity In Six-Dimensions*”, Phys. Lett. B **147**, 47 (1984).

[190] R. Geroch and J. H. Traschen, “*Strings And Other Distributional Sources In general relativity*”, Phys. Rev. D **36**, 1017 (1987).

[191] D. Garfinkle, “Metrics with distributional curvature,” Class. Quant. Grav. **16** (1999) 4101 [arXiv:gr-qc/9906053].

[192] C. de Rham and A. J. Tolley, “*Gravitational waves in a codimension two braneworld*”, arXiv:hep-th/0511138.

[193] N. Kaloper and D. Kiley, “*Exact black holes and gravitational shockwaves on codimension-2 branes*”, arXiv:hep-th/0601110.

[194] S. J. Poletti and D. L. Wiltshire, S. J. Poletti and D. L. Wiltshire, “*The Global properties of static spherically symmetric charged dilaton space-times with a Liouville potential*”, Phys. Rev. D **50**, 7260 (1994) Erratum-ibid. D **52**, 3753 (1995) [arXiv:gr-qc/9407021].

[195] K. C. K. Chan, J. H. Horne and R. B. Mann, “*Charged dilaton black holes with unusual asymptotics*”, Nucl. Phys. B **447**, 441 (1995) [arXiv:gr-qc/9502042].

[196] S. B. Giddings, E. Katz and L. Randall, “*Linearized gravity in brane backgrounds*”, JHEP **0003**, 023 (2000) [arXiv:hep-th/0002091].

[197] D. Garfinkle and T. Vachaspati, “*Cosmic String Traveling Waves*”, Phys. Rev. D **42**, 1960 (1990).

[198] M. Abramovitz and I.A. Stegun, *Handbook of Mathematical Functions*, (Dover, New York, 1965).

[199] B. M. N. Carter and A. B. Nielsen, “*Series solutions for a static scalar potential in a Salam-Sezgin Supergravitational hybrid braneworld*”, Gen. Rel. Grav. **37**, 1629 (2005) [arXiv:gr-qc/0512024].

[200] G. W. Gibbons, R. Guven and C. N. Pope, “*3-branes and uniqueness of the Salam-Sezgin vacuum*”, Phys. Lett. B **595**, 498 (2004) [arXiv:hep-th/0307238].

[201] G. W. Gibbons and K. i. Maeda, “*Black Holes And Membranes In Higher Dimensional Theories With Dilaton Fields*”, Nucl. Phys. B **298**, 741 (1988).

[202] S. Mignemi and D. L. Wiltshire, “*Spherically Symmetric Solutions In Dimensionally Reduced Space-Times*”, Class. Quant. Grav. **6**, 987 (1989).

[203] B. M. N. Carter, A. B. Nielsen and D. L. Wiltshire, “*Hybrid brane worlds in the Salam-Sezgin model*”, arXiv:hep-th/0602086.